DEVELOPMENT OF ANTIOXIDANT AND SELF-HEALABLE GELATIN-POLYANILINE FILMS EXTRACTED FROM RED TILAPIA FISH SCALE

By

NAZATUL SHIMA BINTI AZMI

Thesis Submitted to the School of Graduate Studies, Universiti Putra Malaysia, in Fulfilment of the Requirements for the Degree of Doctor of Philosophy

February 2023

FK 2023 33

Abstract of thesis presented to the Senate of Universiti Putra Malaysia in fulfilment of the requirement for the degree of Doctor of Philosophy

DEVELOPMENT OF ANTIOXIDANT AND SELF-HEALABLE GELATIN-POLYANILINE FILMS EXTRACTED FROM RED TILAPIA FISH SCALE

By

NAZATUL SHIMA BINTI AZMI

February 2023

Chair : Roseliza Kadir Basha, PhD
Faculty : Engineering

Gelatin is promising biomass for developing active biofilm due to its good film-forming properties and compatibility with active substances such as solid polyaniline (PANI). In addition, interestingly, the damaged gelatin-based film has the potential to self-heal the damaged zone by physical interaction in the presence of moisture. Nevertheless, the potential of this active film properties in the current research has not been explored in-depth. Hence, the aim of this research is to develop a self-healable active film from gelatin extracted from red tilapia's fish scale incorporated with polyaniline (PANI). 4.34% dry weight basis of snowy white, crystal and light textured of gelatin was extracted from red tilapia's fish scale. The extracted gelatin also has high amounts of glycine (20.79g/100g) and hydroproline (14.38g/100g), contributing to the filmogenic properties. Several chemical interactions on the peptide bonds are indicated as amide A, amide I, amide II, and amide III. Then, the good film-forming gelatin was further developed into gelatin-based film with the incorporation of 25% (w/w of gelatin) of glycerol using the solution casting method. The mechanically significant variations altered the G-Gly (with glycerol) film flexibility by more than 90% and decreased the tensile strength (TS) to 14.83 MPa. From the investigation via color, morphology, addition of functional group in Fourier transform infrared spectroscopy (FTIR), moisture content, mechanical, thermal, water vapor permeability (WVP) analysis, it was conclusive that G-Gly film was effectively developed with the addition of glycerol as plasticizer. The gelatin-based film was further explored with the incorporation PANI (G-Gly-PANI) in various sizes (x) (50μm ≤x≤ 100μm, 100μm ≤x≤ 125μm, 125μm ≤x≤ 250μm) and concentrations (0.5, 1 and 2 g/L) with feature characteristics of the films were further explored as active film. PANI dispersion inside the film was seen clearly as the green spots and the moisture content of G-Gly-PANI film decreased due to the hydrophobic properties of PANI. Based on the different T_g values obtained, G-Gly-PANI composite film was heterogenous and immiscible. Additionally, G-Gly-PANI films show differences in thermal degradation temperature and weight loss. From the mechanical aspects, the TS of the films increased and decreased

in elongation at break (EAB) with the addition of small size of PANI due to the rigidity properties of PANI. Meanwhile, it contradicted with the larger size of PANI where the arrangements of PANI were more spacious, reducing the effect on the flexibility. The G-Gly-PANI film exhibited more than 40% in antioxidant activity. Out of the analyses subjected, it is noteworthy that the small size (50μm ≤x≤ 100μm, 100μm ≤x≤ 125μm) and high concentration of PANI can transition gelatin as the active film, which denoted its high capability as antioxidant. Next, G-Gly-PANI film was further investigated the ability and behaviour of self-healing properties of the film. The G-Gly-PANI film can repair the scratches that reach the underlying substrate by utilizing water stimuli. The absorbed water disrupted the intermolecular hydrogen bonds, allowing the polymer chains to move around and begin the self-healing process. Nevertheless, the mechanical properties of the self-healed film showed a significant decrement in flexibility compared to the non-damage films. From the sorption analysis of the films, based on R^2 values (more than 0.95), Peleg and Guggenheim Anderson de Boer (GAB) models were respectively found to be the best-fitted model for representing the experimental data within the RH (23%, 33%, 57%, 75%) and temperature (5, 30, 40 °C) studied. Additionally, high relative humidity (75%) and low temperature (5 °C) does trigger the healing progress in a more incorporating way. After 7 days stored the films, the scratched film only nearly self-healed. The moisture was absorbed on the whole film and not only at the scratched area. Thus, when the films reach equilibrium, they will stop absorbing moisture and the healing process. In conclusion, this study revealed the feasibility of developing a self-healable active gelatin-based film incorporating with PANI as an active substance. Therefore, the complement of this study shows that the developed G-Gly-PANI film shows excellent potential as an active and self-healing film with potential applications in the food packaging industry, especially perishable fruit and vegetable.

Abstrak tesis yang dikemukakan kepada Senat Universiti Putra Malaysia sebagai memenuhi keperluan untuk ijazah Doktor Falsafah

PEMBANGUNAN ANTIOKSIDAN DAN SWASEMBUH GELATIN-POLIANILINA FILEM TERSARI DARI SISIK IKAN TILAPIA

Oleh

NAZATUL SHIMA BINTI AZMI

Februari 2023

Pengerusi : Roseliza Kadir Basha, PhD
Fakulti : Kejuruteraan

Gelatin merupakan biojisim yang boleh diolah untuk menjadi bio-filem aktif kerana sifat pembentukan filemnya yang baik dan keserasian dengan bahan aktif seperti pepejal polianilina (PANI). Di samping itu, filem berasaskan gelatin yang rosak berpotensi untuk swasembuh kawasan yang rosak dengan sendiri melalui interaksi fizikal dengan adanya kelembapan. Walaupun begitu, potensi filem aktif ini dalam penyelidikan semasa belum diperinci secara mendalam. Oleh itu, tujuan penyelidikan ini adalah untuk mengembangkan swasembuh filem aktif daripada gelatin tersari dari sisik ikan tilapia merah yang digabungkan dengan polianilina (PANI). Sebanyak 4.34% berat kering gelatin putih seperti kapas, kristal dan ringan yang tersari dari sisik ikan tilapia merah. Gelatin yang tersari juga mempunyai jumlah glisin yang tinggi (20.79g / 100g) dan hidroprolina (14.38g/100g) yang menyumbang kepada sifat filemogenik. Terdapat beberapa interaksi kimia pada ikatan peptida yang ditunjukkan sebagai amida A, amida I, amida II, dan amida III. Kemudian, pembentuk filem gelatin dihasilkan lebih lanjut menjadi filem berasaskan gelatin dengan penggabungan 25% (w/w gelatin) gliserol menggunakan kaedah tuangan larutan. Variasi yang signifikan secara mekanikal mengubah fleksibiliti filem G-Gly (dengan gliserol) lebih daripada 90% dan menurunkan kekuatan tegangan (TS) menjadi 14.83 MPa. Dari penyelidikan melalui analisis warna, morfologi, tambahan kumpulan fungsional dalam analisis spektroskopi inframerah transformasi Fourier (FTIR), kandungan kelembapan, mekanikal, termal, kebolehtelapan wap air (WVP), dapat dirumuskan bahawa filem G-Gly dikembangkan dengan berkesan dengan penambahan gliserol sebagai pemplastik. Filem berasaskan gelatin diselidiki lebih lanjut dengan penggabungan PANI (G-Gly-PANI) pada pelbagai ukuran saiz (x) (50μm ≤x≤ 100μm, 100μm ≤x≤ 125μm, 125μm ≤x≤ 250μm) dan kepekatan (0.5, 1 dan 2 g/L) dengan ciri-ciri filem ini diselidiki lebih lanjut sebagai filem aktif. Penyebaran PANI di dalam filem dilihat dengan jelas sebagai bintik-bintik hijau dan kandungan kelembapan filem G-Gly-PANI menurun kerana sifat hidrofobik PANI. Berdasarkan nilai T_g yang diperoleh berbeza, filem komposit G-Gly-PANI adalah heterogen dan tidak dapat dicampur. Selain itu, filem G-Gly-PANI

menunjukkan beberapa perbezaan dari segi suhu degradasi termal dan penurunan berat jisim. Dari aspek mekanikal, TS filem meningkat dan menurun dalam pemanjangan pada rehat (EAB) dengan penambahan PANI yang bersaiz kecil kerana sifat ketegaran PANI. Sementara itu, ia bertentangan dengan PANI yang bersaiz lebih besar di mana susunan PANI lebih luas yang mengurangkan kesan pada fleksibiliti. Filem G-Gly-PANI mempamerkan lebih daripada 40% aktiviti antioksida. Dari analisis yang dilakukan, didapati bahawa PANI bersaiz kecil (50μm ≤x≤ 100μm, 100μm ≤x≤ 125μm) dan kepekatan PANI yang tinggi dapat mengubah gelatin sebagai filem aktif yang menunjukkan kemampuan tinggi sebagai antioksida. Seterusnya, filem G-Gly-PANI diselidik lebih lanjut mengenai kemampuan dan tingkah laku mengenai sifat swasembuh filem ini. Filem G-Gly-PANI dapat memperbaiki calar yang mencapai substrat yang mendasari filem menggunakan rangsangan air. Air yang diserap mengganggu ikatan hidrogen intermolekul, yang membolehkan rantai polimer bergerak dan memulakan proses swasembuh. Walaupun begitu, sifat mekanikal filem yang disembuhkan sendiri menunjukkan penurunan fleksibiliti yang ketara berbanding dengan filem yang tidak rosak. Dari analisis penyerapan filem, berdasarkan nilai R^2 (lebih daripada 0.95),Peleg dan Guggenheim Anderson de Boer (GAB) model masing-masing didapati sebagai model yang paling sesuai untuk mewakili data eksperimen dalam RH (23%, 33%, 57%, 75%) dan suhu (5, 30, 40 °C) yang dikaji. Selain itu, kelembapan relatif tinggi (75%) dan suhu rendah (5 °C) dilihat membantu proses swasembuh. Setelah 7 hari menyimpan filem, filem yang digores itu hampir swasembuh. Ini kerana kelembapan menyerap pada keseluruhan filem dan bukan hanya di kawasan yang tergores. Oleh itu, apabila filem mencapai keadaan keseimbangannya, ia akan menghentikan kelembapan yang diserap dan proses swasembuh. Sebagai kesimpulan, kajian ini menunjukkan kemungkinan mengembangkan filem berasaskan gelatin aktif sebagai filem swasembuh disamping menggabungkan dengan PANI sebagai bahan aktif. Oleh itu, pelengkap kajian ini menunjukkan filem G-Gly-PANI yang dikembangkan menunjukkan potensi yang sangat baik sebagai filem aktif dan swasembuh dengan aplikasi yang berpotensi dalam industri pembungkusan makanan terutama buah dan sayur yang mudah rosak.

ACKNOWLEDGEMENTS

First and foremost, I would like to thank to ALLAH S.W.T because with His blessing, I had completed this research after a few years of struggles. Special thanks and gratitude to my supervisory committee, Dr. Roseliza Kadir Basha, Assoc. Prof. Dr. Siti Hajar Othman and Dr Mohd Afandi P. Mohammed for their guidance, advices and support.

I also would like to express my thanks to my husband, mother, father and others family members whom has been very supportive and always be on my side. Not to forget, to all my friends who are always there to support and especially during the hard time.

Lastly, my sincere thanks to all staffs and Assistant Engineer from Department of Process and Food Engineering for their kindness, willingness and cooperation in helping me.

Besides, I would like to convey my deepest appreciation to the Universiti Tun Hussien Onn and Ministry of High Education for awarding me a scholarship program (STAB and SLAB/SLAI), which has been my primary financial support throughout my study. Last but not least, my sincere thanks to Universiti Putra Malaysia for the financial support provided through Geran Putra IPS (9547500) and Geran Putra (957400).

This thesis was submitted to the Senate of Universiti Putra Malaysia and has been accepted as fulfilment of the requirement for the degree of Doctor of Philosophy. The members of the Supervisory Committee were as follows:

Roseliza Kadir binti Basha, PhD
Senior Lecturer
Faculty of Engineering
Universiti Putra Malaysia
(Chairman)

Siti Hajar binti Othman, PhD
Associate Professor
Faculty of Engineering
Universiti Putra Malaysia
(Member)

Mohd Afandi bin P. Mohammed, PhD
Senior Lecturer
Faculty of Engineering
Universiti Putra Malaysia
(Member)

_____
ZALILAH MOHD SHARIF, PhD
Professor and Dean
School of Graduate Studies
Universiti Putra Malaysia

Date: 21 July 2023

TABLE OF CONTENTS

LIST OF TABLES

LIST OF FIGURES

LIST OF ABBREVIATIONS

AOAC	Association of Official Analytical Chemists
APS	Ammonium persulfate
CH_3CO_2K	Potassium acetate
CSA	Camphorsulfonic acid
EAB	Elongation at break
EMC	Equilibrium Moisture Content
FTIR	Fourier-transform infrared spectroscopy
GAB	Guggenheim Anderson de Boer
HCl	Hydrochloric acid
HPLC	High performance liquid chromatography
k_1	Water sorption rate
k_2	Water sorption capacity
K_2CO_3	Potassium carbonate (K_2CO_3)
MgCl	Magnesium chloride
NaBr	Sodium bromide (NaBr)
NaCl	Sodium chloride (NaCl)
NaOH	Sodium Hydroxide
PA	Polyamide
PANI	Polyaniline
PE	Polyethylene
PET	Polyethylene terephthalate
PHA	Polyhydrooxyalkanoates
PLA	Polylactic Acid

PS	Polystyrene
R^2	Regression square
RH	Relative humidity
SEM	Scanning electron microscopy
T_g	Glass-transition temperature
TS	Tensile strength
WVP	Water vapor permeability

CHAPTER 1

INTRODUCTION

1.1 Background of study

Packaging is an integral part of the food industry. Global consumption of plastics as the packaging was approximately 390.7 million tonnes in 2021 (Europe & EPRO, 2022). Based on the statistics, the major contributors include Asia (52%), Europe (15%), Middle East and Africa (7%) (Europe & EPRO, 2022; Shaikh et al., 2021). In Asia, Malaysia is one of the leading nations for the production and use of plastic. The primary function of packing is to preserve and protect food from external contamination. Packaging also aids in the protection of food from external contaminants and effects such as heat, light, moisture, oxygen, germs, dirt, and dust particles, all of which contribute to food degradation (Baghi et al., 2022; Marsh & Bugusu, 2007). Furthermore, it helps to globalize the food sector by stabilizing food items so they may be delivered across vast distances.

Due to evolving customer expectations and market developments, the food sector has been engaged in various advancements in packaging technologies and applications during the previous several decades. These demands or requests can be summarized in the high quality, freshness, and extended shelf life of the food products, coupled with the use of the handle and resistant packaging made with lighter, cheaper and recyclable materials. In response to these continuous changes and requests, active packaging has been introduced. Active packaging systems are an innovative technology that is attracting academic as well as industrial interest (Drago et al., 2020). Active packaging techniques are directly related to substances that absorb oxygen, ethylene, moisture, carbon dioxide, flavors/odors, and those which release carbon dioxide, antimicrobial agents, antioxidants and flavors (Vermeiren et al., 2000).

As good resistant packaging, the films should be mechanically reliable, transparent and exhibit good gas and vapour permeability properties to protect the quality of the inner products (Hu et al., 2018). Accidental damage with exposure to the harsh environment that occurred during the handling and transportation could affect and weaken the protection functions of the package and resulting in deterioration of the product (Andersson et al., 2009; Hu et al., 2018). Micro cracking is one of the fatal deteriorations which later will bring to catastrophic failure of the materials and hence significantly shorten the lifetime of the polymers. Numerous self-healing materials have been created to date, and when stimulated by pH, temperature, light, and humidity, these materials may self-healed themselves (Ding et al., 2015; Hu et al., 2018; Skorb & Andreeva, 2015; Thakur & Kessler, 2015). Exposure to a harsh environment would lead to the degradation of polymeric components and later affect the quality of the product inside the package. Moreover, the external force during processing and employment will affect the material by fracture or breakage.

Given that self-healing properties could extend the life of materials, realize recycling and reusing, and reduce a string security issues and environmental problems, the use of self-healing materials is great significance. A self-healing polymer has the ability to transform physical energy into a chemical and/or physical response able to heal damage - a process which normally does not present in conventional -non-self-healing" polymers (Fainleib & Purikova, 2019).

1.2 Problem statement

Plastic is extensively used in food packaging because it is affordable, simple to use, and readily accessible. The majority of plastic is produced from nonrenewable fossil resources. Because of their good structural characteristics, performance, gas or water barrier capabilities, aesthetic features, and cheap cost, petrochemical-based plastics such as polystyrene (PS), polyamide (PA), polyethylene terephthalate (PET), and polyethylene (PE) are the most often used. Unfortunately, some materials are not eco-friendly. As a result, it causes major environmental problems since it creates large amounts of non-biodegradable trash, which is then disposed of in landfills or incinerated at recovery sites. It will literally have a bad influence on the environment and public health. As a result of the growing concern over diminishing petroleum resources, severe government laws and growing social and environmental consciousness, the demand for "greener" packaging is more important than ever. As a result, biomass-based products may aid in reducing the environmental effect of non-biodegradable trash (Soo & Sarbon, 2018). However, in terms of cost and performance, new biomass materials fall behind traditional plastics.

Proteins, lipids, polysaccharides, and gelatin are examples of renewable resources that may be used to produce biomass film. Gelatin can be derived from the fibrous insoluble protein called collagen obtained from either skin, bones, or scales (Mariod & Adam, 2013). The gelatin-based film is made up of bovine and porcine skins to exhibit much stronger mechanical properties than other raw materials (Said & Sarbon, 2022). Unfortunately, due to the religious matter in consumption of this mammalian and health concern about the spread of disease to human, biomass film from fish gelatin have drawn more attention (Chuaynukul et al., 2017; Said & Sarbon, 2022; Weng et al., 2014). The usage of gelatin extracted from by-products of fish processing such as scale not only resolves the religious and health issues but also reduces the abundance of waste produces. Collagen-rich fish scale gelatin has been extensively used in the production of edible films and encapsulating materials. It also has been reported that fish gelatin exhibits excellent film-forming properties compared to other biopolymers (Mohammad et al., 2014a; Weng & Wu, 2015). With the good film-forming ability of gelatin, this property will give an advantage in developing a good film. Despite the many advantages of fish gelatin films, the films usually exhibit a lack of mechanical behavior due to their brittleness (Gómez-Guillén et al., 2009; Weng & Wu, 2015). Hence the application of fish gelatin films as a packaging material is restricted. To overcome the problem, a small percentage of low molecular-weight hydrophilic plasticizers is frequently added. The addition

of the plasticizer can help to increase the hydrogen bonding and electrostatic interactions with the protein chains, hence improving the flexibility of the films. Among all the potential plasticizers that can be added to the films to improve the limited properties, glycerol is favored due to its stability and compatibility with hydrophilic bio-polymeric film apart from having high hygroscopic characteristics (Limpisophon et al., 2009; Tongnuanchan et al., 2012).

In recent years, gelatin-based films have piqued the interest not only because of the product but also because they are compatible with active compounds. Thus, the gelatin-based film incorporated with active compounds can help extend the shelf life of the food and safety. An antioxidant is one of the active substances that can be incorporated with gelatin-based film to protect the food product from oxidation and increase its shelf-life of the food product. Due to safety concerns, current research is mainly concerned with using natural antioxidants as alternatives to synthetic antioxidants like butylated hydroxyl toluene (BHT) and butylated hydroxyl anisole (BHA) (Flieger et al., 2021). Previously, the most natural active substance used as antioxidants was mainly essential oils which extracted from natural resources (tea tree oil, lemon oil, cinnamon oil, and various other plants) due to their major components of thymol, carvacrol, and cinnamaldehyde (Bhavaniramya et al., 2019). However, essential oil has a few drawbacks such as instability and volatility. To overcome the problem, conducting polymer such as polyaniline (PANI) has attracted attention as an antioxidant material by having the advantage of its free radical scavenging properties. Antioxidants such as PANI can interface with the oxidation process by scavenging active oxygen species, chelating catalytic metals, or by terminating the free radical chain reactions by incorporating it into the film material. PANI is a proficient and superior scavenger of 2,2-azino-bis-(3-ethylbenzothiazoline-6-sulfonic acid) (ABTS) and 1,1-diphenyl-2picrylhydrazyl (DPPH) free radicals (Nand et al., 2012). Several conventional food science radical scavenging assays and accelerated storage procedures have been altered to use solid conducting polymer to estimate the effectiveness of different samples and preparations. In the previous study, PANI has been incorporated into several matrix such as polyvinyl alcohol, polyethylene, polystyrene, low-density polyethylene, chitosan, and starch to produce conducting polymer (Annala & Löfgren, 2006; Bhadra et al., 2017; Nand et al., 2011; Saikia et al., 2010; Yavuz et al., 2009; Zareh et al., 2011). However, it is hard to obtain flexible composite film with good antioxidant activity without any usage of commercial petroleum-based material. Hence, this study investigated the physico-chemical and antioxidant properties of PANI/gelatin-based film with incorporation different sizes and concentration of PANI. In this present study, the PANI and gelatin was mixed using solution blending method.

The others aspect that triggers the safety concern is the ability of the packaging film to withstand external forces. Micro cracking is one of the fatal deteriorations which later will bring to catastrophic failure of the materials and hence significantly shorten the lifetime of the polymers (Andersson et al., 2009; Hu et al., 2018). Self-healing is a key property of the materials that allow them to sustain repeated damage. Gelatin in particular is an interesting biomaterial that has been studied extensively not only due to its excellent gas barrier properties,

exhibit excellent film-forming property among the biopolymer, and consist of various amino acids but also due to its self-healing properties (Mohammad et al., 2014b; Sharma et al., 2017; Tongnuanchan et al., 2014; Tyuftin & Kerry, 2021; Weng & Wu, 2015). Gelatin is an interesting biomass-based material that consists of amino acids like proline (Pro), hydroproline (Hyp), and Glycine (Gly). These amino acids are the main components that contribute to the self-healing properties of the gelatin (Sharma et al., 2017). The mechanism of the intrinsic self-healing stimulus by water is due to the ability to develop back the inter- and intramolecular chain-chain hydrogen bonds (Wittmer et al., 2018). The high sorption capacity of the gelatin film will also help accumulate the water on the surface and stimulus self-healing. Additionally, the incorporation of PANI into the film matrix will also contribute to the self-healing process by immediately forming an overlap junction to create a water depletion region which facilitates the film healing. This can be related to the hydrophobic characteristics of PANI which will create stronger hydrophobic forces that lead to faster recovery and restore the rigidity after healing. The timescale of the self-healing event is dependent on the water sorption of the film (Li et al., 2013; Wittmer et al., 2018). There were two elements that influence the amount and rate of moisture that can absorb or diffuse which were humidity and ambient temperature (Othman et al., 2017). These elements or factors need to be considered and investigated to guarantee the self-healing efficiency of the film as well as the integrity of the film developed.

Herein, in the recent study considering the ability of PANI as active substances for PANI/gelatin-based films, the effects on the overall properties of the film are anticipated including antioxidant activities and self-healing aspect. Extending the working life of the film could be depending on the fabrication of novel self-healable active gelatin-based with the ability to reduce the oxidation and repair the scratches. Therefore, preparing self-healable PANI/gelatin-based active film became necessary for further food packaging applications.

1.3 Aim and objectives

This research aims to develop a self-healing active film from gelatin extracted from red tilapia's fish scale incorporated with polyaniline (PANI). The fulfilment of this aim will result in the availability of PANI active materials with antioxidant capabilities for use in the self-healing gelatin-based film and widen its scope of application, specifically in perishable fruits and vegetables products.

The objectives of the study are as follows:

1 to assess the red tilapia's fish scale gelatin-based film with the addition of glycerol as a plasticizer's physical, chemical, morphological, thermal, and barrier properties.

2 to evaluate the effect of size and concentration of PANI powder (active compound) in the develop gelatin-based film on the physical, chemical, mechanical, morphological, thermal, barrier, and antioxidant properties

3 to evaluate the self-healing ability and self-healing behavior of PANI/gelatin-based film stored at different control conditions (relative humidity and temperature)

1.4 Significance of the study

Biomass material development has been employed exceedingly efficiently as an alternative to petroleum-based packaging materials, which are non-biodegradable and have a detrimental influence on the environment. Biomass products are environmentally friendly, non-toxic, and have several favourable physicochemical properties over manufactured materials. According to the findings of this study on the extraction of gelatin from red tilapia's fish scale, gelatin has good film-forming ability and can be developed further as a gelatin-based film with the addition of glycerol as a plasticizer, providing improved properties (physical, chemical, thermal, morphological, mechanical, and barrier). Gelatin is advantageous when combined with active chemicals such as PANI to form an active film. Boeva & Sergeyev (2014) define PANI as a conductive polymer generated from aniline polymerization. PANI was previously loaded in-situ and polymerized directly into the matrix, according to our knowledge, and numerous studies have used solid PANI. PANI is a conducting polymer that derived by aniline polymerization (Boeva & Sergeyev, 2014). PANI was previously loaded in-situ and polymerized directly into the matrix, according to our best knowledge numerous studies have used solid PANI (Annala & Löfgren, 2006; Azmi et al., 2019; Bhadra et al., 2017; Nand et al., 2012; Saikia et al., 2010; Yavuz et al., 2009; Zareh et al., 2011). Therefore, various sizes and concentrations of solid PANI were incorporated into the gelatin matrix to develop the active film was study and measure the physical, chemical, morphological,

thermal, water vapour permeability, and antioxidant activity of the PANI/gelatin-based film. Interestingly, our research has shown that PANI/gelatin-based films able to self-heal by physical touch in the presence of moisture. However, the potential of this characteristic has not been thoroughly investigated in current study. The ability of PANI/gelatin-based films to self-heal was published in this study. The discovery of this films self-healing ability may broaden its applicability in food packaging applications, particularly for perishable goods and vegetables. Furthermore, the sorption analysis of the film under various environmental circumstances (RH and temperature) is associated to the understanding of the self-healing behaviour of the PANI/gelatin-based films described in this work. The mechanical strength and self-healing capabilities of these films were moderately balanced. This extended knowledge of self-healing behavior can contribute to the design of self-healing films in the future. Hence, self-healable active gelatin-based film for use as a new packaging film was developed, and verifying the possibility for packaging of perishable products especially fruits and vegetables was studied by measuring various properties including physical, chemical, mechanical, WVP, thermal, antioxidant and sorption. As a result, it was confirmed that the performances of these films especially in term of their capabilities as antioxidant film can be applied for packaging of perishable fruits and vegetables. These films have the potential to control oxidation and ability to self-heal if accidental damage occur during storage and distribution. However, these modified self-healable active film lack of physical performances regarding their tensile strength and durability in low humidity and high temperature. In addition, this PANI/gelatin-based film, has limitation in antioxidant activity where once the active compound was consumed in the reaction the protection will ceases.

1.5 Structure of thesis

The descriptions of this work are divided into five chapters, as shown in Figure 1.1. The first chapter serves as an introduction to the study, including the statement and importance of the issue, the purpose and objectives, and the relevance of the research.

Chapter 2 reviews the overall background of the active biobased and self-healing film, including the concepts and system that form a core of the thesis, and give a brief overview of previous work. This overview provides a general discussion of related research.

Chapter three presents the materials and methods relevant to the extraction of the gelatin and developing self-healable PANI/gelatin-based active film. This includes the experimental details, procedures, and analytical method used in the thesis.

Chapter four is the working chapters which divided into four subtopics based on the objectives set in Section 1.3. The first subtopic is initiated with the characteristics of the red tilapia's fish scale and further extracts the gelatin from the scale. The extracted gelatin was then analyzed for physical, chemical, and morphological characteristics whereby to the suitability to form a good film forming solution was attained. Then, for the second sub-topic was detailed discussion on preparation and characterization of red tilapia's fish scale gelatin-based film with the addition of glycerol as plasticizer. The develop gelatin-based film was characterized for physical, chemical, morphological, mechanical, thermal, and barrier properties. To conclude, the develop gelatin-based film with glycerol (G-Gly) was further incorporated with polyaniline (PANI) as continued in the next sub-section. The third subtopic is on the development and characterization of the gelatin-based active films incorporated with different sizes and concentrations of PANI. This subtopic is initiated with the synthesis of PANI from aniline and its physical and chemical characteristics. In addition, the details explanation of the compatibility and ability of the solid PANI as antioxidants in the gelatin-based film was further discussed in terms of physical, chemical, morphological, mechanical, thermal, barrier, and antioxidant properties. Forth subtopic describe and presented the efficiency and behavior of self-healing properties of PANI/gelatin-based films. In this subtopic, the model isotherm for sorption analysis is also presented. The findings and analysis obtained from sorption analysis is further elaborate and discussed with the observation of self-healing of the damaged film stored at different temperature and relative humidity.

As for the final chapter, chapter five presented the overall conclusions of the research based the three objectives achieved by the findings discussed in the chapter four. The recommendations for future research on the self-healable active biobased film was also included in this final chapter.

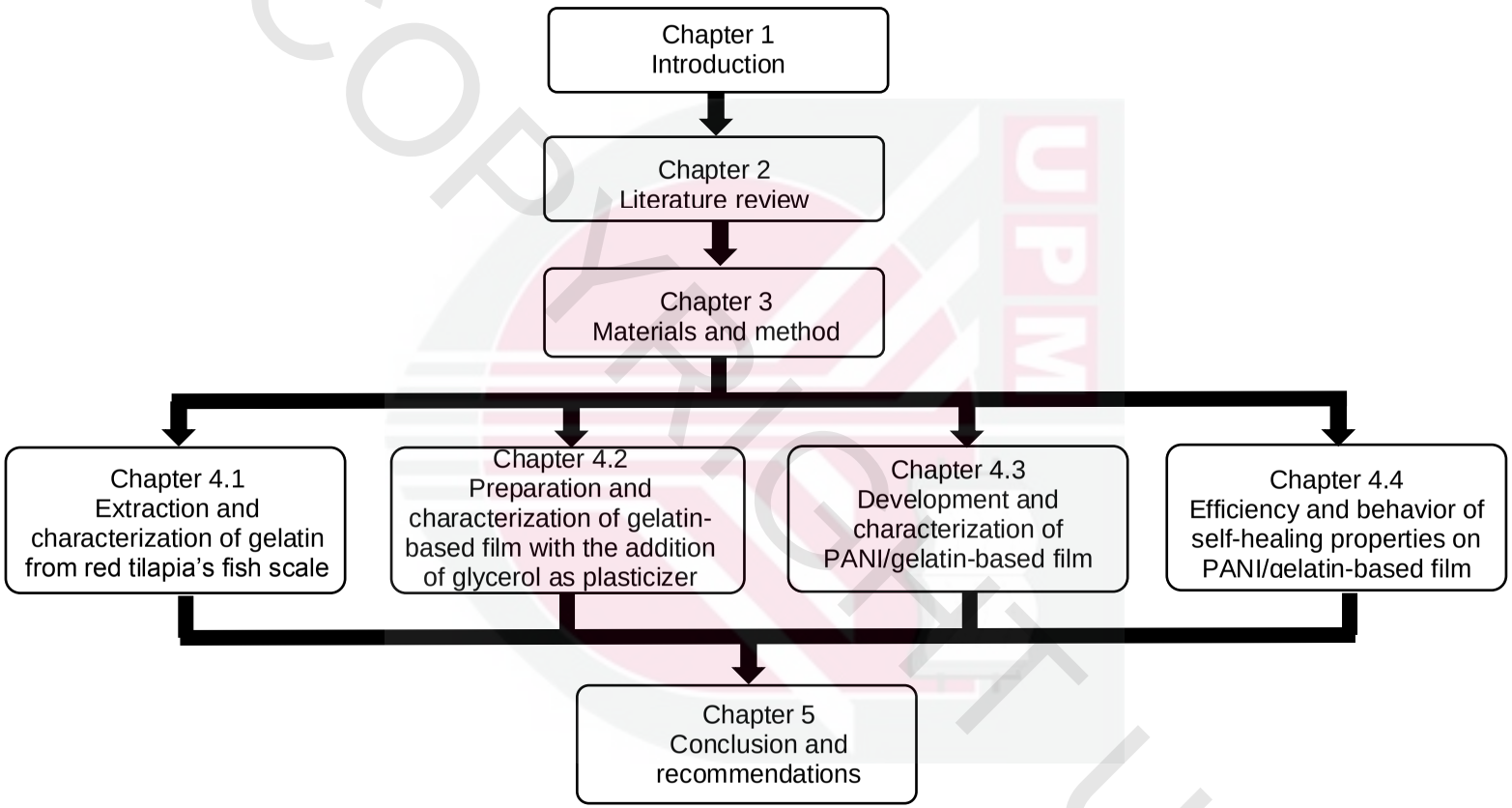

Figure 1.1: Thesis outline

CHAPTER 2

LITERATURE REVIEW

2.1 Biobased polymer

Biobased polymers are materials derived from renewable sources and have diverse chemistry and architecture in relation to their side chains (Shalini & Singh, 2009). Moreover, biobased polymers guarantee eco-friendly, non-toxic, environmental stability and have many desirable physico-chemical characteristics over synthetic ones. Biobased polymers are made from different polymer types (Figure 2.1), which include polysaccharides, proteins, and lipids or combinations of these materials, which can be categorized depending on their origin and production method (Abdul Khalil et al., 2018; Shaikh et al., 2021; Tongnuanchan et al., 2012). Based on the market values in 2019, biobased plastic packaging was at USD 4.65 billion and by the end of 2025, it is expected to reach the market value of up to 12.06 million (Shaikh et al., 2021). A part from that, food packaging industry holds the largest portion (Abdullah et al., 2022).

Bio-based polymers can be directly extracted from biomass, commonly from polysaccharides, protein and lipids derived from marine and agricultural products. These polymers naturally tend to be hydrophilic and crystalline, causing issues during the processing and functionality. Advantageously, they have excellent oxygen, carbon dioxide and volatile compounds barrier properties under low relative humidity conditions (Limpan et al., 2010; Tongnuanchan et al., 2012).

Another category of bio-based polymers is classically chemically synthesized from bio-derived monomers. The use of chemical synthesis to produce these polymers is to be applied in a wide range of possible bio-polyesters, especially from agricultural resources such as corn, wheat or agricultural waste (Shalini & Singh, 2009). The common polymeric material synthesize from bio-derived monomer is polylactic acid (PLA). It has the highest film utilization potential due to the good water vapour barrier and low gas transmittance. Other bio-based polymers can be produced directly by natural or genetically modified organisms. This type of based polymers is more biodegradable and biocompatible compared to others. The most common ones are polyhydrooxyalkanoates (PHA) with low water vapour permeability.

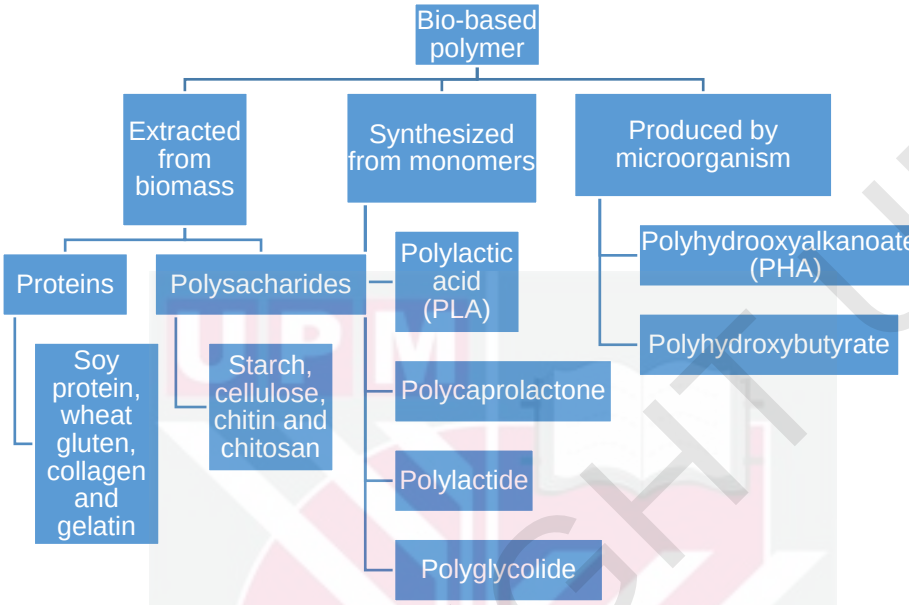

Figure 2.1: Classification of biopolymer
(Source: Abdul Khalil et al., 2018 and Shaikh et al., 2021)

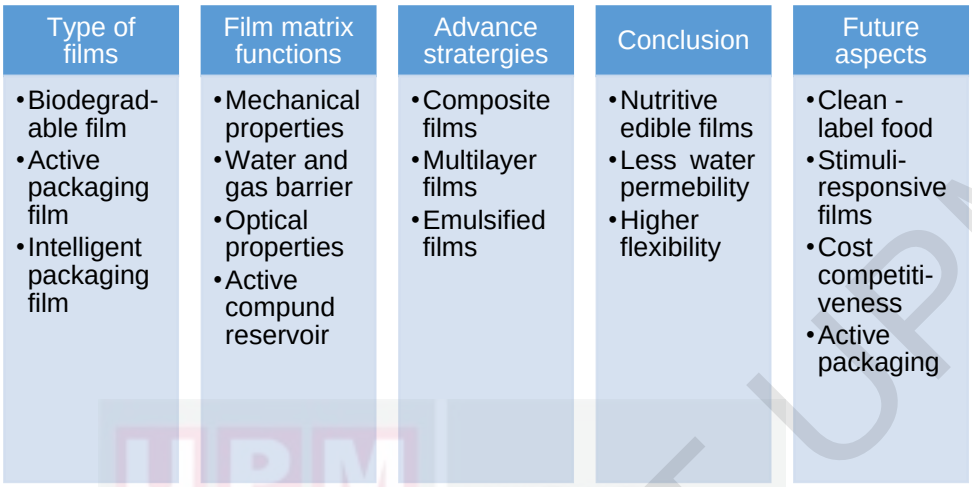

Figure 2.2: An overview diagram elaborating bio-polymer based films
(Source: Abdullah et al., 2022)

Numbers of industries have focussed towards the development of commercially viable and sustainable food related packaging applications using various biopolymers. Table 2.1 showed companies that involved in production of bioplastic. One of the biofilm produce by Novara company in Italy is Novamont. They produce a wide range of biodegradable film including monolayer and multilayer coextruded film based on a blend of biodegradable polyesters Previously, Del Nobile et al. (2008) has been used Novamont (Novara, Italy) films to prolong the shelf life of minimally processed lettuce by 5 days in compared to traditional film (oriented polypropelyne) which extend the shelf life until 4 days only at 4 °C. Furthermore, Novamont commercializes MaterBi®, a type of granular starch that can be processed as a thermoplastic material for manufacturing of films or bags.

Table 2.1: Bioplastic companies for food-related packaging applications

Company	Biopolymer	Application
Bioenvelop	Starch	Moisture barrier coating films for food
EverCorn, Inc. (subsidiary of Japan Corn Starch Co., Ltd.)	Starch	Films for food wrapping
FKur Kunststoffe GmbH	Cellulose/polylactic acid	Composite film for food packaging applications
Metabolix	Polyhydroxyalkanoates	Utilized as cast film
NatureWorks LLC	Polylactic acid	Food wrapping
NODAX	Polyhydroxyalkanoates	Good odor and oxygen barrier properties, customizable mechanical properties, thus highly suitable for food packaging
Fresh Del Monte Produce Inc	Polylactic acid	Packaging of fresh-cut fruits
ILIP	Polylactic acid	Packaging of fresh-cut to fresh whole produce

(Source: Del Nobile et al., 2008)

For the present research, protein has been selected as the source of bio-based polymer. Proteins have been extensively studied, as they exhibit valuable behaviours in biodegradable film production owing to their abundance, good film-forming ability, transparency, and excellent barrier properties against gas O_2, CO_2, and lipids (Etxabide et al., 2017; Jongjareonrak et al., 2006; Said & Sarbon, 2022). Thus, many researchers have been intensive to further study protein-based film from various protein sources such as collagen (Hua et al., 2014), gelatin (Jahit et al., 2016; Soo & Sarbon, 2018), and wheat gluten (Nataraj et al., 2018).

2.2 Protein

Proteins are polymers containing over 100 amino acid residues and are made of 20 proteinogenic amino acids joined together by amide bonds called polypeptides. Proteins form and functions differ depending on their origin, structures and amino acids compositions (Table 2.2). Each of the amino acids composition is comprised of a central (α-carbon) bonded to hydrogen, a carboxyl group (COOH), an amino acid (NH_2) and a unique amino acids side chains or R group. The R-group distinguished one amino acid from another, as shown in Figure 2.3.

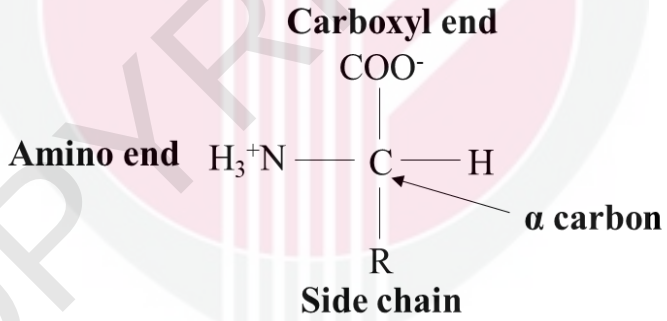

Figure 2.3: The basic chemical structural formula of protein

Table 2.2: Amino acids listing and basic properties

Amino acids name	Abbreviations	Properties
Alanine	ala (A)	Hydrophobic (non-polar)
Arginine	arg I	Positively charged
Asparagine	asn (N)	Hydrophilic (polar)
Aspartic acid	asp (D)	Negatively charged
Cysteine	cys I	Hydrophilic
Glutamic acid	glu (E)	Negatively charged
Glutamine	gln (Q)	Hydrophilic
Glycine	gly (G)	Hydrophobic
Histidine	his (H)	Positively charged
Isoleucine	ile (I)	Hydrophobic
Leucine	leu (L)	Hydrophobic
Lysine	Lys (K)	Positively charged
Methionine	met (M)	Hydrophobic
Phenyl-alanine	phe (F)	Hydrophobic
Proline	pro (P)	Hydrophobic
Serine	ser (S)	Hydrophilic
Threonine	thr (T)	Hydrophilic
Tryptophan	trp (W)	Hydrophobic
Tyrosine	tyr (Y)	Hydrophilic
Valine	val (V)	Hydrophobic

(Source: Nur Hanani et al., 2014)

The smallest and simplest amino acid is glycine which the R-group is a hydrogen (H). The amino acids can be subdivided according to their properties uttered by the functional groups. They are divided by charge, hydrophobicity and polarity, as listed in Table 2.2. These properties effects the way of they interact with surrounding amino acids in polypeptides. Thus, impacts on the 3D structure and properties.

The sequence of amino acids is classified as primary, secondary, tertiary and quaternary forms, as shown in Figure 2.4. A primary protein structure is the linear sequence of amino acids in its polypeptide chains. The peptide bonds which connect the amino acids together maintain the primary structure of a protein. Meanwhile, a secondary protein structure is one local folded structure that forms within a polypeptide due to interactions between atoms of the backbone. The shape of the protein molecules exists as either α helix or β sheet (folding and coiling) and is brought about by hydrogen-bonding between -C=O and N-H groups in between the chain and the primary amino acids building blocks. As for the tertiary protein structure, it arises from the further folding of the secondary structure of the protein. The folding and bending of the secondary structure of protein occurs due to the interactions with the R groups on the individual amino acids. These interactions may happen due to the hydrogen bonding, dipole-dipole interactions on the polarity of the R groups. A quaternary protein structure results in the spatial arrangements of various tertiary structures. It is a consequence of non-covalent interactions that bind multiple polypeptides into a large macromolecular complex (Sun et al., 2004).

The major insoluble fibrous protein is called collagen. Collagen contains large domains of helical conformation shaped by three α-helix chains, each containing 1050 amino acids. The chains are, in turn, coiled together to form a right-handed triple helix, as shown in Figure 2.5.

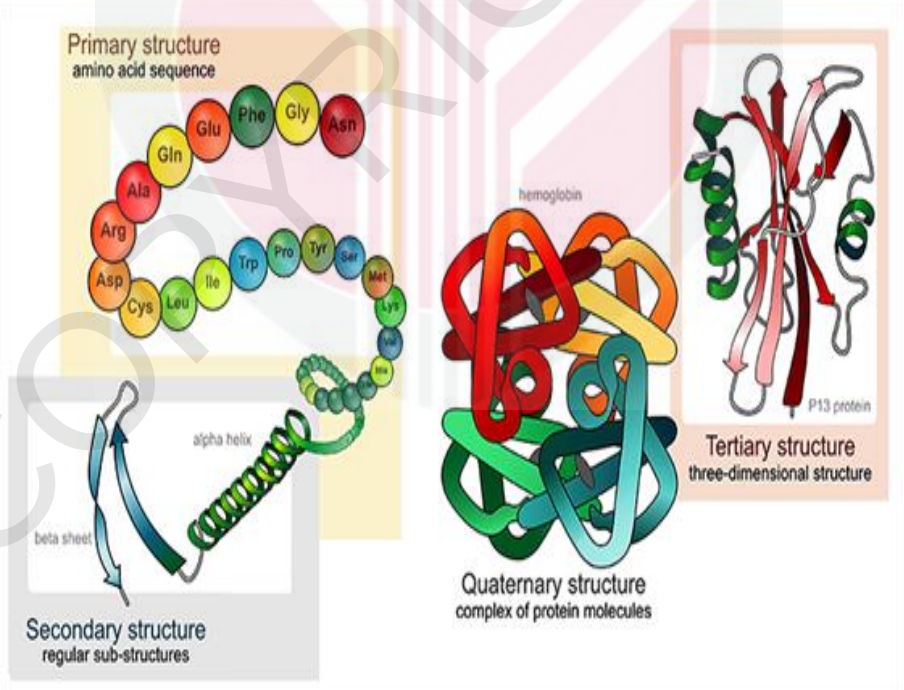

Figure 2.4: Four basic structures of protein
(Source: Byjus, 2022)

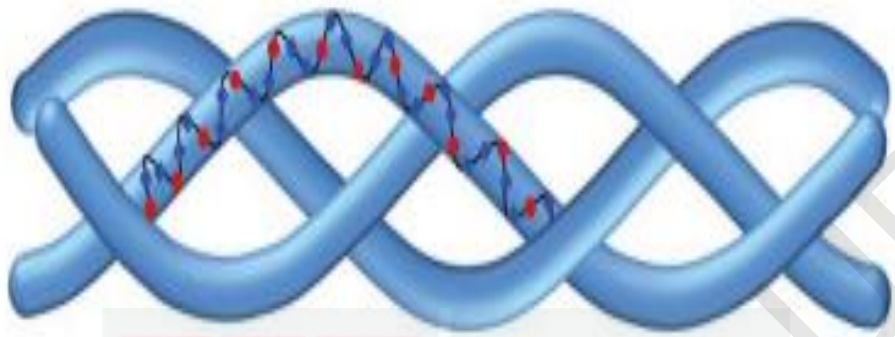

Figure 2.5: Schematic of the collagen triple helix (glycine, other amino acids)
(Source: Korossis, 2018)

2.2.1 Collagen

Collagen is abundant in many animal body parts, including tendons, skin, bone, the circulatory system, scales, and the connective tissue sheath that surrounds muscles, which helps to make muscles more durable. Compared to fish, which typically have far less collagen, on average 10% of mammalian muscle protein is collagen (Karim & Bhat, 2009). On a molecular level, collagen is a right-handed helical rod composed of three parallel-intertwined alpha chains (Haug et al., 2004). The triple helix of collagen assembles from specific polypeptide chain (α chains), made up of three amino acids residues in the sequence of Gly-X-Y (X and Y are often proline and hydroxyproline) (Asghar & Henrickson, 1982). Tropocollagen is formed from each α chains coil is a left-handed helix associated with three residues per turn, and the three chains are twisted right-handed.

The collagen molecule and collagen with a small concentration of both amino acids are stabilized hydroproline, denatures at lower temperatures than those with high concentrations (Jafari et al., 2020). Fish collagen generally has lower imino acid contents than mammalian collagens, which may be why denaturation at low temperature (Karim & Bhat, 2009).

2.2.2 Gelatin

Gelatin is a denatured protein synthesized by the partial hydrolysis of collagen extracted, and the properties of the gelatin produced are greatly affected by the sources, age of animal, collagen type and the extraction method used (Cho et

al., 2005; Said et al., 2021). It has a rheological property of thermos-reversible transformation between sol and gel. The gels are formed by cross-linking between amino and carboxyl components of amino acids residue side groups. As for the gelatin structure, it consists of a mixture of single and double unfolded hydrophilic chains. Gelatin is hygroscopic, which consequently adsorbs water depending on the relative humidity at which it is dried and stored. Physically, gelatin is produced in powdered and granulated form, colorless and tasteless.

Hydrogen and covalent bonds (which stabilize the structure) need to be broken to generate gelatin from collagen. During the gelatin extraction, covalent and hydrogen bonds are broken down by heat with the beginning of the conversion collagen into gelatin via the transition from helical to coil structure (Ahmad et al., 2019, 2020). It can be done by acid and/or alkali pre-treatments followed by extraction in hot water. The pre-treatment with acid or alkali functionally in removing non-collagenous protein material, degrade covalent bonds and inactive native proteases (Zhou & Regenstein, 2005). Figure 2.6 shows the representative of gelatin structure of a mixture of single and double unfolded chains.

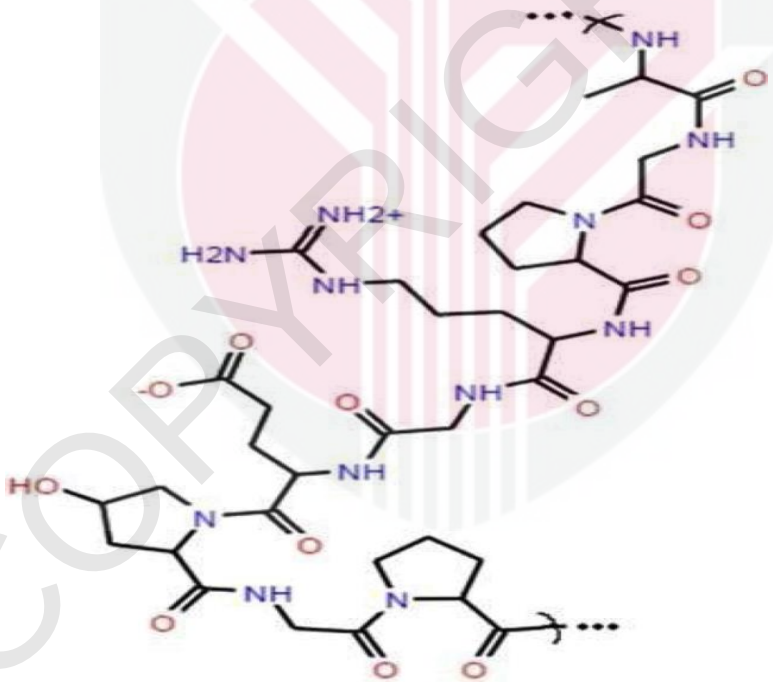

Figure 2.6: Representative gelatin structure
(Source: Ramos et al., 2016)

After the gelatin is produced and the temperature is lowered to below the critical value, there is partial renaturation of the collagen molecule. This phenomenon is called “collagen fold”. Those parts of collagen rich in proline and hydroproline

residues will regain some of their structure by following which they can apparently interact (Roff & Allen Foegeding, 1996). It has been reported by Ross-Murphy (1997) that gelatin aqueous solutions will be in the sol state at 40°C and during the gelation process its chains will undergo a conformational disorder-order transition. A three-dimensional structure will be produced when many molecules are involved. The strength of the gel formed is proportional to the molecular weight (Cho et al., 2004). Circular dichroism analysis reveals that gelling involves refolding denatured collagen chains into the typical triple helix conformation and conversely unfolding upon reheating. This folding process is directly related to the stabilization of the gels without disregarding its role in triggering the gelation process (Gómez-Guillén et al., 2002).

Gelatin can be extracted from different sources, and the properties of the gelatin are intrinsic affect by the source, age of the animal and type of the collagen. The most commonly used commercial gelatins are derived from bones and hide from cattle and pigs. Rapid progress and development of gelatin sources from skin, bones, and scale of the fish and poultry is underway and potentially serve as important commercial gelatin sources in the future. This is because the gelatin extracted from these sources never had any relationship with bovine spongiform encephalopahthy, BSE ("made cow disease"), more ethically and religiously acceptable and may possess novel and unique functional properties (Nur Hanani et al., 2014). For these reasons, there is high demand for fish gelatin. This has created a huge shift in the production of gelatin from bovine sources toward marine sources (Karim & Bhat, 2009).

2.2.3 Extraction of gelatin

The method of gelatin extraction involves three stages which are pre-treatment of the raw material, extraction of the gelatin and purification with drying (Karim & Bhat, 2009). Gelatin can be classified into two classes and determined by the pre-treatment. Type A gelatin with an isoionic point of 6-9 is obtained from acid treated collagen. Meanwhile, type B with an isoionic point 5 gelatin is derived from an alkali-treated precursor (Guerrero et al., 2011; Nur Hanani et al., 2014). Gelatin extracted from pig skin and fish is normally referred to as type A gelatin, and gelatin derived from beef skin or bovine is called type B gelatin. Acidic pre-treatment is suitable for the less covalently cross-linked collagen type A gelatin meanwhile alkaline treatment is favorable for the more complex collagen found in type B collagen. The extraction process effect on the length of the polypeptide chains and the functional properties of the gelatin. It commonly depends on the processing parameters, including temperature, time and pH, the pre-treatment, and the properties of the raw materials (Karim & Bhat, 2009).

Gelatin can be extracted from various fish species by several steps, which are non-collagenous protein elimination, demineralization and swelling with acid solution prior to conversion of collagen to gelatin by immersing in certain water temperature and finally recovery of gelatin in the final form (Roff & Allen Foegeding, 1996). As for the raw material with high content of lipids, it is better

to degrease first before another pre-treatment (Montero & Gómez-Guillén, 2000)(Montero & Gómez-Guillén, 2000) has been extracted gelatin from mergim skin that pre-treated by acetic- and propionic-acid rendered the gelatins with the highest elastic modulus, viscous modulus, melting temperature and gel strength. In other findings by Gómez-Guillén et al. (2002) gelatin from flat-fish species (sole and megrim) showed the best gelling ability and thermostable than those from cold-adapted fish (cod and hake). This difference was affected from the amino acid composition, the α_1/α_2 collagen-chain ratio, and the molecular weight distribution.

Pre-treatment is one of the factors that influences the functional properties if the gelatin. Pre-treatment with alkaline solutions of calcium hydroxide ($Ca(OH)_2$) and/or acetic acids (HAC) of sturgeon (*Acipenser baeri*) skin develop gelatin with favaroble color. It was proven that alkali pre-treatment removed non-collagenous proteins effectively, whilst acid induced some loss of collageous proteins. Resulting from pre-treated gelatin with HAC or alkali will improve the gel strength and viscosity in the presence of protease inhibitors (Hao et al., 2009). A previous study has been done by Yang et al. (2008) based on the relationship between the physical properties and nanostructure of channels catfish (*Ictalurus punctatus*) skin. The skin was sodium hydroxide, acetic acid or water and then extracted with hot water before further analyzed. The acid pretreatment group showed the highest gel strength and protein yield with reasonable viscosity from the findings. Meanwhile, by using water pre-treatment, the result showed the lowest values for all the physical properties.

2.2.4 Fish gelatin

Gelatin extracted from marine sources (warm- and cold- water fish skins, bones, fins and scale) is a possible alternative to bovine gelatin (Nurilmala et al., 2022). Normally all of these parts are known to cause waste and pollution as they are by-products from the fish processing industry. Advantageously, it can be a valuable source of gelatin as it contains collagen. The production of fish gelatin is known conceptually and has been present since 1960 (Karim & Bhat, 2009). Fish gelatin commonly has lower bloom values (0-270 g) compared to mammalian gelatin (Said & Sarbon, 2022b). However, the study by (Cho et al., 2005) that extracted gelatin from yellowfish tuna skin has obtained high bloom values, which is 426 g. This might be due to their differences in proline and hydroproline content in collagen from different species types and habitat temperatures. Fish gelatin contains a low concentration of amino acids, including proline and hydroproline compared to the other gelatin sources (mammalian). In the study of gelatin extraction from warm-water fish like big-eye-tuna tilpaia species have higher amino acids than cold-water fish such as cod, whiting, and halibut species (Ninan et al., 2014).

From the study by Weng & Wu (2015), the amino acids obtained from tilapia's scale gelatin was higher in comparison to tilapia skin gelatin with 212 residues per 1000 amino acids. Fish gelatin exhibits good film properties, with transparent, almost colorless, water-soluble, and highly extensible films (Alfaro et al., 2014). Additionally, fish scales are a captivating by-product of fish that are widely available in Malaysia fresh markets. Statistically, 94% of tilapia contribute to the red tilapia's (*Oreochromis* spp.) (Mohamad et al., 2021) (Figure 2.7). Red tilapia's fish are a durable, fast-growing species and highly resistant to disease (Foh et al., 2011). The wastes from fish filleting industries alone comprise 75%, and nearly 30% come from skins, scales and bones. Therefore, huge amounts of fish waste are discarded in the processes every day. Waste from fish scales can be found abundantly and transformed into a value-added product used in various applications.

Figure 2.7: Red tilapia fish (Length : ±15 cm)
(Source**:** Reátegui-Pinedo et al., 2022)

Fish scales are hierarchically ordered structures of mineralized collagen with stiff fibers easily swell like the bone (Zhang et al., 2010). The gelatin extracted from the fish scale was mainly composed of β-chains, α-chains and their degraded products with amino acids. Reportedly, the gelatin extracted from fish scale has higher amino acids than the fish skin (Weng & Wu, 2015). The higher content of imino acid and alanine exhibit better viscoelasticity and ability to develop the triple-helix structures, which relatively affected the film-forming properties of the gelatin (Giménez et al., 2009). However, there are limited studies conducted on the fish scale whereby most of the studies concerning the fish gelatin-based films were limited to fish skin only (Irwandi et al., 2009; Jongjareonrak et al., 2006; Muyonga et al., 2004; Sarabia et al., 2000; Tongnuanchan et al., 2016).

2.3 Properties of gelatin-based film

Gelatin has been explored extensively on account of its film-forming ability, especially in film production due to its exceptional filmogenic properties and used widely in the food packaging area (Alemán & Martínez-Alvarez, 2013; Hosseini et al., 2016; Lv et al., 2019). Gelatin might undergo a different conformational transition of disorder-order rearrangement according to the formation of gelatin and solutions (Aguirre-Alvarez et al., 2011).

Thickness of the film is one of the important properties that need to be measured as it is relates with other properties such as mechanical, and WVP. Differences in film thickness might influenced by the viability in nature, composition and solid content that present in the film structure (Said & Sarbon, 2022). Thickness of the film varied when incorporation of additives or plasticizer. Villasante et al. (2020) have found that by incorporation of pecan walnut and shell into the gelatin increased the thickness (0.047 – 0.150 mm) significantly in compared to the control (0.032±0.01 mm). This is due to the all the samples were prepared with different percents of extracts that contain different solid components (dry mass), this resulting in ticker film after evaporation of the solvent. In line with this study, the thickness of the gelatin-film incorporated with root essential also increased in thickness values that related to the interaction of essential oils with the peptide chains that reduced the ordered alligment (Tongnuanchan et al., 2013). In addition, film thickness value may vary according to the gelatin types, inclusion of other components into the films as well as the methods involved during the development process.

The other properties of the gelatin-based film that need to be measured is the color. Generally, gelatin color depends on raw materials used and extraction conditions (Jongjareonrak et al., 2006). The color of food products was commonly measured in L*, a*, b* which indicated lightness, redness/greenness and yellowness/blueness axis, respectively. Color of the film is an indicator for consumer satisfacness, quality attributes and marketability. Commonly, transparent film packaging has higher customer demands due to the clear in viewing the color, textures and quality of the food. Fish gelatin films were observed to perceived more yellowish color. This might be attributed to hogher content of cysteine (1 residues per 1000 residues) and methionine amino acids (10-17 residues per 1000 residues. (Gómez-Guillén et al., 2009).

Meanwhile, the L*, a* and b* values composites fish-gelatin based films with addition of natural extratcts such bergamot, lemongrass, epigallocatechin gallate, ginger, turmeric,plai, Ziziphora clinopodioides and grape seed were in the range of 55.12–91.11, 3.02–16.77 and 1.79–13.43, respectively (Nalinanon et al., 2008; Said et al., 2021; Tongnuanchan et al., 2013, 2015). The color of the films can also attribute from the natural coloring components of additives added such as in the study by Liu et al. (2019) have recorded as darker and reddish color as compared to single gelatin film. The L*, a*and b* color value for

intelligent marine's gelatin film has been observed at 75.55–90.35, 1.32–9.09 and -4.47–(-1.48), respectively.

Thermal properties of the film can be determined by using DCS analysis. The thermodynamic characteristics are useful in determining the quality of the films when it is found under different conditions such as temperature, gas pressure or atmosphere. Commonly from DSC thermograph, Tg can be obtained by measured the midpoint of the heat flow change at the glass transition in the first heating scan. Tg may be varied in term type of gelatin and incorporation of additives (Perazzo et al., 2014; Tongnuanchan et al., 2013; Weng et al., 2014). Inclusion of plasticizer in the gelatin-based film might reduce the Tg due to the hydrophilicity of glycerol that increased the water holding capacity in the gelatin later affected on the TS of the film (Sanyang et al., 2015a; Tongnuanchan et al., 2014). Hence, the determination of T_g is vital as it related with other characteristics and factorized by the chemical structure, moisture content and free volume.

Generally, fish gelatin films are generally developed from warm-water fish species because they are good in tensile, elongation at break, and water vapor permeability (WVP). The cold-water fish species usually have high hydrophobicity, while warm-water fish species show good hydrophilicity due to the high content of proline and hydroproline in their structure (Lv et al., 2019). Gelatin properties are affected by certain physical parameters that are involved in film processing, such as the inclusion of plasticizers (Nor et al., 2017), polymers (Soo & Sarbon, 2018) and cross-linker (Ramos et al., 2016b). The preparation of biobased film can be executed through casting or extrusion method (Said & Sarbon, 2022). Commonly casting methods have been widely used in the film formation process. The mechanism of gelatin film formation involves dispersing and solubilizing the gelatin in the solvents (water), which then is incorporated with either plasticizer or additives, cast onto the plates followed by drying (Jomlapeeratikul et al., 2017). The benefit of using the casting method for film preparation compared to other processes (extrusion) are lower production cost, greater film thickness uniformity, excellent dimensional stability and free from pinholes, gels, residual stress and superior optical properties (Suhag et al., 2020). Moreover, casted films also produced isotropic orientation in terms of mechanical and optical as the film was not stretched during the process. The solvent casting method is feasible only for laboratory scale rather than industrial as it requires longer drying time and shape and amount restriction (Said & Sarbon, 2022; Suhag et al., 2020).

Gelatin structure contains more glycine, proline and hydroproline residue, which on dehydration, conformational changes take place and may be utilized in the formation of the surface film (Bergo et al., 2010). Such films are strongest with the high availability of triple-helix content. Nevertheless, gelatin films present have limitations in brittleness and stiffness due to the extensive interactions between polymer molecules. Hence, to overcome these issues, a small percentage of the plasticizer can help to increase the hydrogen bonding and

improve the flexibility of the films. The addition of plasticizers does not only effects on the elastic modulus and other mechanical properties but also the resistance to permeation of vapor gas (Gómez-Guillén et al., 2009). Most of plasticizers are hydrophilic and hygroscopic, which can attract water molecules and form a large hydrodynamic plasticizer-water complex.

Plasticizers such as glycerol, sorbitol, and glycol are constitutive to make the films more flexible, softer and avoid pores and cracks in the polymeric matrix (Nur Hanani et al., 2014). Among all the potential plasticizers, glycerol is favored due to its stability and compatibility with hydrophilic biofilm apart from having high hygroscopic characteristics (Limpisophon et al., 2009; Nordin et al., 2020; Nur Hanani et al., 2014; Tongnuanchan et al., 2012). However, adding plasticizers can significantly change some properties, including reduced tensile strength (TS), increased film permeability to water, and increased water sorption capacity (Nur Hanani et al., 2014; Suderman et al., 2018). The amount of plasticizer added can cause an adverse effect on the films properties. Hence, the amount of plasticizer added must be used with caution. Based on some studies, 20-25% glycerol is required to plasticize gelatin film successfully (Nur Hanani et al., 2014; Pushpadass et al., 2008). It was previously reported that at 25% addition of glycerol in the film, maximum TS and optimum modulus of elasticity (Pushpadass et al., 2008). Moreover, the amount of plasticizer used in film formation should be small enough in order to avoid probable toxic effects.

Films with gelatin are hydrophilic which tend to retain water in their structure, which cause swelling and showing insufficient performance. The WVP of the packaging material can be used as a reference for the application of relatable food product. WVP also can be varied based on the chemical structure of the gelatin, plasticizer used and incorporation of other substances such as antioxidant. Based on the previous study showed that gelatin-films exhibit lower WVP ($6x10^{-13}$ – $2.5x10^{-10}$) compared to the bovine films (Hosseini et al., 2016; Hosseinzadeh & Ramin, 2018; Said & Sarbon, 2022; Tongnuanchan et al., 2014). This can be explained in terms of amino acid composition where by gelatin comprised higher constituent of hydrophobicity (lower proline and hydroproline contents). The hydroxyl group of hydroxyproline is normally available to form hydrogen bonds with water. Meanwhile, other study showed that incorporation of natural extracts such as ginger, turmeric, and plai into the film improve the water barrier properties of the film ($1.88 – 2.91 \times 10^{-11}$ $gm^{-1}s^{-1}Pa^{-1}$) (Tongnuanchan et al., 2013). These occurrences were due to the hydrophobic nature that exhibited by the essential oil which consequently increase the hydrophobicity of films and thus reduced the water vapor migration through the film.

2.4 Gelatin-based active packaging

The idea of active packaging started with changing the packaging from passive protection to active protection. In the past, primary packaging materials were known to be "passive", functioning only as inert shields to protect products from

moisture and oxygen. Several new packaging materials have recently emerged to provide 'positive' safety to products. Active packaging refers to the incorporation of specific additives into packaging systems that have the ability to maintain or extend product quality and shelf life. The active ingredient or ingredients can be incorporated directly into the packaging matrix, attached to the inside of the packaging material, or placed in a separate container such as a sachet within the packaging system (Kerry et al., 2006) as demonstrated in Figure 2.8.

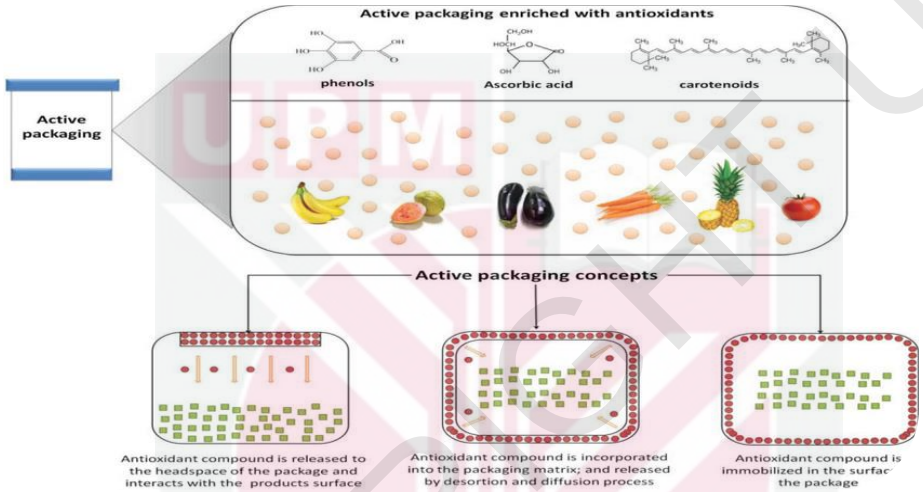

Figure 2.8: Active packaging models
(Source: Kerry et al., 2006)

Previously in Section 2.3, it has been discussed how gelatin exhibits good film-forming capacity. These excellent properties can be utilized to improve the shelf-life of food products by acting as an outer film that inhibits direct exposure of light and oxygen into the food material (Gómez-Guillén et al., 2009; Said & Sarbon, 2022b). The application of gelatin-based film can be extended by adding different additives and agents in the film matrix, which help enhance the physical, mechanical and biological properties of food products. Research on gelatin-based active film has opened the window on worldwide interest.

All active packaging technologies involve physical, chemical, or biological effects that alter the interaction between the package, product, and package headspace to achieve the desired result (Lee et al., 2008). Various active packaging systems have been established and developed, including oxygen and carbon dioxide scavenging, antibacterial and antioxidant activity. Active substances released from biopolymer packaging involve various mechanisms directly related to food or food analogues, such as melting, diffusion, swelling, and degradation (Said & Sarbon, 2022). The melting mechanism is based on melting the structural matrix

to release bioactive compounds. The diffuse release mechanism involves diffusion of the active ingredient through the micro- or macroporous structure of the polymer matrix and transport from the film surface to the food. Swelling behavior, on the other hand, means that the matrix must be placed in a compatible liquid or wet food if the diffusion coefficient of the active ingredient is low, and the matrix will swell when the liquid enters. On the other hand, polymer degradation, cleavage or deformation is accompanied by the release of decomposition or particle fracture (Quirós-Sauceda et al., 2014) .

In addition, appropriate packaging is one of the important methods used by growers to preserve, improve quality and extend the shelf life of their goods by controlling the oxygen inside the package. This is because fresh produce continues to be metabolized in large amounts after processing and spoils quickly. The respiration process still occurred even after harvested by using oxygen (O_2) from the environment to breakdown the carbohydrate which is glucose ($C_6H_{12}O_6$) and release carbon dioxide (CO_2), water vapor (H_2O) and energy.

$$C_6H_{12}O_6 + 6\ O_2 \longrightarrow 6\ CO_2 + 6\ H_2O + \text{energy} \qquad \text{Equation 2.1}$$

Fresh produce with very high respiration rates such as mushroom, strawberries, broccoli and asparagus require high permeable films (Wilson et al., 2018). The package should be able to control transmission of water vapor or gases to maintain the freshness and quality of the products. In order to slower the respiration rate of the fresh vegetables without harming it taste, texture and appearance, the level of the oxygen in the packaged need to be in lowest level. Hence, oxidation might trigger the enzymatic oxidation of phenolic compounds, resulting in brown color substances forming (Jiang et al., 2016). This phenomenon is called enzymatic browning. Enzymatic browning is the second largest cause of quality of fresh fruits and vegetables. The successive stages of fresh fruit and vegetables handling, transportation and marketing entail different needs and therefore place differing demands on the packaging. One of the most effective means of removing oxygen from the package is the inclusion of antioxidants in the packaging material. Active packaging refers to incorporating certain additives into the packaging systems to remain or extend the product quality and shelf life.

Recent research showed that gelatin-based film used as food packaging has been making improvements in various types of food products including fruits (strawberry, fresh apples cut, banana) and fresh vegetables (tomatoes) (Said & Sarbon, 2022) It has been proven that gelatin as an additional protective layer for fresh products by increasing the shelf-life.

2.5 Antioxidants agent in active gelatin-based film

Antioxidants are incorporated in packaging materials that greatly delay or avoid oxidation of that substrate when present at low concentrations compared to those of an oxidizable product (Halliwell & Gutteridge, 2015). This antioxidant activity occurs as antioxidants migrate to the surface through the bulk of the polymer.

The reaction chain of antioxidants can be seen from equation 2.2 to 2.6, which is often caused by the presence of oxygen and free radicals. Antioxidants can impede the oxidation process by scavenging the oxygen species or terminating the free radical chain reaction. In a chemical system, the strength of an antioxidant can be evaluated by examination of its ability to scavenge free radicals and thereby terminate the chain reaction. The termination of a chain reaction by an antioxidant is shown as follows (Kamal-Eldin & Pokorn, 2005).

$X\bullet + RH \rightarrow R\bullet + XH$ Equation 2.2

$R\bullet + O2 \rightarrow ROO\bullet$ Equation 2.3

$ROO\bullet + RH \rightarrow ROOH + R\bullet$ Equation 2.4

$R\bullet + AH \rightarrow RH + A\bullet$ Equation 2.5

$R\bullet + A\bullet \rightarrow RA$ Equation 2.6

Where X• = oxidizing agent; RH = substrate; AH = antioxidant

Hydrogen atoms are moved from a substrate to an oxidizing agent with free radical (R) development during the oxidation processes, which are usually very unstable and can easily react with oxygen to form peroxyl radicals (ROO•). The resulting peroxyl radicals react with other compounds to obtain the required hydrogen atoms. The new molecule loses an atom of hydrogen when struck by free radicals and becomes a free radical in a chain reaction in Equation 2.4. Antioxidants remove free radical intermediates and terminate these chain reactions by donating electrons or hydrogen atoms to the free radicals, as in Equation 2.5, and/or by combining with the free radical in Equation 2.6. The antioxidant radical (A•) produced as a consequence of hydrogen loss is generally much more stable, and the chain reaction will not proceed. Antioxidants are also reduction agents because they are electron or hydrogen donors. Antioxidants shield other materials from damage by free radicals as a "sacrificial" reactant.

2.5.1 Intrinsically conducting polymer (ICP)

Intrinsically conducting polymers with the combination of electrically conducting materials are a comparatively current class of novel organic materials with typical characteristics of conventional polymers (Holze, 2011). Usually, they are

insulating, have metal electrical and optical properties, thus maintaining the mechanical properties of conventional polymers. Typically, ICPs have π-conjugation along the backbone of the polymer, which has single and double bonds that are the basis of their conductivity. Polyaniline, poly(3,4-ethylenedioxythiophene) and polyacetylene are examples of ICP.

PANI is generally considered to have the optimum combination of stability, high conductivity and low cost (Cao et al., 1992; Min, 1999; Pud, 1994). The antioxidant capability of ICP polymers was reported by Ismail et al. (1998), they evaluated the ability and performance of PANI in protecting styrene butadine rubber vulcanizes against oxidation deterioration.

2.5.2 Polyaniline (PANI)

Polyaniline (PANI) is a representative of the conducting polymers distinguished by easy synthesis and high environmental stability. PANI consists of monomer units built from reduced benzenoid amine (y) and oxidized quinoid imine (1-y) blocks, as shown in Figure 2.9:

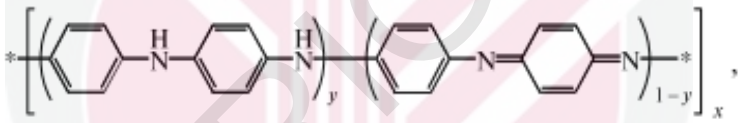

Figure 2.9: Chemical structure of PANI

where 0≤ y ≤ 1 (Boeva & Sergeyev, 2014). Chemically, as shown in the figure, PANI is a polymer based on phenylene with -NH groups on either side of the phenylene ring. This -NH group will undergo oxidation, allowing the PANI to exist in a continuum state (Palaniappan & John, 2008). The redox state of the polymer can be determined by the value of y: at y=0.5, PANI occurs in the form of emeraldine; y=0 corresponds to the fully oxidized form, pernigraniline, while y=1 correspond to the fully reduced form, leucoemeraldine (Figure 2.10) (Beygisangchin et al., 2021; Scherr et al., 1991). Leucomeraldine is a colorless substance that can slowly oxidize in the air and not electrically conducting (Boeva & Sergeyev, 2014). Meanwhile, pernigraniline is composed of alternating aminobenzene and quinod imine fragments. Quinod imine group is unstable in the presence of nucleophiles, specifically water will affect pernigraniline and its salt stability to decompose in the air. The emeraldine salt of PANI is formed during the protonation of the emeraldine base with organic and inorganic acids.

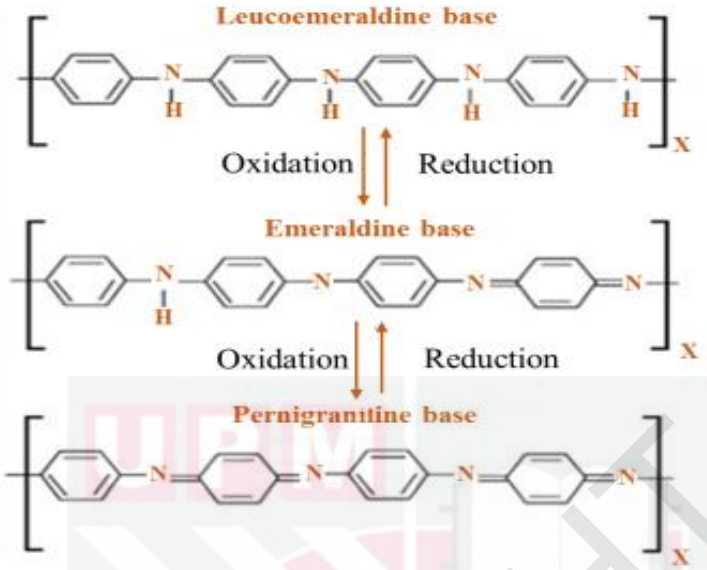

Figure 2.10: Basic PANI in three dissimilar types ($0 \leq x \leq 1$)
(Source: Beygisangchin et al., 2021; Gospodinova & Terlemezyan, 1998).

2.5.3 Synthesis of PANI

PANI can be prepared via chemical or electrochemical polymerization of aniline. Several factors need to be considered in the procedure, such as the temperature and the time regimes, the types of oxidant, dopant, and solvent, the voltage applied on the electrode etc (Boeva & Sergeyev, 2014). These will affect the PANI structure, morphology and redox state. However, chemical synthesis is the preferred technique for obtaining large quantities of PANI. Moreover, the chemical polymerization technique is the simplest way to prepare PANI with various physicochemical properties and supermolecular structures.

In the mechanism of oxidative polymerization of aniline, the aniline dimer is formed through the reaction of an anilium cation with aniline (Altamirano et al., 1994; Genies & Lapkowski, 1987; Liau et al., 2006). Then, the dimer is oxidized via a single two-electron step to quinoidal diamine form. It is because its lower oxidation potential in comparison with aniline leads to the formation of the polymer (Mohilner et al., 1962; Wei et al., 1989). The polymerization of aniline is efficient in acidic conditions by which the aniline exists as an anilinium cation.
The use of various oxidants conducts the chemical polymerization of aniline ammonium persulfate (APS) is the most commonly used (Boeva & Sergeyev, 2014; Stejskal & Gilbert, 2002). The polymerization process is usually carried out in acidic conditions, and several organic and inorganic as well have been used for chemical synthesis of PANI. The product is the corresponding acid-doped emeraldine salt form of PANI.

The commonly used synthetic antioxidants in food applications are butylated hydrxoytoluene (BHT) and butylated hydroxyanisole (BHA), which currently interest in the use of α-tocopherol, L-ascorbic acid, L-tyrosine, carvacrol and aromatic plant extracts as replacement (Nand et al., 2012; Robertson, 2008). This is due to the consumer preference for natural food ingredients that have shifted to natural antioxidants. Even though natural antioxidants have lower antioxidant activity than synthetic antioxidants, due to availability and acceptance by health authorities, they positively affect the sensory properties and act as preservation agents which are easily accessible (Shafiur Rahman, 2007).

2.5.4 PANI based polymer substrate

PANI has been successfully utilized as a solid antioxidant requires blending with commercially available polymers with suitable mechanical properties and processability. Several techniques have been used in preparing PANI containing polymer substrates, such as solution blending, melt processing, surface deposition and surface grafting. Solution blending is preferable for the lab scale purpose, incorporating PANI into the biopolymer matrix. In the previous study, PANI has been incorporated in several matrices such as polyvinyl alcohol, polyethylene, polystyrene, low-density polyethylene, chitosan and starch to produce conducting polymer (Annala & Löfgren, 2006; Azmi et al., 2019; Bhadra et al., 2017; Nand et al., 2012; Saikia et al., 2010; Yavuz et al., 2009; Zareh et al., 2011). Figure 2.11 shows the applications of PANI in the food industry. PANI can be incorporated into the polymer substarte and being used widely as electric nose, biodegradable food packaging, active food packaging and intelligent food packaging due to the several characteristics of PANI such antioxidant, antimicrobial, sensor and others (Chia et al., 2022).

Figure 2.11: Application of PANI in food industry
(Source: Chia et al., 2022)

The compatibilization of polyethylene/polyaniline (PE/PANI) blends, and the preparation of plasticized PANI/camphorsulfonic acid (CSA) complexes suitable for melt blending were studied by Annala & Löfgren (2006). Through the study, significant findings were found where the mechanical properties of the PE/PANI blends were improved and increased with the addition of functionalized metal-locane polyethylene. In addition, this study also developed plasticized PANI/CSA complex and showed good electrical conductivity.

PANI has also shown compatibility with starch and synthesized using oxidative polymerization of PANI in an aqueous dispersion of starch isolated from Colocasia esculenta corn (Saikia et al., 2010). This study was found from the

SEM image the growth of PANI on the surface of the starch granules. The developed composite also successfully shows antioxidant activity by using DPPH scavenging analysis. Composite possesses an antioxidant nature which increases with the concentration of polyaniline. The materials show great potential for biomedical applications.

Polyethylene terephthalate (PET) was blended with a nanorod form of polyaniline (NR-PANI), formed by a falling pH synthesis, were prepared by dispersion in a melt of PET at 265 °C (Nand et al., 2012). Optical microscopy showed an even distribution of NR-PANI particles within the PET matrix. The blends were characterized using FTIR, XPS, DSC and DMTA. While the PET glass transition temperature was not changed, the degree of PET crystallinity was increased with the addition of NR-PANI. With higher NR-PANI loading in the matrix, PET's electrical conductivity and capacity to scavenge free radicals both improved. However, when NR-PANI loading increased, the mechanical characteristics of PET decreased, indicating insufficient interfacial adhesion between the NR-PANI particles and the PET matrix.

Other study on the compatibility of PANI was done by substituting PANI with chitosan. The composites were chemically synthesized by measured conductivity, FTIR, UV-vis, SEM and TGA techniques. The composites obtained showed higher conductivity, thermal stability and agglomerated granular morphology can be seen through SEM.

In the work by Bhadra et al. (2017), it has been presented exclusively on the effect of feeding ratio of the aniline on the structural, thermal, mechanical and electrical properties of PANI and polyvinyl alcohol (PVA) blends. The morphological analysis reveals a heterogenous distribution of conducive PANI particles in the PVA. The tensile strength (TS) of the blends remained unchanged as the aniline concentration increased. The conductivity of the blends was also increased.

Evaluation of the effect of concentrations and size of PANI loading into the starch film was done by Azmi et al. (2019). The composites showed favorable mechanical properties and antioxidant activity at different concentrations and size of PANI. Based on the FTIR spectra, the starch/PANI film spectra were similar to the starch/glycerol without PANI. However, one notable weak pick near 1455 cm^{-1} can be found in sample B and C.

Recently, a study has been conducted in developing chitosan-polyaniline nanocomposite film that prepared with different concentration of PANI at various synthesis times (Pirsa & Mohammadi, 2021). The developed chitosan-PANI nanocomposite film reduced in transparency which became advantageous in package products that are susceptible to oxidation in the light. The result also indicated that the by increasing PANI concentration and synthesis time, it cause

reduction in water solubility and water vapor permeability. These characteristics is important in expanding the usage in food application. By using chitosan as matrix, PANI also has proven to improve the mechanical properties, electrical conductivity, and antimicrobial activity in other study by Mohammadi et al. (2019). It has been found that PANI-coated PMMA/CNC showed slight antioxidant strength.

PANI has been exploited for its electrical conductivity; however, its application as a solid antioxidant is an emerging field of study. Yet, PANI is to be applied in active food packaging systems. PANI based active packaging system have a huge potential in food packaging applications as the food packaging industry continuously need improvement in packaging systems.

2.5.5 Determination of antioxidant capacity

There were several methods used to determine the antioxidant capacity of active substances. These can be based on the metal-reducing agents (Yadav & Bhatnagar, 2007), quantification of products formed during lipid peroxidation (Siriwardhana et al., 2014) and various free radicals scavenging activities (Aruoma, 2003; Frankel & Meyer, 2000; Sánchez-Moreno, 2002). The most common methods used are free radical scavenging methods to evaluate the antioxidant activity of the active compounds due to their simple, faster, sensitive and reproducible nature. The antioxidant activity of PANI that is characterized using free radical scavenging activities is attributed to its ability to switch easily between the reduced and oxidized states. PANI with a lower formal potential, act as strong reducing agents when it in contact with free radicals to neutral species (Marija Gizdavic-Nikolaidis et al., 2004; Hsu et al., 2008). Commonly the most used methods to assess the free radical scavenging capacity of PANI using $DPPH^{\bullet}$ (1,1-diphenyl-2-picrylhydrazyl) (M. Gizdavic-Nikolaidis et al., 2004; Marija Gizdavic-Nikolaidis et al., 2004; Saikia et al., 2010) and $ABTS^{\bullet+}$ (2,2-azino-bis(3-ethylbenzothiazoline--sulfonic acid) assays (Hsu et al., 2011). The $DPPH^{\bullet}$ and $ABTS^{\bullet+}$ radicals are colored but are decolorized upon reduction. The extent of free radical reduction on the degree of decolorization can be measured by UV spectrophotometry.

The DPPH assay is based on electron transfer (ET) between two constituents, the antioxidants and the blue colored DPPH• radical (a weak oxidant). This method evaluates the reducing ability of antioxidants towards $DPPH^{\bullet}$. $DPPH^{\bullet}$ will accept an electron from the antioxidant when the ET reaction takes place, which causes a color change in the system, and the rate and extend of color loss provide a measure of the efficiency of the antioxidant. The test procedure protocol for DPPH analysis is suitable for 24 hours of reaction time before the final reading is taken. DPPH assay also involves a hydrogen atom transfer reaction consisting of a fast electron transfer process and a slow hydrogen atom transfer reaction from antioxidants to DPPH radicals, especially when the reactions occur in strong hydrogen bond-accepting solvents such as methanol

and ethanol. One of the advantages of this method is $DPPH^{\bullet}$ is quite stable organic nitrogen radical and does not have to be generated before use.
The other determination of antioxidant activity method is by using the ABTS assay. ABTS assay is also an ET-based method. This is simple in terms of its operation. In this method, the blue/green ABTS radical is formed through the reaction between ABTS and ferrymyoglobin radical species. During the reaction, ABTS donates an electron to the ferrymyoglobin radical, changing to $ABTS^{\bullet+}$ radical and regenerating metymyoglobin. One of the disadvantageous of ABTS radical is cannot be found in biological systems and only represents a 'nonphysiological' radical source.

2.5.6 Biocompatibility of PANI as antioxidant

PANI has always been treated with extra precautions as the aniline monomer, and subsequent polymerization intermediates, such as aniline dimmers and oligomers can be potentially active. It is due to the threat of carcinogernic effect of benzidine, the aniline dimer. Fortunately, after removing low molecular weight polymerization products, purified PANI has been proven to be biocompatible and non-cytotoxic (Humpolicek et al., 2012). Other studies have confirmed that PANI is biocompatible and non-cytoticity.

Previously, Kumar et al. (2010) have demonstrated the biocompatibility of heavy ion irradiated PANI nanofibers by studying their haemolysis prevention activity. In the study, the PANI showed reduced potency to damage blood cells and enhanced hemolysis prevention activity. The other study by Kamalesh et al. (2000) assessed the biocompatibility of PANI through subcutaneous implantation into rats and concluded that the films were biocompatible. Moreover, other studies on polymer composites (Dispenza et al., 2006; Kim et al., 2009; Prabhakar et al., 2011) and hydrogels (Dispenza et al., 2012) incorporated with PANI has also been found to be biocompatible. As a priority consumer concern, the biocompatibility and non-cytotoxicity of PANI gives advantageous for applications such as food packaging where it will be in contact with food stuff.

2.6 Self-healing materials and behavior

Exposure to harsh environments during storage and transportation processes due to microcracks can degrade the polymer material and product inside the package (Fainleib & Purikova, 2019). Damage deep within the film material is difficult to detect and especially difficult to repair, so the material must be capable of repair. In recent decades, various types of self-repairing materials have been developed and inspired by the healing phenomenon of natural organisms. A polymer with self-healing properties needs to convert physical energy into a chemical and/or physical response capable of healing a damage-a mechanism

that is not typically present in "convectional non-self healing polymers" (Binder et al., 2013). The healing process can be divided into autonomic or non-autonomic, related to the requirement of external stimulus such as heat or water. If no external stimulus is required and the healing agent has to be pre-embedded then the mending is called autonomic, whereas its triggering with additional treatment when polymers are able to heal cracks by themselves (heat) is called non-autonomic (Fainleib & Purikova, 2019).

Much literature is related to self-healing material (Aïssa et al., 2012; Andersson et al., 2009; Fainleib & Purikova, 2019; Mauldin & Kessler, 2010). The self-healing materials could generally be divided into two categories: intrinsic self-healing materials and extrinsic self-healing materials (Fainleib & Purikova, 2019). The intrinsic self-healing materials depend on the non-covalent of the materials, for example, the type of hydrogen bonding, hydrophobic interactions, and electrostatic attractions. The mechanism is due to the physical, and/or chemical interactions. On the other hand, extrinsic self-healing materials depend on healing agents embedded in the material matrix in advance during the manufacturing of the material.

The self-healing mechanism can be involved in various interactions on bonding, including hydrogen bonding, Schiff base linkage, hydrophobic interaction, electrostatic interactions, reversible covalent bonding and encapsulated healing agent. Based on the study on polysaccharide film layered with acrylamide-modified chitosan and alginate aldehyde, the excellent self-healing ability of the films could be due to the water-induced swelling and high mobility of the polymer network that facilitate the reconstruction of Schiff base linkage underwater assistance (Hu et al., 2018). The film can be healed several times due to the more free amino groups and aldehyde groups in the thicker film, which improved the repeated damage-healing property of the film. In terms of hydrogen bonding, it is one of the non-covalent bodings which forms between the hydrogen atom ad another atom. In 2015, Zhang & He, prepared the hydrogen bonding assisted self-healing using partly cross-linked poly(vinyl alcohol) (PVA) and poly(acrylic acid) (PAA). By designing the molar ratio of hydroxyl groups to carboxyl groups, the cross-linked polymer thin film can maintain abundant hydroxyl groups at the scratched interfaces to reform H-bonds across the interfaces. Other studies by Haque et al. (2011) prepared a lamellar structure hydrogel with a soft network of hydrophobic interactions. Hydrophobic interactions describe the entanglement of the aliphatic molecular chains, and it was found that a double network polymer consists of a weak and a strong network.

Previously, Wool & O'Connor (1981) proposed five stages of crack healing that involve (a) surface re-arrangement; (b) surface approach; (c) wetting; (d) diffusion and (e) randomization. That approach has been proven successful in separating the multi-convoluted time dependencies of the different mechanisms controlling crack healing and their underlying molecular processes and being strongly related to molecular interdiffusion at or above the glass-transition temperature, T_g. It was also in agreement with the study by (Kausch & Jud,

(1982)whereby they observed that the development of the mechanical strength during the crack healing process of glassy polymer is related to inter diffusion of the molecular chains and subsequent formation of molecular entanglements.

2.6.1 Hydrogen bonding

A hydrogen bond is one type of reversible non-covalent relationship that can develop between a hydrogen atom and another atom. Recently, gelatin-based adhesive hydrogel has been developed with self-healing ability. The gelatin was functionalized by dopamine to form dopamine grafted gelatin (GelDA). Then, it was mixed with 1,4-phenyleneisboronic acid and graphene oxide (GO) obtained by horseradish peroxidase catalytic system. Based on the healing properties, the behavior was attributed to the coordination bond between the catechol groups and boronic groups (Narkar et al., 2016), the hydrogen bonds between catechol groups and the π-π stacking between catechol groups and GO (Tu et al., 2019). The hydrogel developed has great potential applications in both multifunctional wound dressing and the booming developed wearable devices in the medical field.

Chen et al. (2019) prepared the hydrogen bonding assisted self-healing polymer composited reinforced with graphene oxide. The polymer matrix was based on amino-terminated hyperbranched developed by dimer acid and diethylene triamine, and graphene oxide is synthesized by the modified Hummers methods. From the findings, the composite materials suffer damage, the hydrogen bond tends to break first due to the weak strength, which the non-associated groups will appear in the fractured area, and the new hydrogen bonds can be produced again at room temperature. As also proven in the study, the composite polymer is an intrinsic self-healing polymer with infinite healing cycles.

Another study by Cordier et al. (2008) prepared the hydrogen bonding assisted self-healing rubber by synthesizing fatty acid and urea. In the fatty acids components made of vegetable oil composed of carboxylic acids functional group, and urea consists of the amine group (N-H). The C=O groups in the COOH played a role as hydrogen bonding acceptors, and N-H groups were the hydrogen bond donor. These two groups tend to produce strong hydrogen bonds in the materials when they combine. The samples were divided in half for the investigation and then brought together for certain healing intervals. The re-association of hydrogen bonding at the cutting surfaces was thought to be the cause of the self-healing behaviour. In fact, it was found that the self-healing ability was affected by the healing time. When there is a time delay before the cut touch each other, the self-healing ability will be decreased. This was most likely due to the creation of pairs between the free hydrogen bonding acceptors and donor within each part of the cut specimens. The hydrogen bonding can help generate another covalent bonding which is π-π stacking (Xu et al., 2010). Sufficient of free hydroxyl groups that appear at the cut interfaces of the materials increased the self-healing efficiency. The smart design approaches in the study

of Zhang et al. (2014) by fabricating partly cross-linked poly(vinly alcohol) (PVA) and poly(acrylic acid) (PAA) with the designated molar ratio of hydroxyl group to carboxyl group, kept abundant of free hydroxyl groups to facilitate later in the healing process (Zhang et al., 2014).

pH value was also found to be influenced by self-healing ability. In the study by Phadke et al. (2012) prepared a rapid self-healing material using acyrloyl-6-aminocaproic acid (A6ACA). The hydrogen bonding of this material was formed by the COOH groups, which acted as both acceptors and donors. This material lost the self-healing ability when the pH value was higher than the ionization points of COOH groups. The phenomenon was due to the COOH that deprotonated to be COO^- and lost the function of hydrogen bonding donors. However, in an acid environment COO^- can be protonated when the pH value is less than the ionization point of COOH groups. Thus, the self-healing ability of the materials can be restored.

2.6.2 Hydrophobic interactions

Hydrophobic interactions refer to the entanglement of the aliphatic molecular chains. Based on the study by Sharma et al. (2017) that has demonstrated at room conditions the iongels consist of 1-ethyl-3-methylimidazolium chloride (1L) solutions made through the thermal treatments showed self-healing properties after they were cut using a surgical blade. The healing process does not need any stimuli to trigger the process. The healing mechanism was based on the rejuvenating of their network structure via hydrophobic interactions between the aliphatic hydrocarbon chains of the two gel pieces. The hanging hydrophobic tail of 1L will immediately form any overlapping junction in creating the water depletion regions, facilitating the healing. Thus, the healing is mostly governed by hydrophobic interactions.

Furthermore, the potential reversibility of hydrophobic interactions would be utilized in the creation of the self-healing material. A self-healing hydrogel has been prepared via the polymerization reaction of large hydrophobic stearyl methacrylate with a hydrophilic in the presence of sodium dodecyl sulfate (SDS) as surfactant. The samples were observed to be stretched to a strain similar to the original samples and exhibit self-healing at room temperature. It was revealed that SDS plays a significant role in the self-healing ability of the samples. It was due to the SDS increases the solubility of the hydrophobic interactions, which generates the reversible cross-linked (Akay et al., 2013).

Furthermore, in the surfactant structure, the length of alkyl chains also affected the mechanical strength and self-healing ability of the polymer. The self-healing ability was shown with samples with 18 carbon atoms in the alkyl chains (Tuncaboylu et al., 2012). It was associated with a structure that achieved a favorable equilibrium between the flexibility of the molecular chains and the

accessible hydrophobic interactions. The hydrophobic interactions also react with the hydrogen bonding to enforce each other (Song et al., 2013). The polymer synthesized with the stearyl methacrylate with the poly(acrylic acid) demonstrated an elongation of up to 5 mm/mm (Gulyuz & Okay, 2013). This polymer showed a strong self-healing ability with an efficiency of 80% when the temperature rose to 80 °C after 30 minutes. This was due to the synergy between the hydrogen bonding and the hydrophobic interactions (Phadke et al., 2012).

2.6.3 Influential factors of self-healing

Generally, the main functional properties of hydrophilic materials, such as gelatin are strongly dependent on their water content. The adsorption of water vapor by the dried film normally involves the binding of the water molecules to specific hydrophilic sides, such as carboxylic, amino and hydroxyl residues in addition to the backbone of peptide groups at lower humidities (Cuq et al., 1997) . Meanwhile at higher relative humidity, multimolecular adsorption is by swelling and changes in the macromolecular structural. As a good food packaging material, knowledge of the barrier properties, including water sorption of the film is much needed and important as it leads to the final applications of the film. Moisture contents play a vital role in determining the performance of the film as food packaging. This is because moisture is transferable element that can pass through the film either by adsorption or desorption and instantly may affect the properties of the film and packaged product (Bourlieu et al., 2009).

A mathematical modelling was developed previously by Zemskov et al. (2014) for bacterial self-healing of cracks in concrete by using Galaerkin finite element method in understanding and monitoring the healing process of the concrete using bacteria as a catalyst agent. Another study by Li et al. (2013) proposed using water absorption in monitoring and characterizing the crack network and void in the healing process as the prime driving force for absorbing the water as it greatly affects the healing process. A water absorption test can also be vital in characterizing and evaluating the scratch film's healing process. This is because the process involves releasing, gradually filling and repairing the film back (Li et al., 2013).

2.6.4 Sorption analysis and isotherm

Permeability is the process that involves absorption (dissolution) of low-molecular-weight gas or water vapor onto the side of the polymer film, followed by diffusion through the film and finally by desorption from the other side. Several factors influence the amount and rate of moisture that can transfer or diffuse, such as temperature and relative humidity (Basha et al., 2021; Othman et al., 2017). These factors need to be controlled to ensure the efficiency of the edible film as well as the integrity of the products. Hence, in this present study, water

sorption analysis is considered as one of the vital parameters in developing self-healable packaging films with excellent properties.

The study on sorption isotherm provides information regarding the moisture-binding capacity of samples under different relative humidity at different temperatures. It is also useful in analyzing the moisture plasticizing effect and its effect on mechanical properties (Al-Muhtaseb et al., 2002). Furthermore, the sorption isotherm of bio-plastic can also be used to study and predict the stability and quality changes during the packaging of food products (Srinivasa et al., 2003).

The moisture sorption isotherm model is useful to forecast the water sorption characteristics of a material under certain circumstances. Moisture sorption isotherm represents the sorption behavior of the material in a graphical method. It is able to describe the relationship between the equilibrium moisture content of the material and water activity at a constant temperature. Using moisture sorption isotherm can effectively evaluate the effect of temperature and relative humidity on sample properties (Cadden, 1988; Lai & Padua, 1998). There were several isotherm models can be fitted using the experimental data, such as Peleg, Guggenheim Anderson de Boer (GAB), Smith, Halsey, Osmin and Henderson model (Andrade P et al., 2011; Basha et al., 2021; Saberi et al., 2015).

For the moisture sorption kinetic study, Suppakul et al. (2013) proposed a method in which the samples were conditioned in a desiccator for three days of silica gel to reduce initial moisture content before placing it over saturated salt solutions with different relative humidity. The weight of the samples was determined as a function of time while the moisture content was determined by drying them in an oven at 105^{o}C for 3 hours. Then, moisture adsorption curves of samples were obtained from the data and fitted to a mathematical model named Peleg Model to investigate the sorption kinetic of film.

Peleg Model is mainly used for moisture sorption kinetic study. The water absorption of bio-based films over a period can be determined by using the equation proposed by (Peleg, 1988):

$$M_t = M_i \frac{t}{K1+K2t} \qquad \text{Equation 2.6}$$

Where, M_t is a moisture content at a known time, (% dry basis), M_i is an initial moisture content, (% dry basis), t is a the water absorption time, (in hour), and, K_1 and K_2 are Peleg constants. By rearranging the equation gives:

$$\frac{t}{Mt-Mi} = K_1 + K_2 \qquad \text{Equation 2.7}$$

From the plot of t/(Mt-Mi) versus t, a straight line was obtained with K_1 as intercept value while K_2 is the gradient of the graph. The characteristic of Peleg's constant was determined from the plot.

The most well-fitted isotherm model that is commonly used in many studies for the moisture sorption analysis of film is the GAB model (Bajpai et al., 2017; Coupland et al., 2000; Cuq et al., 1997; Othman et al., 2019; Othman et al., 2017). Fitting the experimental data in the isotherm model will provide information on the quantities of the water that is strongly adsorbed to the specific sorption site of the film and the number of the sorption sites. In addition, the isotherm model also states the monolayer moisture content which corresponds to the minimum moisture to avoid autooxidation and to improve the stability of the films (Othman et al., 2019).

2.7 Summary

As a replacement for petroleum-based packaging materials that are not biodegradable and have a detrimental influence on the environment, the creation of biomass material has been employed incredibly and efficiently. Biomass materials, as opposed to synthetic ones, provide environmental safety, non-toxicity, environmental stability, and a host of attractive physico-chemical properties. This chapter reviewed some of the biomass materials from different sources. Previous researchers have come to an interest in extracting gelatin from different animal sources as an alternative to biomass materials, including fish. From the fish processing, the by-product generated was abundant and rich in protein content for gelatin extraction. Fish processing by-products include bones, skin, and scales. Fish scales have become an attention interest nowadays due to their high protein content and good film-forming ability. Gelatin has also shown good compatibility as an active film, incorporating antioxidants as active substances. Previously, PANI has been utilized as an active substance (antioxidant) in different fields with high antioxidant efficiency through DPPH analysis. Most of the studies used in-situ methods to incorporate PANI into the matrix, and numerous studies have applied solid PANI into the gelatin-based film. Further study on the effect of size and concentration of PANI loaded into the gelatin-based film on several characteristics has been suggested in this study to be further investigated.

Gelatin with high content of hydrophobic amino acids, including glycine and hydroproline has been proven to be excellent and gives good structural characteristics to the film. It also has been reviewed that these properties help in the self-healing behavior of the gelatin-based film. One of the influential factors affecting the properties of the gelatin-based film is the water sorption ability of the films. The phenomenon of self-healing is known to be related with

the stimuli of water. To date, there is still no study on the effect of the self-healing ability of the PANI/gelatin-based film at different surrounding conditions, including RH and temperature.

In order to facilitate future food packaging applications, it was therefore required to develop a self-healing PANI/gelatin-based active film. Thus, improved knowledge will be provided on the self-healing behavior of PANI/gelatin-based film with the understanding of the non-covalent bonding process related with the water sorption activities at different surrounding conditions (relative humidity and temperature).

CHAPTER 3

METHODOLOGY

3.1 General experimental plan

The experiments were conducted in four major phases, as shown in Figure 3.1. The first and second phases are related to the first goal. The first step involves extracting gelatin from the red tilapia's fish scale and calculating yield as well as physical, chemical, and morphological properties. The research then moved on to the second stage, which involved the preparation of a red tilapia fish scale gelatin-based film with the addition of 25% (w/w of the gelatin) glycerol as a plasticizer, which was then characterised for physical, chemical, morphological, mechanical, thermal, and barrier analysis. Following the successful preparation of the gelatin-based film, the third step of the research focused on developing an active bio-based film by inserting PANI as an active ingredient in the gelatin matrix. The PANI/gelatin-based film was developed at these step in terms of the sizes and concentrations of PANI put into the film. The physicochemical properties and antioxidant activity of the PANI/gelatin-based film were assessed. The last part of the research focussed on the efficiency and behaviour of the PANI/gelatin-based film in terms of self-healing characteristics. This step comprises an examination of the various variables (temperature and relative humidity), which were then documented and discussed based on the film's water sorption analysis.

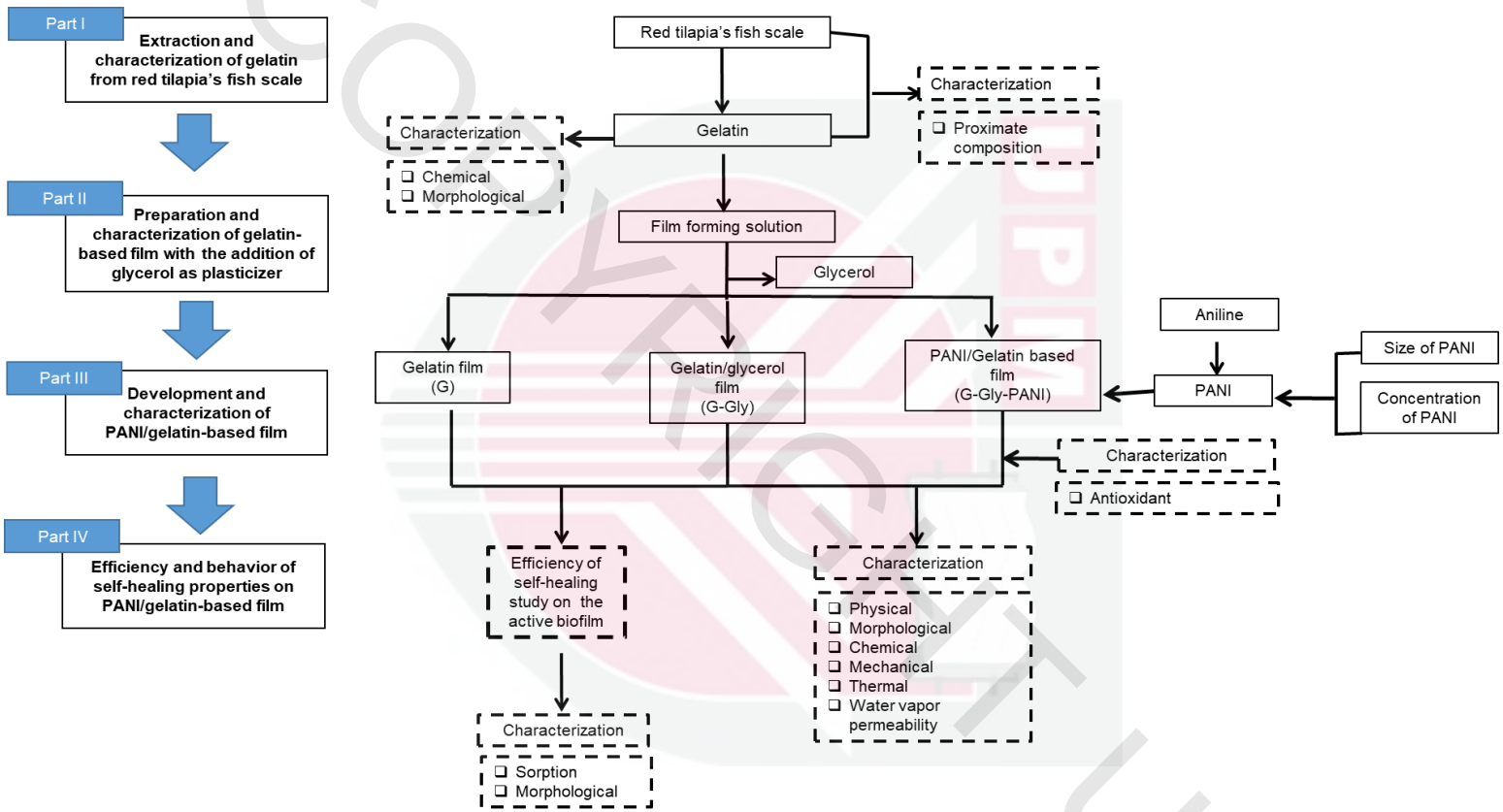

Figure 3.1: Research flow chart

3.2 Extraction of gelatin from red tilapia's fish scale

A red tilapia fish scale was bought at a local wet market in Pahang, Malaysia, and delivered to the laboratory in a plastic bag. When the fish scale arrived at the laboratory, it was maintained frozen at -20 °C in the freezer (Elba, Fiamma Sdn. Bhd., Malaysia) until further processing. The scales were properly cleansed and rinsed before being utilised for gelatin extraction to eliminate debris and leftover blood. Proximate analysis was used to determine the chemical composition of the fish scale.

Figure 3.2 shows the extraction process of the gelatin from the red tilapia's fish scale. Gelatin was extracted according to the procedure of Limpisophon et al. (2009) and Weng & Wu (2015). First, the scales were washed to remove the dirt. Then, the scales were soaked in a solution containing 0.05M sodium hydroxide (NaOH) (R & M chemicals, Ever Gainful Enterprise Sdn. Bhd., Malaysia) and 25% of methanol (Systerm, Chemar, Malaysia) with a ratio of scale:solution is 1:4 (w/v) at 10 °C for 24 hours to remove the lipid, pigments and non-collagenous proteins. Alkaline treated scales were then washed again. The scales were then soaked to five time volumes of 0.05M hydrochloric acid (HCl) (J. T. Baker, Avantor Performance Materials, Inc., Pennsylvania) for 2 hours at room temperature for the demineralization of the scales. After that, the swollen scales were washed thoroughly with clean water. After the pre-treatment, the swollen scales were soaked in distilled water at 80 °C for 1 hour to extract the gelatin. The mixture was centrifuged (Universal 320, Hettich GmbH & Co., Canada) at 15,000xg for 30 min. The supernatant of gelatin extract was freeze-dried, Then, the yield of the gelatin powder obtained was calculated and stored at -20 °C in the freezer (Elba, Fiamma Sdn. Bhd., Malaysia) until further use.

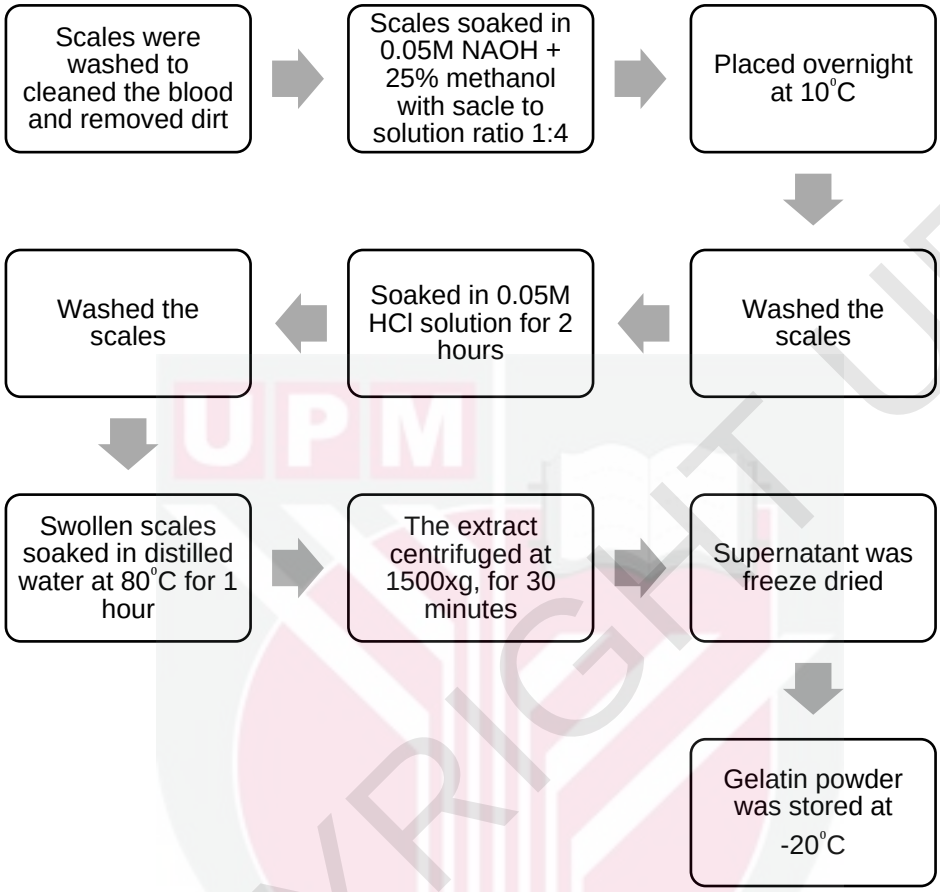

Figure 3.2: The process flow of gelatin extraction from red tilapia's fish scale

3.3 Preparation of gelatin-based film

The gelatin films were developed using the same protocol for the solution casting method as mentioned by González et al. (2016) with some modifications on the heating temperature and stirring time. The film-forming solution for the gelatin-based film without glycerol (G- film) was prepared by dissolving 2% (w/v) of the freeze-dried gelatin in 60 °C distilled water for 30 min with continuous stirring. As for the gelatin-based film with glycerol as plasticizer (G-Gly film) 25% (w/w of the gelatin) glycerol (Sigma Aldrich, Sigma Aldrich (M) Sdn. Bhd., Malaysia) was added into the film-forming solution. 25% (w/w of the gelatin) of glycerol was selected based on the previous studies (Nur Hanani et al., 2014; Pushpadass et al., 2008) due to the maximum TS and optimum of elasticity with the suitable limit to avoid probable toxic effects. Then, the solution was sonicated using an ultrasonic probe (Q500, Qsonica L.L.C., USA) for 10 minutes (Chang et al.,

2010) to remove the air bubble. The film-forming solution was cast into 14 cm internal diameter petri dishes resting on a level surface for casting and were dried at room temperature for 48 hours. After completely drying, the film was carefully peeled off. The film was conditioned in sealed plastic and placed inside a desiccator containing saturated magnesium nitrate (R & M chemicals, Ever Gainful Enterprise Sdn. Bhd., Malaysia) 51% of RH at a temperature of 30 °C (Y. X. Xu et al., 2005). The developed film was characterized for moisture content, optical, chemical, mechanical, morphological, thermal, and barrier properties.

3.4 Preparation of PANI/gelatin-based film

3.4.1 Synthesis of polyaniline (PANI)

PANI powders were synthesized chemically according to the Nand et al., (2011) procedure. The procedure was carried in the ice bath by adding 50 ml of 0.5M of ammonium persulfate (APS) (Sigma Aldrich, Sigma Aldrich (M) Sdn. Bhd., Malaysia) solution to 50 ml of 1M aniline (Sigma Aldrich, Sigma Aldrich (M) Sdn. Bhd., Malaysia) and 1M HCl (J. T. Baker, Avantor Performance Materials, Inc., Pennsylvania) with vigorous stirred using a magnetic stirrer (Favorit, PLT Scientific Sdn. Bhd., Malaysia). After reacting for 2 hours, the PANI was kept still in the chiller at 5^0 C for 24 hours. Then, the PANI solution was separated using vacuum filter and washed repeatedly using distilled water and methanol until the supernatant became colorless. Then, the supernatant which is the PANI was dried in the oven at 40^0 C for 24 hours. The dried PANI was then ground using a dry grinder (EBG-J1536FJ) for 10 minutes and sieve by siever shaker (RS200, Restch, Germany) using several different size ranges more than 50 µm, 100 µm ,125 µm, and less than 250 µm. The PANI powder was placed in air-tight plastic container until further characterized.

3.4.2 Formulation of PANI/gelatin-based film

The PANI/gelatin-based film were developed using the same protocol for solution casting method as in sub-section 3.3. The film forming solution was prepared by dissolving 2% (w/v) of the freeze dried gelatin with 25% (w/w of the gelatin) glycerol and PANI in the 60 °C distilled water for 30 min with continuous stirring. Table 3.1 shows each of the film composition. The mesh sizes (US measurement standard) used for the sizes of PANI were 60, 120, 140 and 270. Three groups of PANI particles size were proposed in this study; A for the group size of PANI more than 50 µm and less than 100 µm, B for group size of PANI more than 100 µm and less than 125 µm and C for group size of PANI more than 125 µm and less than 250 µm. Size of PANI must be less than the thickness of the film as to avoid damaged on the surface of film. Each of the group size of PANI, the concentrations of PANI loaded were varied 0.5, 1 and 2 g/L. The films were characterized for moisture content, optical, chemical, mechanical, morphological, thermal, barrier and antioxidant properties.

Table 3.1: Film composition of different PANI/gelatin-based film

Sample	Gelatin (w/v) (%)	Glycerol (25% w/w of gelatin) (g)	size of PANI powder (x)	Concentration of PANI (g/L)
G-Gly	2	0.25	-	-
G-Gly-PANI(A0.5)	2	0.25	50μm≤x≤100 μm	0.5
G-Gly-PANI(A1)				1.0
G-Gly-PANI(A2)				2.0
G-Gly-PANI(B0.5)	2	0.25	100μm≤x≤125 μm	0.5
G-Gly-PANI(B1)				1.0
G-Gly-PANI(B2)				2.0
G-Gly-PANI(C0.5)	2	0.25	125 μm≤x≤250 μm	0.5
G-Gly-PANI(C1)				1.0
G-Gly-PANI(C2)				2.0

G: Gelatin; Gly: Glycerol

3.5 Self-healing test

The observation technique was used to characterize the self-healing characteristics of the fish gelatin-based film, in which the film was cut with a 5 mm incision using a razor blade until its underlying substrate was reached. A light microscope (Nowex B series, Holand) was used to examine and record the damaged film. Then, using syringe, droplets of water were injected to the damaged zones of the films to aid in the healing process. The damage-healing process of the film was viewed and recorded using a light microscope (450X magnification) to study the evolution of the self-healing from time to time. The tensile strength of the film was then observed using a mechanical test to investigate the underlying damage-restoring behaviour of the gelatin film network. The damage-restoring behaviour was predicated on the film's capacity to repair itself after damage utilizing water stimuli without the requirement for detection or repair by manual intervention. The films were then tested for sorption at various RH (23%, 33%, 43%, 57%, and 75%) and temperatures (5 °C, 30 °C, and 40 °C).

A 10 x 10 mm film strip with a 5 mm incision in the centre was put inside the desiccators to test the impact of varying RH and temperature on self-healing abilities. For each temperature (5 °C, 30 °C, and 40 °C), three different sets of desiccators were employed with varied RH values (43%, 57%, and 75%). Using a light microscope (450X magnification), the damage-repair process was detected on the gap of the incision section on days 1, 4, and 7.

3.5.1 Sorption isotherm of the films

The film was cut into square shape with dimensions 30 mm x 30 mm and placed inside the desiccator containing silica gel (R & M chemicals, Ever Gainful Enterprise Sdn. Bhd., Malaysia) (0% RH) for 3 days at temperature, 30 °C (Othman et al., 2019) . For a constant surrounding temperature, the desiccator was put in an incubator (Incucell, MMM, Germany). A relative humidity meter (NT-312, ProsKit, USA) was used to ensure the relative humidity inside the desiccator was constant. The weight of the film before it was placed inside the desiccator was measured and labeled as W_d. Then, weight of the film after it was pre-dried inside the desiccator for five days was measured and labelled as W_d. the initial moisture content was determined as follows (Equations 3.1):

$$M_i = \frac{Wi - Wd}{Wd} \qquad \text{Equation 3.1}$$

Where, M_i is an initial moisture content (% dry basis), W_i is an initial weight of sample, (mg) and W_d is a dry weight of sample after being pre-dried in desiccator (mg).

The five-day pre-dried films were then placed inside separate desiccators with different RH conditions (23%, 33%, 43%, 57% and 75%) in triplicate samples for each salt solution. In order to set five different RH conditions, various saturated salt solution has been used as listed in Table 3.2. The water sorption properties of the films were studied at three different temperatures; 5 °C, 30 °C and 40 °C. Therefore, the desiccators were placed separately in conditioning equipment such as chiller (Remi, India) set as 5 °C and incubator 30 °C and 40 °C respectively. After that, the weight of the film was measured periodically every 24 hour for seven days. Equilibrium moisture content was calculated from the increase in mass of dried sample after equilibration at given RH. The resulting data was the equilibrium moisture content of the sample at different RH and temperature. The weight of the product had reached the steady state with the testing time, indicated that it reached the equilibrium state. Determination of the equilibrium moisture content of the sample corresponding to different water activity was carried out by using the following Equation 3.2:

$$M_e = \frac{We}{Wi}\left(Mi + 1\right) - 1 \qquad \text{Equation 3.2}$$

Where, M_e is an equilibrium moisture content of the sample (% dry basis), (mg) ,W_i is an initial weight of the sample, (mg), M_i is an initial moisture content of the product, (% dry basis) and W_e is an equilibrium weight of the sample, (mg).

Table 3.2: Relative humidity of saturated salt solutions

Saturated salt solutions	RH (%)
Potassium acetate (CH_3CO_2K) (Systerm, Chemar, Malaysia)	23
Magnesium chloride (MgCl) (Systerm, Chemar, Malaysia)	33
Potassium carbonate (K_2CO_3) (Systerm, Chemar, Malaysia)	43
Sodium bromide (NaBr) (Systerm, Chemar, Malaysia)	57
Sodium chloride (NaCl) (Systerm, Chemar, Malaysia)	75

The moisture sorption data of the film was fitted to a mathematical model, specifically the Peleg model. The Peleg's model has been used widely to describe the sorption process in various food applications (Othman et al., 2017; Turhan et al., 2002).

The water absorption of starch-based plastic over a period of time was determined using the equation proposed by Peleg, (1988) :

$$M_t = M_i \frac{t}{K1+K2t} \qquad \text{Equation 3.3}$$

Where, M_t is a moisture content at a known time, (% dry basis), M_i is an initial moisture content, (% dry basis), t is a the water absorption time, (in hour) and, K_1 and K_2 are Peleg constants. By rearranging the equation gives:

$$\frac{t}{Mt-Mi} = K_1 + K_2 \qquad \text{Equation 3.4}$$

From the plot of t/(Mt-Mi) versus t, a straight line was obtained with K_1 as intercept value while K_2 is the gradient of the graph. The characteristic of Peleg's constant was determined from the plot.

The were four isotherm models applied in this studied which were GAB (Guggenheim Anderson de Boer), Smith, Halsey and Caurie model. All the models fitted with the experimental data using MS Excel Software (Saberi et al., 2015).

(i) GAB model

The used of GAB model is generalized by its theoretical bases, mathematical simplicity and ease to interpret. The equation of the model is as followed:

$$\frac{Me}{Wm} = \frac{C\ k\ aw}{(1-kaw)(1-kaw+Caw)}$$ Equation 3.5

where, M_e is an equilibrium moisture content of the sample (dry basis), (mg), W_m is a GAB monolayer moisture content, C is a Guggenheim constant, a_w is a water activity, (%) and k is a factor correcting properties of the multiplayer molecules corresponding to the bulk liquid. The parameters (k, W_m and C) in GAB models were obtained from its second-order polynomial form:

$$\frac{aw}{Me} = \alpha\ a_w^2 + \beta\ a_w + \gamma$$ Equation 3.6

where: $\alpha = \frac{k}{Wm(\frac{1}{C}-1)}$, $\beta = \frac{1}{Wm(1-\frac{2}{C})}$ and $\gamma = \frac{1}{Wm\ kC}$

(ii) Smith Model

This model was normally used to describe the final curved portion of sorption isotherm of bio-plastic with high molecular weight. The equation was expressed as

$$M = A - B \log (1-a_w)$$ Equation 3.7

Where the dimensionless constants A represents the moisture bound to the surface and B represent the moisture in a unimolecular layer of normally condensed moisture. The constant A and B were computed from intercept and slope of the linear regression of M versus log $(1-a_w)$.

(iii) Halsey Model

Halsey equation was established at 1948 and its equation was expressed as:

$$\ln (M) = a + b\ (\ln(-\ln(a_w)))$$ Equation 3.8

Where a and b were the constants for equation. The Halsey constants were computed from a linear plot of ln(M) versus $\ln(-\ln(a_w))$.

(iv) Caurie Model

The equation was expressed as

$$\ln (M) = \ln A - r a_w$$ Equation 3.9

Where A and r were the constants for equation. The constants were computed from a linear plot of ln(M) versus a_w.

3.6 Analytical methods

3.6.1 Measurement of film thickness

Thickness of the sample film was measured using a digital vernier caliper (Model MIT-500-196-20, Japan) at ten arbitrary points (n=10). Then, the average thickness value were determined.

3.6.2 Yield of gelatin

The average yield of three replications of gelatin was calculated based on dry weight of fish scale using the following equation 3.10 (Das et al., 2017) :

$$Yield\ of\ gelatin\ (\%) = \frac{Weight\ of\ dried\ gelatin\ (g)}{Dry\ weight\ of\ fish\ scale\ (g)} \text{x } 100 \quad \text{Equation 3.10}$$

3.6.3 Proximate analysis of the fish scale and gelatin

The protein, fat, ash and moisture contents of the fish scale and the gelatin powder were determined according to the Association of Official Analytical Chemists (AOAC) (AOAC International, 2016) methods with the analytical number of 981.10, 991.36, 923.03 and 950.46 respectively. Meanwhile, for the carbohydrate analysis, the test followed Food Analysis: Theory and Practice method (Pomeranz & Meloan, 2000).

3.6.4 Determination of amino acid composition of extracted gelatin

The analysis of amino acid constituents in extracted gelatin was carried out by Unipeq Laboratory, Universiti Kebangsaan Malaysia, utilising the Waters AccQ Tag/HPLC technique and all standard protocols for quantifying amino acids. High-performance liquid chromatography (HPLC) using a Waters 410 Scanning Fluorescence AccQ Tag Column (3.9 x 150 mm) was used to run and assess the quantity of amino acid composition. The amino acid compositions were collected from three replications of extracted gelatin samples on average.

3.6.5 Morphological analysis by using scanning electron microscopy (SEM)

The morphology of the surface of sample films were analyzed using SEM (Model JSM-6400, Jeol, USA). The images were taken at an acceleration voltage of 15 kV. All specimens were coated with a thin layer of gold to eliminate charging effects. ImageJ software was used to further analyzed the SEM images obtained.

3.6.6 Chemical functional group analysis by Fourier-transform infrared spectroscopy (FTIR)

FTIR spectra were recorded using Thermonicolet (Model Nicolet 6700, United State) spectrometer and transmission spectra were obtained by forming thin transparent potassium bromide (KBr) pellets. All the spectra were recorded in absorbance mode with a resolution of 4 cm^{-1} in the range of 600 to 4000 cm^{-1}.

3.6.7 Determination on moisture content of films

The moisture content (MC) of the films was determined by measuring the weight loss of the films upon drying. Before the film dried at 105 °C for 24 hours in a ventilated oven C (UF110, Memmert, Germany) the initial weight (W_1) was taken. After 24 hours, the dried films were weight as final weight (W_2). The data obtained were calculated averagely on three replications of each films following Equation 3.11:

$$\mathrm{MC}\ (\%) = \frac{W_1 - W_2}{W_1} \mathrm{x}100 \qquad \text{Equation 3.11}$$

3.6.8 Physical properties of the films

Color of the film was examined by using a color spectrophotometer (HunterLab, Ultrascan, Pro, USA) by measuring the CIELAB coordinates (L*, a*, b*). The color values were averaged based on at least three replications. The total color difference (ΔE) was calculated using Equation 3.12:

$$\Delta \mathrm{E} = \sqrt{(\Delta \mathrm{L})^2 + (\Delta \mathrm{a}^*)^2 + (\Delta \mathrm{b}^*)^2} \qquad \text{Equation 3.12}$$

where ΔL^*, Δa^*, and Δb^* are the difference between standard white tile (L=88.14, a=80.18 and b=85.08) and film samples respectively.

For the opacity, the value of the films was calculated based on the Equation 3.13:

$$\text{Opacity} = A_{600}/L \qquad \text{Equation 3.13}$$

Where A_{600} is the value of absorbance at 600 nm (Nordin et al., 2020) and L is the film thickness (mm).

3.6.9 Mechanical test of the films

The mechanical properties (tensile strength and elongation at break) were studied using Texture Analyzer (TA.XT2, Stable Micro Systems, UK) with a load cell of 5kN according to ASTM D882-02 (ASTM, 2002). The film sample strips, size of 100 x 15 mm, were cut from each sample. Before testing, the thickness of the film was measured using a Digital Vernier Caliper (MIT-500-196-20, Japan) at ten arbitrary points of the film. Then, the averages of these values were used to calculate the cross-sectional area of each film. The film samples were pre-conditioned for 24 hour at room temperature in a desiccator containing saturated magnesium nitrate (R & M chemicals, Ever Gainful Enterprise Sdn. Bhd., Malaysia), 51% of RH before being analyzed. The end of each sample was mounted using a utility tape to prevent cracking and slippage of film during testing. Force (N) and deformation (mm) were recorded with a cross-sectional test speed of 30 mm/min. Property values reported here represents the average of the results for test run on five specimens for each sample with standard error.

3.6.10 Determination of glass transition temperature (Tg) using differential scanning calorimetry (DSC)

Differential scanning calorimetry (Universal V3-9A TA Instrument, New Castle, PA, USA) equipment was used to determine the glass transition temperature of different types of plasticized films. The calibration of the equipment was conducted using indium as standard. For differential scanning calorimetry (DSC) analyses, 5 mg of film samples were weighed and placed in an aluminum sample pan which was immediately sealed. An empty sample pan was used as a reference. Film samples were heated from 30 to 195 °C at a rate of 10 °C/min. Nitrogen gas was used to flush the DSC cell at a flow rate of 50 mL/min to maintain an inert environment. The apparent glass transition temperature (T_g) was measured as the midpoint of the heat flow change at the glass transition in the first heating scan.

3.6.11 Determination of thermal degradation of the films using Thermo-gravimetric analysis (TGA)

Thermo-gravimetric tests were performed using Mettler Toledo thermal analyzer (TA Instruments, New Castle, PA, USA). The tests were carried out at temperature range from 25 to 800 °C with a heating rate of 10 °C/min under nitrogen gas. Film sample of 5–15 mg was placed. The onset decomposition temperature and weight loss profiles were obtained.

3.6.12 Determination on water vapor permeability of the films

The water vapor transmission rate of the film was measured by a modified technique of a dry cup method, according to (Basha, 2011) followed by the ASTM E96 standard (ASTM, 2005). The cup used were according to JIS-Z0208 (Japan Standard for Water Vapor Transmission Rate of Materials) with 28 cm^2 of transmission area. The thickness of the film was measured using Digital Vernier Caliper (MIT-500-196-20, Japan) at ten arbitrary points of the film. The mean value of ten measurements was used as the film thickness to calculate the water vapor permeability. First, the film samples were pre-conditioned for 24 hour at room temperature in a desiccator containing saturated magnesium nitrate (R & M chemicals, Ever Gainful Enterprise Sdn. Bhd., Malaysia), 51% of RH before being analyzed.

10 g of calcium chloride (Chemiz, Malaysia) was placed in the cup. Wax was used to seal the film to the cup. For around 10 minutes, the wax was allowed to cure and relax. The ready set of sample cups was then weighed. The cup was then placed in the desiccator to maintain the humidity and placed at room temperature (25 °C). The cups were periodically removed and weighed. The mass of water loss from the cups was monitored as a function of time. The steady state of the bound water transfer during the experiment was identified when linear relationship between the mass of water loss and time was obtained. There replications for each sample were done and the result calculated averagely.

3.6.13 Measurement of particle size

Particle size analysis was analyzed by using a Mastersizer 2000 (Model APA2000, United Kingdom) laser diffractometer for the analysis of size distribution in different group sizes of PANI. The measurements were conducted using Hydro MU dispersion units with distilled water as a dispersant.

3.6.14 Determination of antioxidant activity using free radical scavenging analysis

DPPH (1,1-diphenyl-2-picrylhydrazyl) assay method (Hsu et al., 2008, 2011) was applied for the assessment of the films. The 20 (1 x 1 cm^2) film pieces were added to 20 mL of a 55 µM methanolic DPPH solution. The samples were left to react in the incubator for 24 hour and after which the absorbance of the supernatant at 516 nm was measured using a UV Spectrophotometer machine (Ultrospec 3100, Amersham Biosciences, Germany). A blank DPPH solution without a sample was also set up as a control. The percentage (%) of $DPPH^+$ which reacted over 24 hour period was then calculated after subtracting away the background loss of $DPPH^+$ solution without sample. There replications for each sample were done and the result calculated averagely.

3.7 Statistical analyses

Each experiment and measurement were performed in triplicate. Statistical analysis was conducted using a statistical program (Minitab 17) with analysis of variance (ANOVA). The significant differences between means were evaluated by Tukey's multiple range test. Differences were considered statistically significant at $p < 0.05$.

CHAPTER 4

RESULTS AND DISCUSSION

4.1 Extraction and characterization of gelatin from red tilapia's fish scale

4.1.1 Yield and approximate composition of extracted red tilapia's fish scale gelatin

Approximate compositions, such as protein, fat, ash, and moisture content of the fish scales and extracted gelatin, were tabulated in Table 4.1. The red tilapia's fish scale was primarily composed of 24.60% protein, 59% moisture, 0.60% fat, and 15.80% ash. The value of protein content is fairly consistent with the findings by Sockalingam & Abdullah, (2015) but different in moisture and ash content as this might be due to the different type of tilapia used (black tilapia's). Besides, there are many factors that can affect the total protein concentration of the fish scale, including the species and age of the fish (Karim & Bhat, 2009). With protein as the major components in the scale, the gelatin has been extracted from red tilapia's fish scale using chemical pre-treatment and thermal denaturation of collagen technique at 80 °C for an hour. In Table 4.1, the approximate compositions analysis of extracted gelatin for the protein, fat, ash, and moisture values were at 85.80%, 0.40%, 2.50%, and 11%, respectively. In compared to the protein content (90.76%) as major contents with low contents of fat and ash in gelatin extracted from tilapia's scale obtained by Weng et al. (2014) it was a bit lowered due to the different method of extraction. The extraction of gelatin using chemical pre-treatment and thermal denaturation technique used in this study obtained protein as the major constituent with low contents of both lipids (fat content) and inorganic matters (inorganic residues in the form of ash).

Table 4.1: Percentage of approximate composition of red tilapia's fish scale and extracted gelatin

Composition	Yield (%)	
	Fish scale	Extracted gelatin
Protein	24.60	85.80
Fat	0.60	0.40
Ash	15.80	2.50
Moisture	59.00	11.00

The yield of extracted gelatin after freeze drying the gelatin solution was 4.30% based on the dry weight basis from fish scales. The result was slightly lower than

reported by Zin et al. (2019) with the yield of extracted gelatin of red tilapia fish scale of 5.8%. The differences in the extraction yield were due to the several factors including the differences in nutrition compositions of the scales, the collagen content, and the amount of soluble components in the scales beside the age of fish and extraction method (Songchotikunpan et al., 2008). Thus, red tilapia's fish scale has shown promising result and has the potential concerning the gelatin extraction with good yield and protein content.

4.1.2 Amino acid composition of gelatin extracted from red tilapia's fish scale

The data in Table 4.2 showed the amino acid composition of gelatin extracted from the red tilapia's fish scale. The result indicated that the glycine content was the highest with a result of 20.79 g/100g, followed by hydroproline 14.38 g/100g, and proline 10.47 g/100g. The high amino contents obtained in this study were similar to the previous studies (Limpisophon et al., 2009; Mohammad et al., 2014a; Weng & Wu, 2015). Glycine content in the red tilapia's fish scale gelatin was abundant, which is relatively similar to gelatin from sardine, red sea bream, and Japanese sea bass scale (Nagai et al., 2004; Weng & Wu, 2015). Proline with hydroproline makes up the imino acid complex, which is particularly important in determining the gel properties of a particular gelatin. Commonly, the triple helix of gelatin molecules is made up of a repetitious sequence of glycine-proline-hydroproline. The significant function of imino acids in the triple-helix structure of gelatin molecules also leads to the gel strength of gelatin and (Tong & Ying, 2013). The stability of the triple helical structure in renatured gelatin is relatively proportional to the total content of imino acids. Hydropoline acts in the stabilization of the triple-stranded collagen helix because of its hydrogen bonding ability through its hydroxyl group (Hoque et al., 2011). Gelatin of animals from high-temperature habitats has higher imino acid content compared to those from low-temperature habitats. Hence, fish gelatin generally has lower imino acids concentration than mammalian gelatin. However, warm water fish have a higher concentration of imino acids compared to cold-water fish. It also has been reported that gelatin with higher content of imino acid and alanine exhibited better viscoelastic properties and have the ability to develop the triple-helix structure (Gómez-Guillén et al., 2009). Consequently, this will positively affect the film-forming properties of gelatin. The lowest amino acids by composition were valine (1.9 g/100g), histidine (1.22 g/100g), isoleusine (1.14% g/100g), phenylalanine (1.02 g/100g), and thyrosine (0.50 g/100g). All these amino acids are inherent properties of gelatin (Mahmoodani & See, 2013). Hence, with high content of imino acid, the gelatin exhibited an excellent filmogenic (ability to form film) property, which later resulted in contributing a positive effect on the development of the gelatin-based film.

Table 4.2: Amino acid composition of red tilapia's fish scale gelatin

Amino acid	Composition (g/100g)
Hydroxyproline	14.38±0.30
Aspartic acid	4.05±0.06
Serine	3.83±0.07
Glutamic acid	8.19±0.13
Glycine	20.79±0.15
Histidine	1.22±0.06
Arginine	10.33±0.05
Threonine	3.04±0.03
Alanine	7.90±0.09
Proline	10.47±0.02
Thyrosine	0.50±0.01
Valine	1.90±0.02
Isoleusine	1.02±0.00
Lysine	2.70±0.06
Leusine	2.39±0.00
Methionine	1.14±0.01
Phenylalanine	2.05±0.02
Total	95.90±1.06

4.1.3 Morphological analysis of the gelatin

The gelatin extracted from the red tilapia's fish scale was in a snowy white crystal-like appearance and had a light texture. The white color appearance of the gelatin imparts a good influence or quality on the develop film in term of color. Moreover, the gelatin extracted has barely detected a fishy odor. Digital photographs of freeze-dried gelatin are shown in Figure 4.1 (a) with the porous structure, as apparent. The flank of the freeze-dried gelatin looks bright, white, and shiny. The surface morphology of the freeze-dried gelatin was observed by SEM and is shown in Figure 4.1 (b). The sample presented a rough surface and porous on the side of the wall. During the freeze-drying process, the materials were dried by sublimation of ice crystals under vacuum at a temperature below the ice freezing point (Federal & Catarina, 2017; Kang et al., 1999). The free water in the polymeric solution was frozen, causing the polymer chains to gather and condense, leading to a honeycomb structure after ice sublimation.

(a) (b)

Figure 4.1: (a) Digital photograph and ; (b) SEM micrograph of freeze dried red tilapia's fish scale gelatin

4.1.4 Chemical functional groups analysis in extracted red tilapia's fish scale gelatin structure

FTIR spectra of extracted gelatin is shown in Figure 4.2. The peptide group of polypeptides and proteins gives movement to many representative vibrational bands (amide A, B and amide I-VII). As shown in Figure 4.2, several characteristics can be observed and depicted by four individual peaks marked by Amide I, Amide II, Amide III, and Amide A from the freeze-dried gelatin. The main vibrational modes of the peptide bond were also shown in Figure 4.2 (Foggia et al., 2012).

The amide I peak occurred at 1731 cm^{-1} is due to the C=O stretch and attributed to the unordered and α-helix structures. Besides that, the amide II band existed due to N-H bending and C-N stretching vibration, being detected at 1538 cm^{-1}. This type of amide existed due to the N-H bending and C-N stretching vibration. As for the amide III, the band observed at 1228 cm^{-1}. For the amide A, the broad peak can be observed at 3284 cm^{-1}. This peak was related to NH stretching coupled with hydrogen bonding and free water (Bergo et al., 2010).

In short, the FTIR spectra indicated four individual's peaks, which were amide A, amide I, amide II, and amide III that were relatively concerned with the vibrational of -C-N and N-H functional groups. Thus, the gelatin extracted from red tilapia's fish scale exhibit excellent characteristics on film forming solution. Next part of this chapter will be focusing on the preparation and characterization of the gelatin-based film with and without the addition the plasticizer that includes moisture content, optical, chemical, mechanical, morphological, thermal, and barrier properties. In the present study, 25% of glycerol (w/w of the gelatin) has been applied to prepare the gelatin-based film.

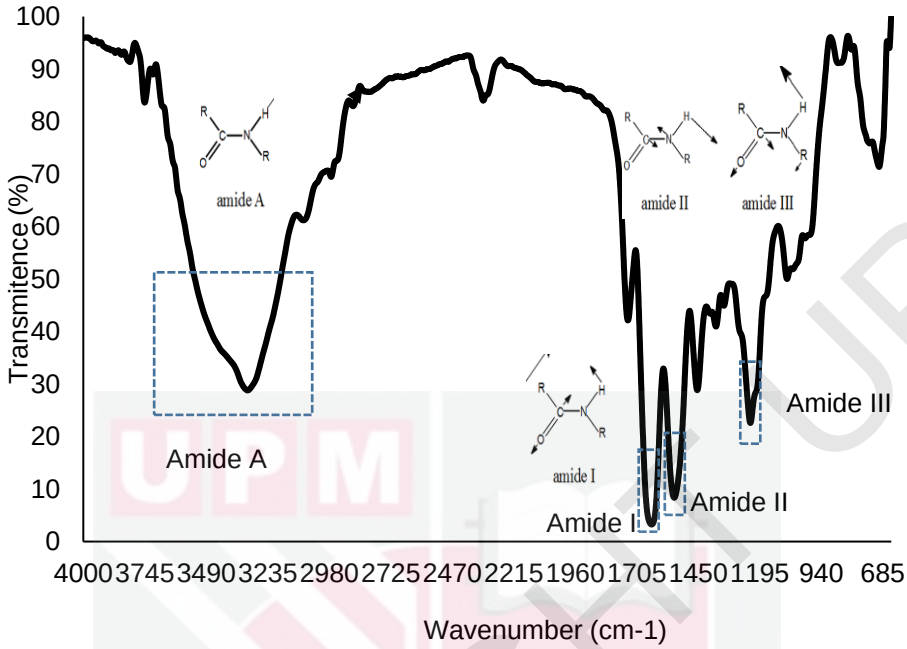

Figure 4.2: FTIR spectra of gelatin

4.2 Preparation and characterization gelatin-based film with the addition of glycerol as plasticizer

4.2.1 Physical and optical properties of the gelatin-based film

Figure 4.3 (a) and (b) are the digital photographs of gelatin-based film with and without the addition of glycerol. Both gelatin-based films with and without glycerol were transparent, as the letter 'S' on the paper can be seen clearly. The thickness measurements were 0.05±0.01 mm and 0.06±0.01 mm for both gelatin-based film without the addition of glycerol (G) and with the addition of glycerol (G-Gly), respectively. The G-Gly film was more transparent compared to the G film due to the decreased protein-protein interactions, associated with the increasing in the free volume in the film matrix, which then easily allowed light to pass through the network (Chuaynukul et al., 2017). Further explanation on the optical properties for the color and opacity of the film were analyzed and explained in the following paragraph.

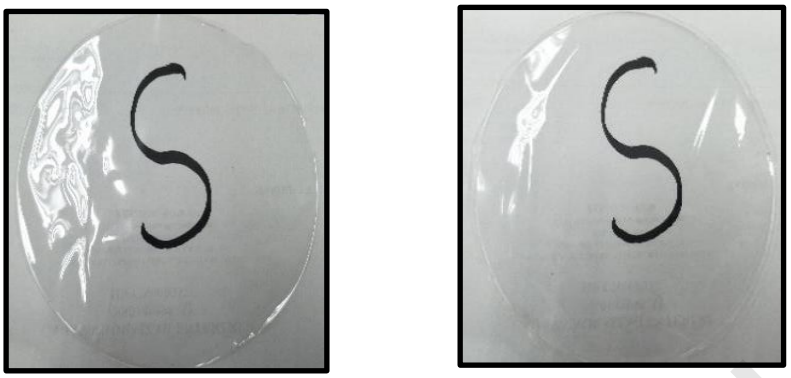

(a) (b)

Figure 4.3: Digital photographs of (a) G: gelatin-based film without addition of glycerol and (b) G-Gly: Gelatin based film with addition of glycerol

The color of the material and degree of transparency are crucial aspects of food packaging that may affect the contained food products, which in turn, determines the consumer's opinion of their acceptability. Table 4.3 displayed the color values (L, a*, b* and ΔE) and opacity of the gelatin-based films. As apparent in Table 4.3, both G and G-Gly generally had similar L, a*, b*, and ΔE values, except for the opacity aspect. This is evident from the visuals shown in Figure 4.4, whereby the color of both films was similar. It was reported by Gennaddios et al. (1996) and Vanin et al. (2005) that plasticizer does not influence color differences, neither caused by type nor concentration of plasticizer. The a* values obtained for both films were low than 0, which indicates that the films were more neutral in terms of red or green chromaticity. The gelatin-based film produces transparent films with a sightly yellowish tint with the b* values of 3.40 and 3.97 for G and G-Gly films, respectively. It is generally known that ΔE values obtained gives better differentiation of color for comparison purpose (Francis, 1983) The ΔE obtained for both films falling in a narrow range with no significance difference between both films. It indicates that both film look similar or alike in term of color as observed from Figure 4.3. However, based on the opacity obtained, G-Gly film had lower opacity values compared to G film, indicating the presence of glycerol resulted in an increase in the film transparency. Such an occurrence is related to the decreased protein-protein interactions and increasing in free volume in the film matrix. Hence, light could pass through such a network more easily (Chuaynukul et al., 2017).

Table 4.3: Optical properties of the gelatin-based films

Sample films*	L	a*	b*	ΔE	Opacity
G	90.63±2.51[a]	-1.02±0.16[a]	3.40±0.54[a]	4.71±1.06[a]	13.92±0.89[a]
G-Gly	90.12±0.21[a]	-1.23±0.06[a]	3.97±0.19[a]	5.07±0.07[a]	11.68±0.09[b]

*****G=Gelatin based-film without glycerol, G-Gly=Gelatin based film with glycerol
a, b Different superscripts indicate a statistically difference ($p<0.05$) within the same column

4.2.2 Moisture content of gelatin-based film

Table 4.4 showed the moisture content of the gelatin-based films without and with the addition of plasticizers. From the result obtained, the moisture content of the gelatin-based film with the addition of glycerol was significantly higher compared to the one without the addition of glycerol. This observation is attributed to the character of glycerol, which is hygroscopic and easy to retain water in the matrix of the film. This finding was also correlated with other studies that reported the addition of plasticizers caused an increment in the moisture content of hydrocolloid films like gelatin (Sanyang et al., 2016; Tarique et al., 2021). The addition of glycerol will generate more hydrophilic hydroxyl groups as active sites could be replaced by water molecules with the hydrogen bonds formed (Sanyang et al., 2016; Sanyang et al., 2015). Thus, glycerol acts as a water-holding agent that has an effect on the moisture content of the film.

Table 4.4: Moisture content of gelatin based-films

Sample films*	Moisture content (%)
G	19.84±0.87[b]
G-Gly	27.11±2.07[a]

*****G=Gelatin based-film without glycerol, G-Gly=Gelatin based film with glycerol
a, b Different superscripts indicate a statistically difference ($p<0.05$)

4.2.3 Mechanical properties of the gelatin-based film

The interaction of protein, hydrocolloids, and other additives, including plasticizers and water, plays an important role in the mechanical properties of the film. The protein chain and plasticizers are partly attributed to the mechanical properties in these interactions (Li et al., 2014; Park et al., 2001). The mechanical properties of the material are related to their chemical structure

(Mchught & Krochta, 1994). From the result obtained, a stress-strain curve was developed (Figure 4.4) to determine the tensile strength (TS) and elongation at break (EAB). From the tabulated data, the values of TS and EAB for the films were calculated, as shown in Table 4.5.

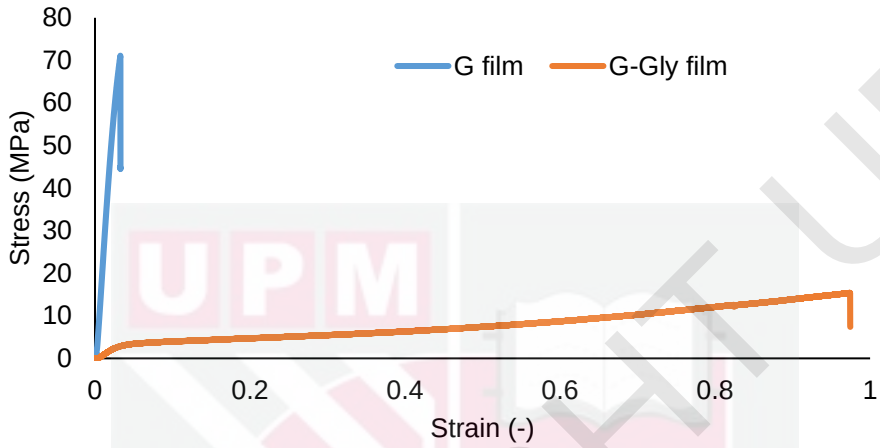

Figure 4.4: Stress-strain curves represent tensile properties of the gelatin-based film

Table 4.5: Mechanical analysis of the gelatin-based films

Sample films*	TS (MPa)	EAB (%)
G	72.23 ± 3.27^{b}	3.25 ± 0.22^{b}
G-Gly	14.83 ± 1.11^{a}	96.44 ± 5.32^{a}

***G=Gelatin based-film without glycerol, G-Gly=Gelatin based film with glycerol
a, b Different superscripts indicate a statistically difference ($p<0.05$) within the same column

The result of tensile tests showed that gelatin-based film without the addition of glycerol broke rapidly, as shown in Figure 4.5, after yielding with the TS of 72.23 MPa and EAB of 3.25%. Meanwhile, gelatin-based film with the addition of glycerol broke after necking and stress increased with strain above the yield stress at 14.83 MPa and 96.44% of TS and EAB, respectively. The mechanical behavior of the gelatin-based film without glycerol was typically brittle and rigid. In this study, the stiffness (Young Modulus) of the G film was not determined although the G film showed high TS that reflected to the blitheness of the film. TS of the film showed the maximum force that the film can stand before break when the film being pulled. To overcome this problem, plasticizer was

introduced. Hence, the efficacy of the glycerol as plasticizer can be compare by analyzed the TS and EAB of the film only. The presence of these characteristics is due to the higher interactions and proximity between protein chains in the absence of the glycerol that was in line with the studies of Yang & Paulson (2000) and Nor et al. (2017b). Polar group (-OH) along a plasticizer's chain are functioning in developing the polymer-polymer interactions in bioplolymer films. A small quantity of plasticizers added in between the polymer chains produced a 'cross-linker' effect that would decreased the free volume and the segmental mobility of the polymer and subsequently decrease the mechanical strength of the films (Ghasemlou et al., 2011).

In additions, based on the moisture content of G-Gly film was higher compared to the G film. Film that contains glycerol reflected with higher moisture content and consequently lower the TS. This is because addition of glycerol offer the chancers of plasticizer-gelatin, plasticizer-water and plasticizer-plasticizer interactions (Sanyang et al., 2015a). G-Gly films generates more hydroxyl groups as actives sites which could occupied by water molecules. Thus, increasing the moisture content and lowering the TS.

On the other hand, the EAB of the gelatin-based film with the addition of glycerol is superior to the gelatin-based film without the addition of glycerol, having a result of an EAB value of 3.25%. Hence, the EAB exhibited an inverse trend toward the TS result. In compared to other fish gelatin-based film, such as from blue shark skin (6.24%) (Limpisophon et al., 2009) and commercial fish skin (24.10%) (Chuaynukul et al., 2017), red tilapia fish scale gelatin showed the highest EAB, whereby the EAB data correspond to the film's breaking point. This indicates that, with the presence of glycerol, it causes the reduction in interactions between the biopolymer chains (Nor et al., 2017) which then results in attaining a higher EAB value. (Bergo & Sobral, 2007) also found that the addition of glycerol reduced the formations of junctions between the adjacent of the biopolymer. The existence of glycerol is also responsible for reducing gelatin crystallinity that increases the film's mobility and flexibility. Therefore, the interactions between proteins chains are reduced, which permits in increasing macromolecular movements and decrease the free volume and segmental mobility of the polymer, enhancing the film extensibility (Ghasemlou et al., 2011; Jongjareonrak et al., 2006; Nor et al., 2017).

Overall, the incorporation of glycerol molecules in gelatin-based film replaced gellan-gellan hydrogen bond by establishing glycerol-hydrogen bonds. This can be related to the result from the FTIR analysis, where the peaks of amide A bands become more intensely widen and sharpen with the addition of glycerol. This explains the hydrogen bonding between the -OH group of amino acids in gelatin with the glycerol (Gueguen et al., 1998; Muyonga et al., 2004). Hence, the chain segmental increase with the extensibility improved and interactions between the molecular chain reduced, thus decreasing in tensile strength. Thus, the addition of glycerol acted as a satisfactory plasticizer and was compatible with gelatin-based film. Moreover, glycerol is favored due to its stability and

compatibility with hydrophilic film, such as gelatin with the 25% addition improved the brittleness properties of gelatin based film (Pushpadass et al., 2008; Limpisophon, at al., 2009; Tongnuachan et al., 2012, Nur Hanani et al., 2014; Nordin et al., 2020).

4.2.4 Chemical functional groups analysis in gelatin-based film using Fourier-transform infrared spectroscopy (FTIR) analysis

Figure 4.5 shown the FTIR spectra obtained in the gelatin-based film with and without the addition of glycerol as plasticizers. Several characteristics of FTIR absorption bands of amide A, I, II, and III can be observed from the spectrum which have similar findings in the sub-section 4.1.4 (chemical interaction analysis for gelatin).

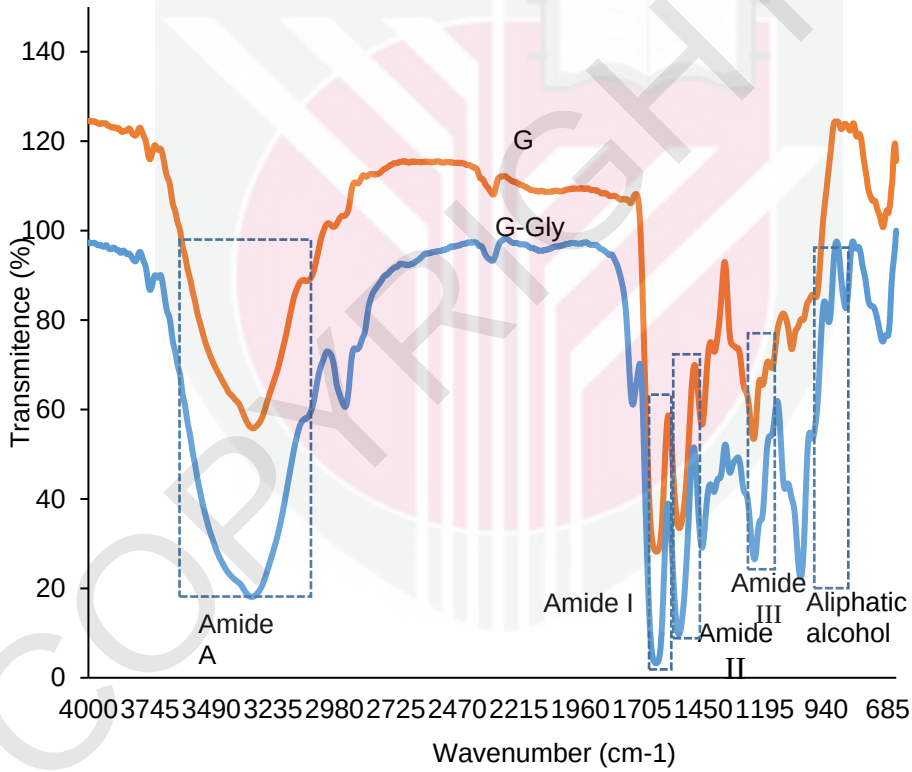

Figure 4.5: FTIR spectra of gelatin obtained from gelatin based-film without (G) and with the addition of glycerol (G-Gly)

The amide I band is very sensitive and is frequently used to study secondary protein makeup. The amide I peak occurred at 1643 cm^{-1} for both extracted gelatin. This peak is corresponded to a combination of a C=O stretching vibration

of the amide group and N-H bending, which usually occurs in the range of 1600 cm^{-1} to1700 cm^{-1} (Ahmad & Benjakul, 2011; Nikoo et al., 2011).
On the other hand, amide II exists due to N-H bending and C-N stretching vibration and reveals less protein conformation than amide I, which was detected at 1549 cm^{-1}. There were various other group characteristics marked by different other bands but rarely used in protein conformational studies (Nikoo et al., 2011).

The amide A in this study is the wide peak occurring in the range between 3317-3322 cm^{-1} for all the samples. This peak corresponds to NH stretching coupled with hydrogen bonding. Hydrogen bonding between OH groups of the amino acids in gelatin is responsible for the width (Muyonga et al., 2004). These peaks changed more intensely, widening and sharpening with the additional of glycerol in the film. Such a reaction is possibly due to the -OH group contribution made by the plasticizers.

Referring to Figure 4.5, it is evident that Amide III bands occurred at the range 1233-1241 cm^{-1}, which is consistent with the observations of Ahmad & Benjakul, (2011). With the addition of glycerol, the changes occurred with the increased in intensity and sharper peaks. This was due to the occurrence of additional interactions between the glycerol and film structure. These bands also reflect the presence of the free water (Nor et al., 2017b). The aliphatic alcohol group presented at a much higher band of 1046 cm^{-1} with the present of glycerol, indicating the concentration of glycerol was high enough to exhibit the signal in the infrared spectrum.

Overall, the shape and positions of the spectra of film were found to be practically unchanged with the addition of glycerol except for the peak intensity. Hence, glycerol permeates the film matrix, occupying positions between the macromolecules, without inducing any new interactions between the macromolecules.

4.2.5 Morphological properties of the gelatin-based film using scanning electron microscopy (SEM)

SEM micrograph of the surface of the gelatin-based film without (G) and with (G-Gly) addition of glycerol are shown in Figure 4.6 (a) and (b) at 100x magnification. Both of the gelatin-based films show homogenous, smooth, uniform, and continuous surfaces. This was in line with the other studies by (Li et al. (2014) and Tongnuanchan et al. (2012). This was due to the presence of ordered phase and homogeneous network structure. It can be anticipated that better mechanical characteristics in term of elasticity can be obtained given the homogeneity of these films' structural integrity and homogeneity (Tarique et al., 2021). It has been proven in Section 4.2.3, whereby the EAB of G-Gly films was increased significantly ($p<0.05$).

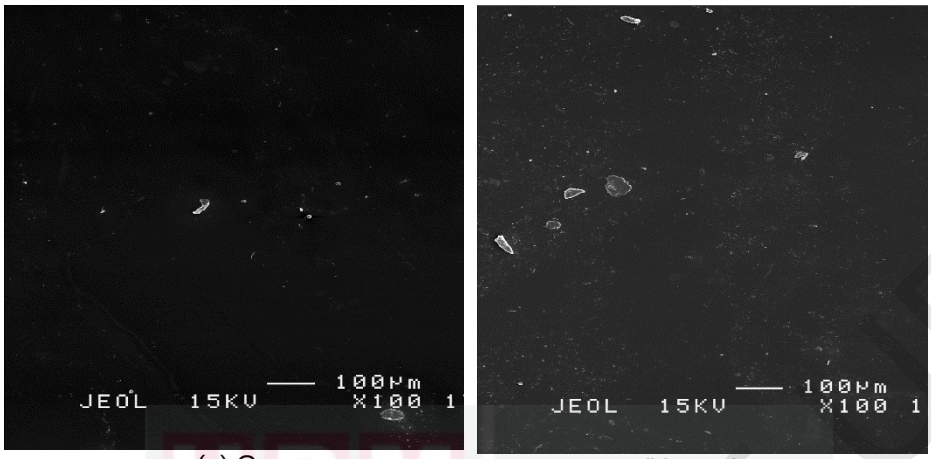

(a) G (b) G-Gly

Figure 4.6: SEM micrograph of gelatin-based film (b) without the addition of glycerol (d) with the addition of glycerol

4.2.6 Glass transition temperature (T_g) analysis of gelatin-based film by differential scanning calorimetry (DSC)

For applications purpposes, the glass transition temperature (T_g) of polymers is an important parameter that affects the thermo-rheological behavior of applications (Backfolk et al., 2007). In this study, only Tg is measured not including melting temperature (T_m) and crystallinity temperature (Tc) due to the fact gelatin is likely amorphous. T_g in the molecular segmental concept of disordered (amorphous) structure which is stabilised by various protein interactions during film forming (Jongjareonrak et al., 2006; Tongnuanchan et al., 2014). T_g dependent on molecular structure and interaction as well as chain stiffness which serves to explain the physical and chemical behaviour of material system. T_g results obtained for DSC thermograph (Figure 4.7 and 4.8) as the midpoint of the heat flow change at the glass transition in the first heating scan of each gelatin-based film with and without the addition of glycerol is shown in Table 4.6.

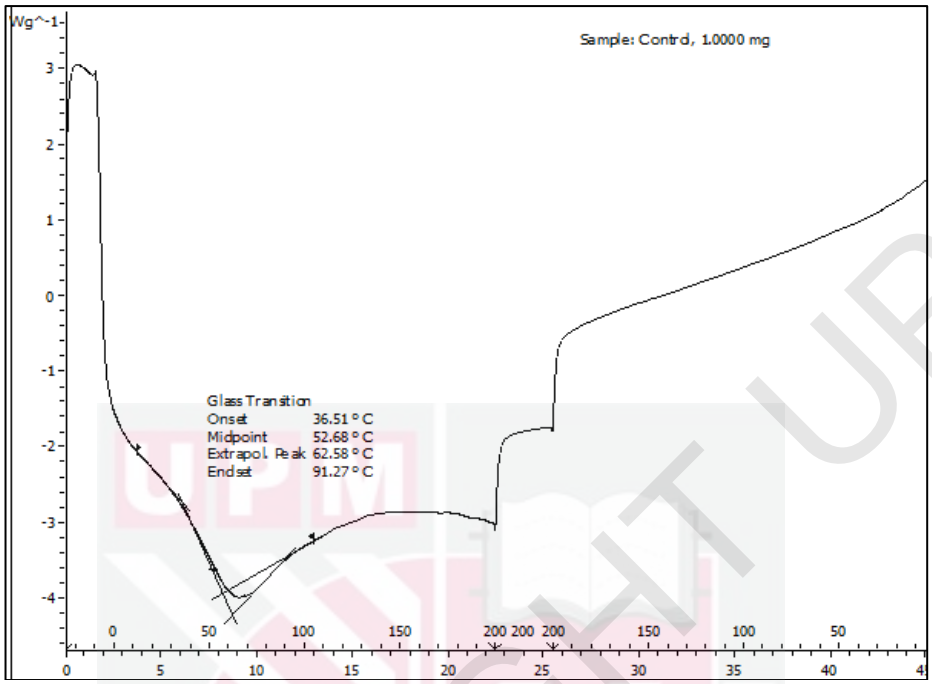

Figure 4.7: DSC thermograph of gelatin-based film without glycerol (G)

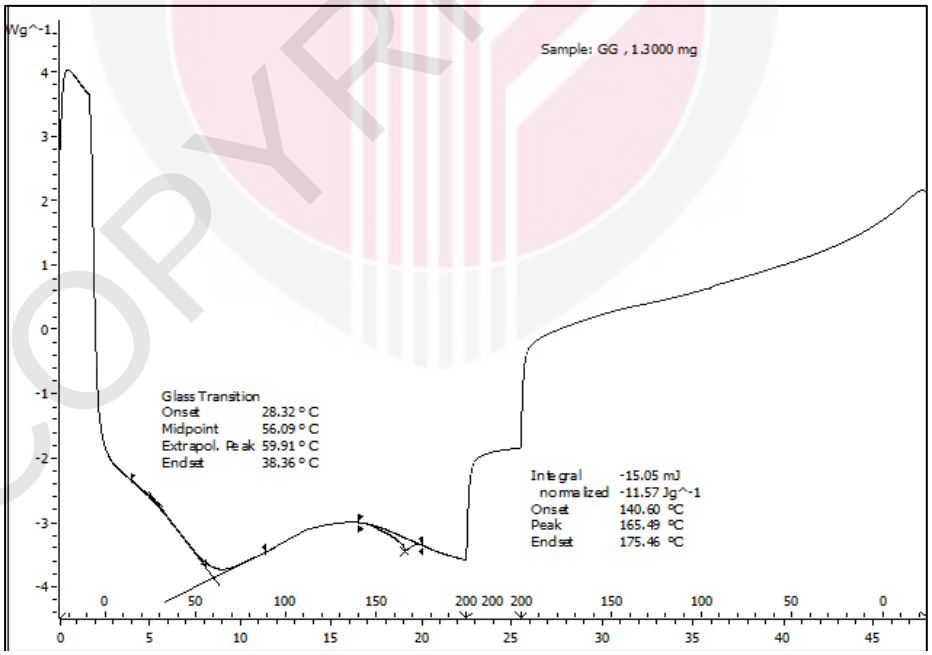

Figure 4.8: DSC thermograph of gelatin-based film with glycerol (G-Gly)

Table 4.6: T_g of the gelatin based-films with and without the addition of glycerol

*Sample	T_g (°C)
Glycerol	-78.6
G film	62.58
G-Gly film	59.91

*G=Gelatin based-film without glycerol, G-Gly=Gelatin based-film with glycerol

From the result in Table 4.6, T_g (59.91 °C) for the G-Gly film reduced after accounting for the addition of plasticizer compared to the G film (62.58 °C). This was due to the glycerol-rich phase in the gelatin matrix film. Based on the literature that used the similar brand of glycerol, T_g of glycerol is obtained at -78.6°C (Arik Kibar & Us, 2013). The addition of glycerol in the gelatin-based film created the hydrophilic hydroxyl groups as active site which attracted the water molecules (Sanyang et al., 2015). This is due to the hygroscopic characteristics of glycerol. As explained in Section 4.2.2, with the high moisture content of plasticized film, the film tends to easily retain the water into the gelatin matrix film. Hence, with high attraction of water molecules retain in the film matrix and it being considered as a polymer inter-chain mobility enhancer, this will lower the T_g value. The incorporation of glycerol increases the free volume and provide several interactions between gelatin-glycerol, glycerol-water and glycerol-glycerol interactions. Moreover, this can be related with the mechanical properties of glycerol plasticized gelatin-based film whereby the TS reduced but EAB increased with the lower T_g. This also probably due to the ability of glycerol to penetrate between the polymer chains and therefore weaken the interaction.

4.2.7 Thermal analysis of gelatin-based film by Thermo-gravimetric analysis (TGA)

TGA is used to analyze the thermal stability and decomposition behavior of the polymer sample, where the sample is heated to a high temperature in a controlled environment. Table 4.7 shows the weight losses during the heating process, described at three thermal degradation stages.

Table 4.7: Thermal degradation temperatures (T_d, °C) and weight loss (Δ_w, %) of tilapia fish scale gelatin-based film

Sample films	Δ_1		Δ_2		Δ_3	
	$T_{d1,onset}$ (°C)	Δ_{w1} (%)	$T_{d2,onset}$ (°C)	Δ_{w2} (%)	$T_{d3,onset}$ (°C)	Δ_{w3} (%)
G	131.67	6.21	455.24	51.08	654.33	6.99
G-Gly	130.67	3.86	277.31	10.72	486.29	46.01

*G=Gelatin based-film without glycerol, G-Gly=Gelatin based-film with glycerol

The initial stage of thermal degradation was due to the loss of moisture due to dehydration on the loosely bound water and/ or the evaporation of volatile components in the films that occurred at a temperature less than 150 °C (Tongnuanchan et al., 2014). It can be observed from Table 4.7 that G film had high weight loss compared to plasticized gelatin-based (G-Gly) film in the range of temperature 130.67-131.67 °C. This was associated with the high amount of water in film ascribed to a higher amount of hydrophilic gelatin components in the films (Tongnuanchan et al., 2013).

The second stage of weight loss (Δ_{w2} = 10.72 – 51.08) occurred at the thermal degradation temperature between 277.31 – 455.24 °C, and it was related to the degradation of plasticizers compound as well as lower molecular weight of protein fractions or the structure of the bound water in the film network (Hoque et al., 2011). The thermal decomposition for the gelatin-based film without glycerol is high, approximately to 450 °C. It is ascribed to the removal of hydrogen functional groups, degradation, and polymerization of the gelatin carbon chains polymer (Nascimento et al., 2012; Tarique et al., 2021).

Next, the third stage of thermal degradation behavior is associated with the degradation of the larger size or highly associated protein fraction (Tongnuanchan et al., 2014). For the third stage of weight loss, $\Delta_{w,3}$ of 6.99% of 654.33 °C were observed for G film, which was the highest in thermal degradation temperature and lower weight loss when compared to others. The higher thermal stability and lower weight loss was plausibly associated with strong hydrogen bond formation with the inter/intra-molecular protein interaction in the film network. Generally, films incorporated with plasticizers had lower thermal stability in comparison to the unplasticized film. Such a finding was in agreement with the weaker film networks, as indicated by the lowered tensile strength (Tongnuanchan et al., 2012, 2014). Thus, it can be stated that plasticizers had a remarkable impact on thermal stability in gelatin.

4.2.8 Water vapor permeability properties of gelatin-based films

The water vapor permeability of packaging materials is a crucial property that can be related to understand the shelf-life stability of food products as water vapor penetration across packaging boundaries affects the microbial growth, products texture and functionality, overall chemical stability, and pack fogging (Siracusa, 2012). As an evaluation, a better barrier was considered to have a smaller transmission rate or permeability value. Meanwhile, a weaker barrier was considered to have a bigger transmission rate or permeability value.

Gelatin-based film naturally possess high water vapor permeability because of hydrophilic properties tend to retain the water in their structure, thus exhibiting insufficient performance. Furthermore, when plasticizing agents are incorporated, this causes the film to become more permeable to water vapor (Villasante et al., 2020). Table 4.8 showed the WVP for both gelatin-based film with and without glycerol. When comparison is made for these films, there is significance difference for WVP ($p<0.05$) between G and G-Gly film. WVP for G-Gly film was higher than G film. The higher value of G-Gly film was also in-line with other studies using fish skin gelatin films (Jongjareonrak et al., 2006), pig skin gelatin film (Vanin et al., 2005), and fish muscle protein film (Paschoalick et al., 2003), all of which also found that with the addition of glycerol, it will increase the WVP. Glycerol has hydrophilic properties, which add the polar properties in the film. Hence, the intermolecular distance will increase, and cause a decrease in the internal hydrogen bonds and intermolecular stresses on the film as well (Yulistiani et al., 2020). Moreover, the hydroxyl group (-OH) of hygroscopic glycerol, which was able to interact with water, increased the WVP of the film (Hoque et al., 2011). Increasing the free volume in the film that enhances the mobility of the polymeric chains, which is caused by the insertion of glycerol between the protein molecules also resulted in the increase of WVP. The network structure of the films become less dense and more permeable and promotes the water vapor to easily diffuse through the formation of free space in the film matrix. In addition, the increase in chain movement was also reflected in the results of the mechanical properties (sub-section 4.2.3), whereby the EAB of the G-Gly film was lower than G film. This increase in chain movement was also reflected in the results of the mechanical properties (Figure 5).

Table 4.8: Water vapor permeability (WVP) measured at 25°C and 50% RH.

Sample films*	WVP (x 10^{-6} g.mm/m^2.day.Pa)
G	1.69 ± 0.14^{b}
G-Gly	3.09 ± 0.33^{a}

*****G=Gelatin based-film without glycerol, G-Gly=Gelatin based film with glycerol
a, b Different superscripts indicate a statistically difference ($p<0.05$) within the same column

In summary, the addition of glycerol as a plasticizer to gelatin-based films resulted in significant differences on theproperties of gelatin-based films. Based on earlier research by Nur Hanani et al. (2014) and Pushpadass et al. (2008), 25% (w/w of the gelatin) of glycerol was chosen, owing to the highest TS and optimal use of elasticity with the necessary limit to prevent possibly harmful effects. In mechanical properties, there were changes in the flexibility of the film by more than 90% and also a reduction in the tensile strength from 72.23 MPa to 14.83 MPa. The plasticized film also showed a significant change in thermal properties, which could be due to its co-relation with the mechanical result. Chemical structure of plasticized gelatin-based film was also observed through a FTIR analysis. In terms of water vapor permeability properties, the addition of glycerol as a plasticizer gives significant impact on the WVP value due to the hydrophilic properties of the plasticizer. Hence, the addition of glycerol as an additive in the gelatin matrix provides positive significant effects on the properties of film by increasing the flexibility and WVP, making changes in thermal properties. Thus, the G-Gly film was further explored on the feature characteristics as an active film with the incorporation of PANI.

4.3 Effects of sizes and concentrations of polyaniline (PANI) on the properties of PANI/gelatin-based film developed from red tilipia's fish scale gelatin

4.3.1 Physico-chemical, FTIR and micrograph analysis of the synthesize polyaniline (PANI) from aniline

PANI can be derived by polymerization from aniline monomer. Figure 4.9 showed the PANI powder synthesized from aniline. During the polymerization of PANI, the color changes at the initial and slow stage of polymerization (induction period). At the first stage of instantaneous mixing of the monomer and initiator solutions, the colorless solution turned pink. Then, the intensity of the color gradually decreased and turned into a light purple color. After several minutes, the color then changed to blue, and eventually permanently stayed blue after the induction period. At this induction stage, the homogenous polymerization system was turned into heterogenous (Abu-Thabit, 2016). Abu-Thabit (2016) mentioned in his study that the polymerization state commences when the reaction temperature suddenly increased rapidly due to the exothermic nature of the redox polymerization. After 24 hours of being left undisturbed, the green precipitate was collected by vacuum filteration with the solution. The filtrate solution (permeate) that was separated was purple colored, indicating the presence of unwanted water-soluble oligomers. This precipitate was washed repeatedly using distilled water and methanol to remove unreacted initiator, monomer, and low-molecular-weight water-soluble oligomers.

Figure 4.9: Granule PANI

The SEM micrographs at a different magnification of the PANI samples were depicted in Figure 4.8. From the figure, it is apparent that the PANI exhibits a granular morphology that is commonly resulted in precipitation polymerization using ammonium persulfate, the strong oxidant in sulphuric acid (Tian et al., 2014a). During the growth of PANI chain to burst, nucleate start to aggregate. In water conditions, the nucleates have limited solubility, and therefore, tend to randomly agglomerates in the continuous phase to form a bigger granule, as shown in Figure 4.8 (a) and (b), by stacking together.

In this study, mechanical stirring was used as the procedure to synthesize PANI, which affects the nucleation of PANI. The heterogenous nucleation occurs on the surface of the preformed particles when the shear force is applied (Tian et al., 2014b). Then, the hydrophobic nucleates are adsorbed on the formed PANI granules as glues to link the particles together and initiates the growth of new granules on the surface of the former. In line with this, the mesoporous structure obtained can be seen from the SEM image (Figure 4.8 (c)) of PANI. As tabulated in Figure 4.9, the size distribution of PANI can be categorized by certain ranges of size. The smaller the mean size of particles and the narrower the size of distributions will subsequently affect the toughness of the matrix (Basha, 2011).

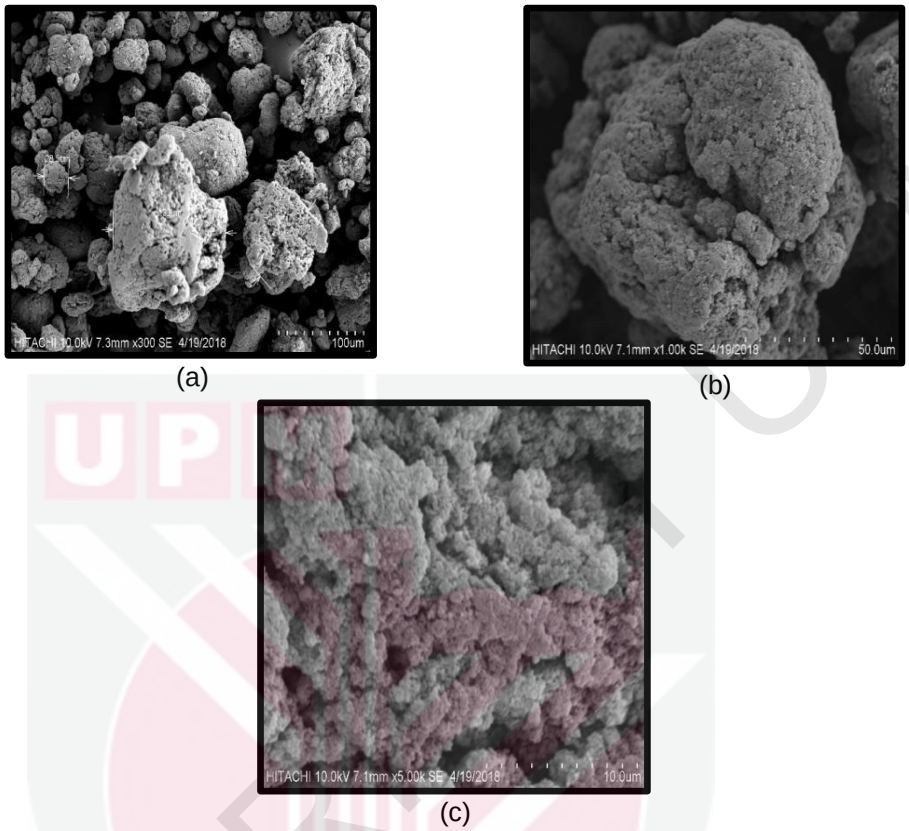

Figure 4.10: SEM image of granular morphology of PANI at magnification (a) x 300 (b) x 1000 and (c) x 5000 .

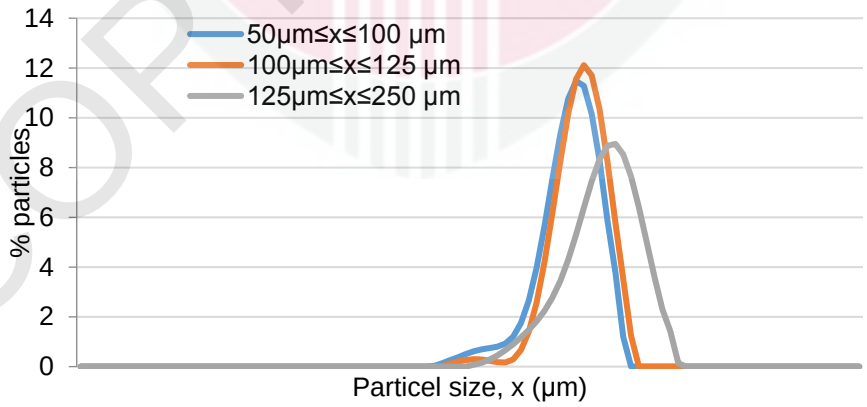

Figure 4.11: Particle size distribution of PANI

As depicted in Figure 4.12, the characteristic peaks of pure PANI were compared with the characteristics from previous literature (Bhadra et al., 2017; Saikia et al., 2010; Zareh et al., 2011). Peaks at 1624 cm^{-1} and 1495 cm^{-1} can be assigned to vibration of quinoid ring (N=Q=N) and benzenenoid ring (N-B-N), respectively. The bands at 1319 cm^{-1} and 1188 cm^{-1} correspond to C-H stretching vibration with aromatic conjugation. The vibrational bands at about 1000 and 825 cm^{-1} are assigned to the aromatic ring in-plane and out of plane (Nand et al., 2012; Parsa & Ghani, 2009). At signal around 825 cm^{-1}, it can also be proved as the structure of PANI is assigned to aromatic C-H vibrational band due to the 1,4- disubstituted benzene ring (Lukasiewicz et al., 2014; Tang et al., 1988). From the result obtained, it confirms that the samples were in partially-oxidized state, referred to as emeraldine PANI state.

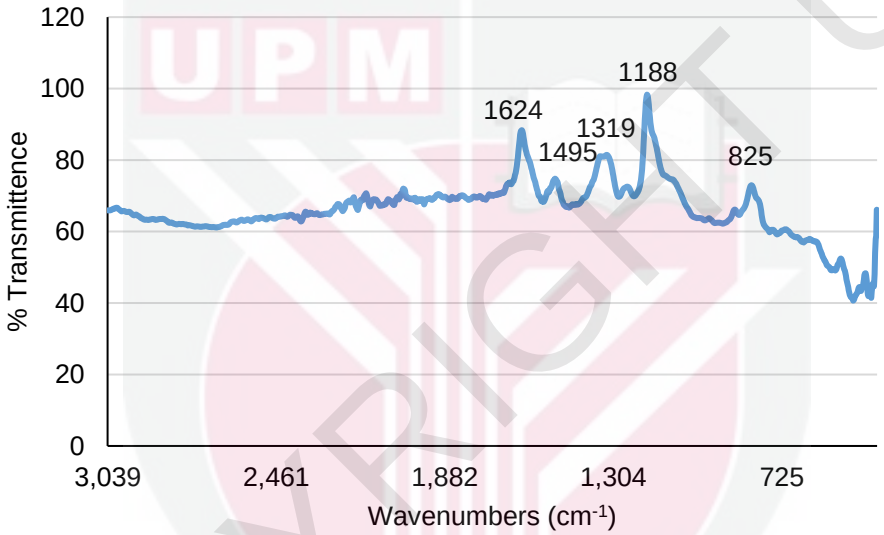

Figure 4.12: FTIR spectra of polyanilne (PANI) powder

4.3.2 Physical and optical properties of PANI/gelatin-based film

Figure 4.13 shows the digital photograph of G-Gly and G-Gly-PANI films. It can be seen clearly by naked eyes the dispersion of PANI in the gelatin matrix. The film was still transparent despite the addition of PANI, as the letter 'S' at the bottom of the film could still be seen. An even distribution of PANI particles in the gelatin matrix can be observed, as indicated by the 'dark spots' in the photograph.

G-Gly G-Gly-PANI

Figure 4.13: Digital photograph of developed active gelatin-based film; Left: G-Gly and Right: G-Gly-PANI

Table 4.9 show the thickness of the G-Gly-PANI film with different sizes and concentrations of PANI. Film thickness could be related with the WVP and mechanical properties of the film (Villasante et al., 2020). The films obtained showed a thickness range 0.0623 to 0.092 mm. The thickness of the G-Gly-PANI with concentration more than 1 g/L film were found higher in compared to the the G-Gly film irrespective to the size of PANI whereas at concentration 0.5g/L do not show any significant different. The different of solid component (dry masss) incorporated into the gelatin-based film resulting in ticker film after evaporation of the solvent. In fact, the film forming solution contains higher dry matter lead to less water evaporated hence increased the thickness.

This finding was line with Villasante et al. (2020), that obtained significant different in the thickness of gelatin-based film incorporated with different size of pecan walnut. Meanwhile, different sizes of PANI incorporated into the gelatin-based films does not effect on the thickness of the film.

Table 4.9: Thickness of PANI/gelatin-based films incorporated with different sizes and concentrations of PANI.

Sample*[1]	Thickness (mm)
G-Gly	0.0060±0.01
G-Gly-PANI(A0.5)	0.0623±0.05
G-Gly-PANI(A1)	0.0795±0.05
G-Gly-PANI(A2)	0.0859±0.00
G-Gly-PANI(B0.5)	0.0675±0.08
G-Gly-PANI(B1)	0.0803±0.00
G-Gly-PANI(B2)	0.0850±0.01
G-Gly-PANI(C0.5)	0.0634±0.03
G-Gly-PANI(C1)	0.082±0.00
G-Gly-PANI(C2)	0.092±0.06

*[1]G-Gly:=Gelatin based-film with glycerol (control), G-Gly(A0.5-C1)=PANI/Gelatin-based film
A=50μm≤x≤100μm; B=100μm≤x≤125μm;C=125μm≤x≤250μm (x: range size of PANI)
a,b,c Different superscripts indicate a statistically difference ($p<0.05$) within the same column

Color of films is an important attribute, which consequently affects its appearance, marketability, and their suitability for various applications. Based on the observations on the digital photograph above, it is evident that the incorporation of PANI in gelatin-based film did impact the appearance of the film. This was further proven by the optical analysis, as tabulated in Table 4.10. The lightness of the films was significantly reduced ($p<0.05$) with the increase in PANI concentrations. This can be explained through the green color (Beygisangchin et al., 2021) and opaque nature of PANI, which later affected the luminosity of the PANI/gelatin-based films. As for the a* values, there was a significant change towards the green chromaticity with the increase of the PANI size irrespective of the concentrations of PANI incorporated in the film. This is due to the attribution of the PANI color. The bigger granule size contributed to the greener color of PANI, thus increasing the a* values. On the other hands, the b* values of G-Gly-PANI films decreased as the sizes of PANI increased irrespective of the concentrations of PANI. This described how the PANI became more prominent when the yellowish tint of gelatin-based film faded. The ΔE shows a significantly increased ($p<0.05$) by comparing the G-Gly with the G-Gly-PANI film. The increasing trend of ΔE was seen with the increase of particle size of PANI. Meanwhile, ΔE of the G-Gly-PANI film at different concentration experienced increased by increasing the concentration PANI loaded from 0.5 g/L to 1 g/L. On the other hand, when the concentration of PANI increased to 2g/L, there were no significant changes on the ΔE. The opacity values of the gelatin-based film decreased substantially after the incorporation of PANI. These results show that the transparency of the film was improved by adding PANI to the gelatin matrix. G-Gly-PANI with low concentration and size of PANI obtained low opacity values

(high transparency). This was due to the existence of a transparent 'window' in the visible region of the spectrum (Cao et al., 1993). This can be inferred that the incorporation of PANI into the gelatin-based film have significant effect on the color attributes of films.

In summary, the dispersion of PANI can be seen with the naked eyes inside the film. From the optical analysis, the PANI color gives major attributes in the PANI/gelatin-based film with the increasing in a* values. Moreover, the opacity of the film was decreased compared to the control film without PANI, which indicates the transparency of the film. For the viewing purpose, high transparency of G-Gly-PANI film gives an advantages to be applied in the food application that are not light sensitives especially perishable fruit and vegetable whereby customer can ensure the freshness of the product.

Table 4.10.: Optical properties of different size and concentration of PANI incorporated into the PANI/gelatin-based films.

Sample*	L*	a*	b*	Opacity	ΔE
G-Gly	90.12±0.21^{a}	-1.23±0.06^{a}	3.97±0.19^{ab}	11.68±0.09^{a}	4.71±1.06^{f}
G-Gly-PANI (A0.5)	82.15±1.55^{bc}	-1.67±0.13^{a}	3.42±0.05^{a}	8.20±0.42^{b}	11.48±1.42^{e}
G-Gly-PANI (A1)	66.98±3.40^{d}	-2.75±0.09^{bc}	3.26±0.25^{bc}	4.68±0.60^{d}	26.32±3.30^{d}
G-Gly-PANI (A2)	66.71±1.34^{d}	-1.22±0.30^{a}	3.07±0.02^{bc}	4.22±0.27^{d}	26.39±1.27^{d}
G-Gly-PANI (B0.5)	86.01±2.83^{bc}	-1.15±0.40^{a}	4.96±0.48^{a}	11.47±0.41^{a}	8.62±2.42^{ef}
G-Gly-PANI (B1)	80.00±1.82^{c}	-2.14±1.92^{ab}	3.50±0.35^{b}	7.01±0.40^{c}	13.59±1.69^{e}
G-Gly-PANI (B2)	80.36±1.52^{bc}	-1.45±0.38^{a}	3.57±0.14^{b}	7.61±0.38^{bc}	13.15±1.45^{e}
G-Gly-PANI (C0.5)	59.17±2.51^{e}	-3.90±0.19^{d}	1.46±0.57^{d}	4.33±0.44^{d}	34.08±2.48^{c}
G-Gly-PANI (C1)	36.37±1.38^{g}	-3.58±0.41^{cd}	1.28±0.04^{d}	1.10±0.09^{e}	56.69±1.35^{a}
G-Gly-PANI (C2)	43.14±1.03^{f}	-4.39±0.70^{d}	2.16±0.88^{cd}	1.41±0.06^{e}	50.06±1.11^{b}

*G-Gly:=Gelatin based-film with glycerol (control), G-Gly(A0.5-C1)=PANI/Gelatin-based film

*1A=50μm≤x≤100μm; B=100μm≤x≤125μm;C=125μm≤x≤250μm (x: range size of PANI)

a,b,c,d,e,f,g Different superscripts indicate a statistically difference ($p<0.05$) within the same column

4.3.3 Moisture content analysis of PANI/gelatin-based film

Table 4.11 shows the moisture content of PANI/gelatin-based film at different concentration and size of PANI loaded. From the result obtained, the moisture content of the gelatin-based film decreased significantly ($p<0.05$) with the addition of PANI. This can be ascribed the less amount of hydrophilic gelatin components in the films caused by the presence of hydrophobic PANI. The findings was in line with the studies by Tongnuanchan et al. (2013) and Tongnuanchan et al. (2014), that incorporate hydrophobic antioxidant into the hydrophilic gelatin matrix and find the reduction in the moisture content. In contrast, there was no significant difference ($p>0.05$) of moisture content when different concentration of PANI incorporated into the film irrespective to the size of PANI.

Table 4.11: Moisture contents properties of different sizes and concentrations of PANI incorporated into the PANI/gelatin-based films.

Sample*[1]	Moisture content (%)
G-Gly	27.11 ± 2.07^{a}
G-Gly-PANI(A0.5)	12.53 ± 3.01^{bc}
G-Gly-PANI(A1)	13.87 ± 1.25^{bc}
G-Gly-PANI(A2)	12.20 ± 1.52^{bc}
G-Gly-PANI(B0.5)	15.58 ± 1.52^{bc}
G-Gly-PANI(B1)	14.71 ± 3.71^{bc}
G-Gly-PANI(B2)	8.67 ± 1.99^{c}
G-Gly-PANI(C0.5)	18.05 ± 3.52^{ab}
G-Gly-PANI(C1)	20.19 ± 1.35^{ab}
G-Gly-PANI(C2)	11.59 ± 5.17^{bc}

*[1]G-Gly:=Gelatin based-film with glycerol (control), G-Gly(A0.5-C1)=PANI/Gelatin-based film
A=50μm≤x≤100μm; B=100μm≤x≤125μm;C=125μm≤x≤250μm (x: range size of PANI)
a,b,c Different superscripts indicate a statistically difference ($p<0.05$) within the same column

4.3.4 Mechanical properties of PANI/gelatin-based film

Tensile strength (TS) and percent of elongation at break (EAB) are important parameters that relate to the mechanical properties of film to their chemical structure (Mchught & Krochta, 1994). Mechanical properties describe how the materials react to force and cause a material to deform. Table 4.12 displays the mechanical properties of PANI/gelatin-based films.

Based on Table 4.12, the tensile properties of the G-Gly-PANI shifted differently, either increase or decrease ($p<0.05$) with the incorporation of PANI. From the results, it can be seen that the films containing PANI with the range size of PANI (x) 50µm≤x≤100µm and 100µm≤x≤125µm had higher tensile strength and low EAB compared to the G-Gly film irrespective of the concentration of PANI. The smaller the mean size of the particles and the narrower the size distribution, the more effectively the particles will enhance the TS of the matrix. Therefore, possessing a small size of the PANI powder is necessary to increase the tensile properties. Based on the PANI concentration loading into the film, as the concentration of PANI increased, the TS is increased with decreasing in EAB. This is due to the fact that pristine PANI is a very rigid material that affects the tensile strength. As observed in Figure 4.15, for the PANI/gelatin-based film, the PANI tend to be in proximity and the rigidity of PANI become dominant (stiffness of the filler), which has an effect on the TS of the film (Girja et al., 2005). In other perspectives related to the moisture content, G-Gly-PANI have less moisture content compared to the G-Gly film as discussed in the previous sub-section. The reduction in moisture content was mainly due to the hydrophobicity of PANI. Hence, it lower the gelatin-water and glycerol-water interaction. On the basis, when the water interaction reduced, the film tends to have higher TS (Sanyang et al., 2015a).

On the other hand, the TS of the PANI/gelatin-based film loaded with larger range size of PANI (x), 125µm≤x≤250 µm, was lower compared to other samples. Concerning PANI/gelatin-based film loaded with PANI in the range size of 125µm≤x≤250 µm, the TS was lower than other samples. The reduction in tensile was expected due to the poor interfacial adhesion between PANI and gelatin matrix, which leads to the poor stress transformation across the interface. This happens due to the increased molecular mobility between the chains, thus enhancing the initial plastic effect (Nand et al., 2012). Moreover, this might also due to the larger particles sizes might damage the film during evaporation of film-forming solution. Meanwhile, G-Gly-PANI (C), exhibit highest EAB value. This was due to the movement and rearrangements of the macromolecules' chains of the matrix, which caused an increase in flexibility (Marana et al., 2013). Furthermore, particle distribution based on the Figure 4.16 (c) were more spacious in between each particle which does not impact on the flexibility of the film. Thus, the flexibility of the film was more likely based on the gelatin itself with minimal effect due to the PANI. In related to the moisture content of G-Gly-PANI (C) was higher in compared to G-Gly-PANI (A) and (B). In can be related to the less particle distribution due to the larger size of PANI and less effect of hydrophobicity of PANI resulting high moisture content and increase elastic deformation.

Table 4.12: Mechanical properties of PANI/gelatin-based films incorporated with different sizes and concentrations of PANI.

Sample*[1]	TS (MPa)	EAB (%)
G-Gly	14.83±1.11^{bc}	96.44±5.32^{a}
G-Gly-PANI(A0.5)	9.41±3.04^{cd}	52.35±15.53^{cd}
G-Gly-PANI(A1)	19.48±2.67^{ab}	46.75±0.35^{cd}
G-Gly-PANI(A2)	19.59±1.54^{ab}	31.62±6.27^{d}
G-Gly-PANI(B0.5)	14.97±0.13^{abc}	70.21±2.48^{bc}
G-Gly-PANI(B1)	21.92±0.75^{a}	50.84±4.31^{cd}
G-Gly-PANI(B2)	19.89±2.54^{ab}	31.41±0.94^{d}
G-Gly-PANI(C0.5)	10.02±0.40^{cd}	95.88±1.71^{ab}
G-Gly-PANI(C1)	8.51±1.86^{cd}	105.52±8.51^{a}
G-Gly-PANI(C2)	4.62±0.49^{d}	93.23±1.59^{ab}

*[1]G-Gly:=Gelatin based-film with glycerol (control), G-Gly(A0.5-C1)=PANI/Gelatin-based film
A=50μm≤x≤100μm; B=100μm≤x≤125μm;C=125μm≤x≤250μm (x: range size of PANI)
a,b,c Different superscripts indicate a statistically difference ($p<0.05$) within the same column

4.3.5 Chemical functional groups analysis in different size and concentration of polyanaline (PANI) incorporated into PANI/gelatin-based films

The FTIR spectra for the G-Gly and G-Gly-PANI are presented in Figure 4.14. The spectra of PANI/gelatin-based film (G-Gly-PANI) were very similar to the spectra of gelatin-based film (G-Gly). Based on the observation and finding, there were no new chemical interactions rise between the PANI and gelatin-based film. Thus, PANI only acts as a filler without change and interaction with the gelatin structure. Although the presence of PANI in the gelatin-based film can be seen as in the Figure 4.14 (Sub-section 4.2.2), peaks that correspond to the PANI were not seen in the FTIR spectra of the composite, as the PANI was still present at a low concentration. The gelatin peaks did not shift or broaden significantly upon loading of PANI. These findings were also similar to the study conducted by Nand et al. (2012), which indicated that, when the NR-PANI powder was deposited on the PET, no chemical interactions were evidenced in the FTIR analysis. The lack of the large shift of peak suggests that specific interactions between the molecules of the two polymers were limited (Woo & Jang, 1999) .

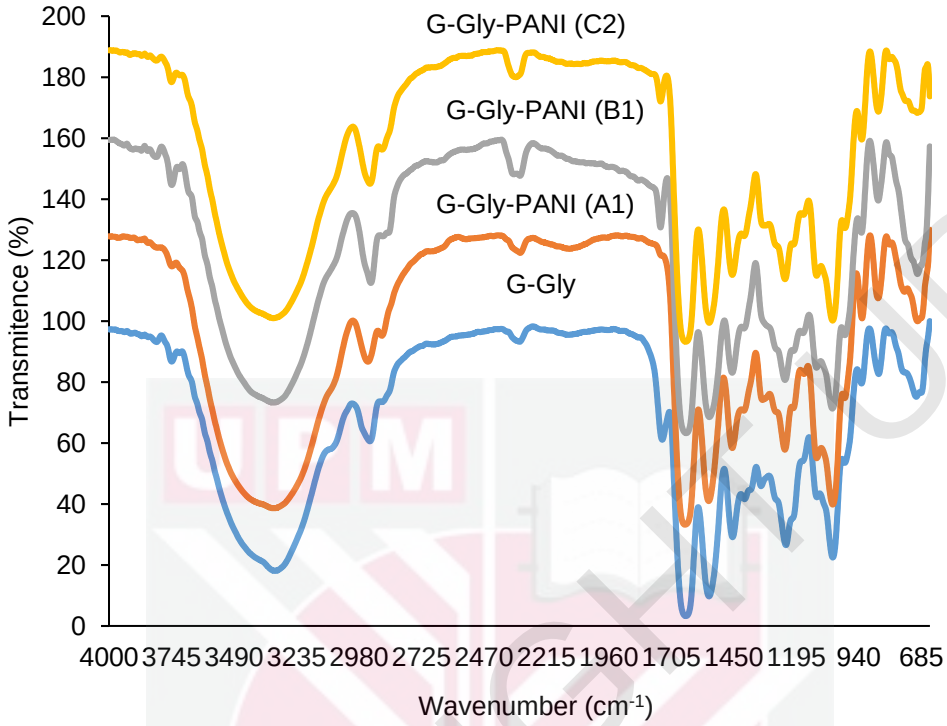

Figure 4.14: FTIR spectra of gelatin-based film without PANI (G-Gly) and with PANI (G-Gly-PANI)

4.3.6 Morphological analysis of PANI/gelatin-based film

The SEM images of PANI/gelatin-based film containing different sizes and concentrations of PANI are presented in Figure 4.15 and 4.16. The particle size of PANI incorporated into the film was measured with the ImageJ software. The size of PANI incorporated into the PANI matrix were the same and did not agglomerate upon dispersing. It can also be noticed that the PANI particles were dispersed uniformly in the micrograph image. Increasing PANI concentration, the matrix, and PANI resulted in it being more heterogeneous. This was due to the phase separation between nature of hydrophilic gelatin and hydrophobic PANI. Similar findings were also reported by Villasante et al. (2020), in which they incorporated the pecan walnut into the gelatin matrix exhibit phase separation in the heterogeneous composite. Acosta et al. (2015) also performed the study involving the addition of ester or fatty acids into the gelatin and yucca starch films resulted in phase separation. The immiscible and heterogenous composite of PANI and gelatin can be proven by from the DSC analysis, whereby the T_g of the control film without PANI will be differed compared to the film with the addition of PANI.

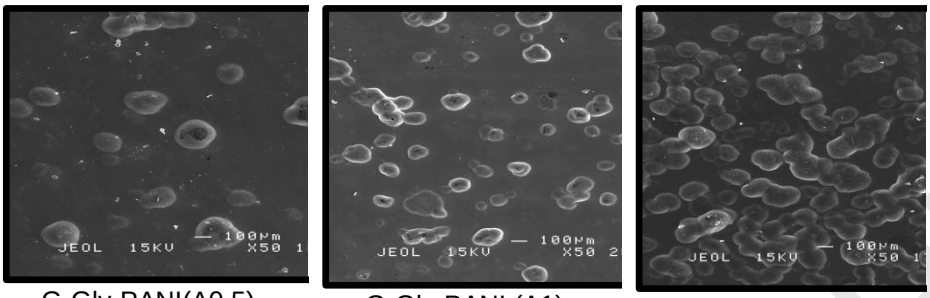

G-Gly-PANI(A0.5) G-Gly-PANI (A1) G-Gly-PANI (A2)

Figure 4.15: SEM micrograph of the PANI/gelatin-based films with different concentration of PANI with the same size of PANI

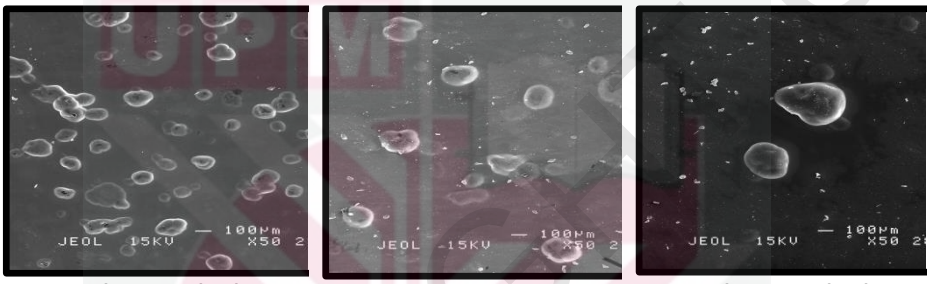

G-Gly-PANI(A1) G-Gly-PANI (B1) G-Gly-PANI (C1)

Figure 4.16: SEM micrograph of the PANI/gelatin-based films with different size of PANI with the same concentration of PANI

Based on the Figure 4.15 and 4.16 at higher concentration of PANI, the PANI particles tends to agglomerate near each others respective to the G-Gly-PANI (A) and (B). The TS of the G-Gly-PANi (A) and (B) were more higher compared to the G-Gly-PANI (C) at concentration 1 and 2 g/L. The increasing in TS can be associated with the reduction in size particles and increase in the surface areas. It was in agreement with Ghadermazi et al. (2019) that found by reducing the mycrocrytal size, the TS of the HPMC film increased and resistance to break. For the G-Gly-PANI (C), the particle distribution was more spacious due to the bigger size of PANI less particle size distribution. Hence, the EAB values for this films were more higher compared to the other size of PANI. The flexibility of the PANI was less effect by the rigidity of PANI.

4.3.7 Glass transition temperature (Tg) analysis of PANI/gelatin-based film

The thermodynamic characteristics are helpful and beneficial in determining the quality of films when they are in different conditions, such as temperature, gas pressure, or atmosphere (reducing or oxidant) (Villasante et al., 2020). The effect of PANI on the T_g of the gelatin films was examined and summarized in Table 4.13.

Table 4.13: DSC results for PANI/gelatin-based film incorporated with different sizes and concentrations of PANI.

Samples*[1]	T_g (°C)
G-Gly	59.91
G-Gly-PANI(A0.5)	64.83
G-Gly-PANI(A1)	67.00
G-Gly-PANI(A2)	61.72
G-Gly-PANI(B1)	68.89
G-Gly-PANI(C1)	67.84

*G-Gly:=Gelatin based-film with glycerol (control), G-Gly-PANI (A0.5-C1)=PANI/Gelatin-based film
*[1]A=50μm≤x≤100μm; B=100μm≤x≤125μm;C=125μm≤x≤250μm (x: range size of PANI)

The gelatin matrix and PANI were known to be immiscible. It has been noticed that the T_g of G-Gly-PANI moves towards lower values than G-Gly. The increasing in T_g value was related with the higher TS and lower moisture content obtained as discussed previously. This indicates lack of miscibility between the components and heterogenous. As increasing the concentration of PANI from 0.5 g g/L to 1 g/L, the T_g of the films showed an increment in value. Meanwhile, the T_g of the film marginally decreased back when the PANI concentration loading into the film increased to 2 g/L. Generally, the shift trend of T_g can be considered as the index of miscibility of polymer blends (Bhandra et al., 2017).

On the other hand, based on the observation on the changes in T_g at different sizes of PANI, the shifted temperature was only at 1 °C irrespective of the concentration of PANI loading into the film. This suggests that the absence of interaction between the two polymers. These findings were in agreement with the study of Nand et al. (2012), in which the T_g of the NR-PANI with PET composite incorporate with different NR-PANI does not differ significantly due to the absence in interactions between those two polymers.

4.3.8 Thermal degradation analysis of PANI/gelatin-based film

TGA parameter presenting thermal degradation behavior of gelatin films incorporated with PANI is tabulated in Table 4.14 with the degradation temperature (T_d) and weight loss (Δ_w). The thermal behavior of both gelatin-based film with and without the addition of PANI proceeds in three stages

irrespective to the size and concentration of PANI. For all the films, the first stage weight loss at 4.72-7.97% was obtained at T_d of 101.48-158.4 °C. The first step of weight loss was caused by the moisture, free acids, and unreacted monomer that were used as solvents and dopants in preparation of the PANI (Bhadra et al., 2017). The major components in the first weight loss are due to the moisture vaporization (loss of free and adsorbed water) (Lewandowska, 2009). The lower weight loss of the G-Gly-PANI(A) with a small size of PANI was observed might be associated with lower water content (sub-section 4.2.3) irrespective of the concentration of PANI. Similar observation was observed by Tongnuanchan et al. (2011), in protein-based film from various sources including tilapia.

Table 4.14: Thermal degradation temperatures (T_d, °C) and weight loss (Δ_w, %) of tilapia's fish scale gelatin based film incorporated with glycerol.

Sample films	Δ_1		Δ_2		Δ_3	
	$T_{d1,onset}$ (°C)	Δ_{w1} (%)	$T_{d2,\ onset}$ (°C)	Δ_{w2} (%)	$T_{d3,\ onset}$ (°C)	Δ_{w3} (%)
G-Gly	130.67	3.86	277.31	10.72	486.29	46.01
G-Gly-PANI(A0.5)	101.48	4.72	252.39	16.45	527.67	46.93
G-Gly-PANI(A1)	114.82	3.55	276.90	12.01	537.68	43.53
G-Gly-PANI(A2)	158.49	6.93	282.83	15.27	537.67	40.68
G-Gly-PANI(B1)	126.44	7.29	282.52	18.41	517.96	39.89
G-Gly-PANI(C1)	158.4	7.97	281.45	18.01	549.72	46.55

A=50μm≤x≤100μm; B=100μm≤x≤125μm;C=125μm≤x≤250μm (x: range size of PANI)

The second stage of thermal degradation for G-Gly-PANI films ranges from 252.39 - 282.83 °C (Δ_{w2} = 12.01-18.41%) that differ when compared to the G-Gly film, 277.31 °C (Δ_{w2}=10.72%). This second degradation step was related to the degradation of glycerol, a small size of protein in the film network together with chemisorb water molecules (Sanyang et al., 2015; Tongnuanchan et al., 2013). G-Gly-PANI films exhibit low thermal stability in terms of temperature and weight loss in the second stage. This is presumed due to the less amount of chemisorb water molecules in the film network.

In general, the T_{d3} of the gelatin-based film loaded with PANI in the range of 517.96-549.72°C was higher than the control film, 486.29 °C (G-Gly film) irrespective of the concentration and size of PANI. This can be correlated with the interruption in protein-protein interaction of gelatin molecules in film network by PANI (Tongnuanchan et al., 2013). Hence, the incorporation of PANI might contribute to the higher stability of the film network.

4.3.9 Water vapor permeabilty properties of PANI/gelatin-based films

One of the principal permeants researched in food packaging applications is water vapor, since it may pass through the polymer package wall from the interior or external environment, changing the quality and shelf life of the product (Kanatt et al., 2012). The water vapor permeability (WVP) of the films stored at 25 °C and 50% RH is shown in Table 4.15. Generally, the incorporation of the PANI in the gelatin-based film at small size of PANI (x) group A (50μm≤x≤100μm) and B (100μm≤x≤125μm) at different concentrations of PANI had less or no notable effect on the WVP of the films. Thus, the incorporation of the small size of PANI filler hardly affected the permeability of the gelatin-based film. This was possibly due to the complexity of the water molecule's sorption and diffusion pathways, as well as the involvement of the microstructure of the polymer matrix. Rather than following the solution-diffusion model, the water molecules could have followed the water-cluster model (Siparsky et al., 1997; Yoon et al., 2000). Water molecules have a significant propensity to create hydrogen bonds with other polar groups and among themselves. It was then suggested that the water molecules would ideally form clusters by forming hydrogen bonds with one another, resulting in poor solubility and low diffusivity of water vapor through the polymer matrix. In the end, it limits the transfer rate of water molecules, and so, the WVP was not affected by the addition of PANI.

Meanwhile, the inclusion of large size of PANI, which was in the range of more than 125 μm but less than 250μm, resulted in a reduction of WVP at low concentration but increment at high concentration of PANI. The reduction in WVP at low concentration of PANI was related to the hydrophobic compound (PANI) that exerts a greater barrier to water vapor. At a high concentration of PANI, the particles tend to be in proximity and behave as large particles, which then provide an additional free surface for the water vapor particles to permeate through the film. Sudár et al. (2007) reported that particle aggregates can act as large particles and de-bonding under the effect of external stress. This phenomenon hinders interactions between the gelatin chains and water molecules; hence, the water molecules can freely pass through the films and consequently caused the increment in WVP (Kavoosi et al., 2013).

Table 4.15: Water vapor permeability (WVP) measured at 25 °C and 50% RH

Samples*[1]	WVP(x 10^{-6}gm/m^2.day.Pa)
G-Gly	3.09±0.33[ab]
G-Gly(A0.5)	3.14±0.99[b]
G-Gly(A1)	2.64±0.02[ab]
G-Gly(A2)	2.43±0.15[b]
G-Gly(B0.5)	2.53±0.57[ab]
G-Gly(B1)	2.83±0.17[ab]
G-Gly(B2)	2.91±0.50[ab]
G-Gly(C0.5)	2.09±0.01[b]
G-Gly(C1)	2.38±0.13[b]
G-Gly(C2)	3.90±1.44[b]

*[1]A=50μm≤x≤100μm; B=100μm≤x≤125μm;C=125μm≤x≤250μm (x: range size of PANI)

a,b, Different superscripts indicate a statistically difference ($p<0.05$) within the same column

4.3.10 Antioxidant activity PANI/gelatin-based film

The free radical scavenging capacity used to measure the antioxidant activity of the gelatin and PANI/gelatin-based film is presented in Figure 4.18. Many researchers have explored the mechanism of the reaction between PANI and DPPH (Nand et al., 2011, 2012; Saikia et al., 2010; Wang et al., 2007). After 24 hours of reacting PANI with DPPH, the emeraldine salt form was converted into fully oxidised pernigraniline, which did not possess any hydrogen atom for reducing DPPH. A material's antioxidant activity is depended significantly on the material's ability to donate hydrogen to minimize DPPH, and thus, the structural conformation of the material plays a crucial role in its antioxidant activity (Saikia et al., 2010).

From Figure 4.17, it can be said that the free radical capacity of the PANI/gelatin-based film significantly increased ($P<0.05$) with the increase in the PANI concentration for 1 g/L and 2 g/L of PANI irrespective of PANI sizes. This observation was in agreement with other studies, where higher free radical scavenging was achieved with increased PANI loading using the same DPPH assay method (Azmi et al., 2019; Nand et al., 2012; Saikia et al., 2010). The increment in free radical scavenging activity capacity with the increase in PANI concentration was expected, since the amount of PANI concentration that exhibits antioxidant property is increased. PANI reduces the DPPH radicals by donating hydrogen atoms, while the PANI segments are, in turn, oxidized to the pernigraniline form when in contact with DPPH radicals (Nand et al., 2011).

Therefore, a higher free radical scavenging capacity was achieved by having a higher concentration of PANI particles being exposed to the DPPH test solution. The low loading of the PANI may be sufficient for the radical scavenging performances of the film, as PANI has a reversible redox property and can be readily oxidized and reduced by species in contact with the film. This can be attributed to the fact that PANI owing to its redox-active nature, is efficient in scavenging the free radical DPPH and such with the increase in the antioxidant activity of the material. This was due to having more hydrogen atom available for donating to eliminate DPPH. The C-N and C-N + groups in the PANI structures are important units when it acts as DPPH free radical scavenger. The C-N and C-N + groups are oxidized through C≡N species, and this is a possible mechanism in this reaction (Hsu et al., 2009).

The relationship of size of PANI loading in PANI/gelatin-based film with free radical scavenging activity was plotted and presented in Figure 4.17. It can be observed that the percentage of DPPH were not significantly different among all three different range sizes of the PANI ($P>0.05$). These granulometric classes showed the highest DPPH scavenging with maximum DPPH percentage of 48.02% (Sample B2) for the $100\mu m \leq x \leq 125\ \mu m$. Zaiter et al., (2016) have made similar observations with green tea powders, where the radical scavenging activity were not significantly difference among three different fractions size of green tea powder.

The results indicated that active conducting polymer (PANI) was available to the test solution (DPPH assay) and was not completely blocked by the presence of gelatin. The prospects for active packaging involving conducting polymer remain exceptionally promising as the effects of solid antioxidant material can be used to extend product shelf-life. Hence, PANI/gelatin-based film has the potential to be used for active film applications.

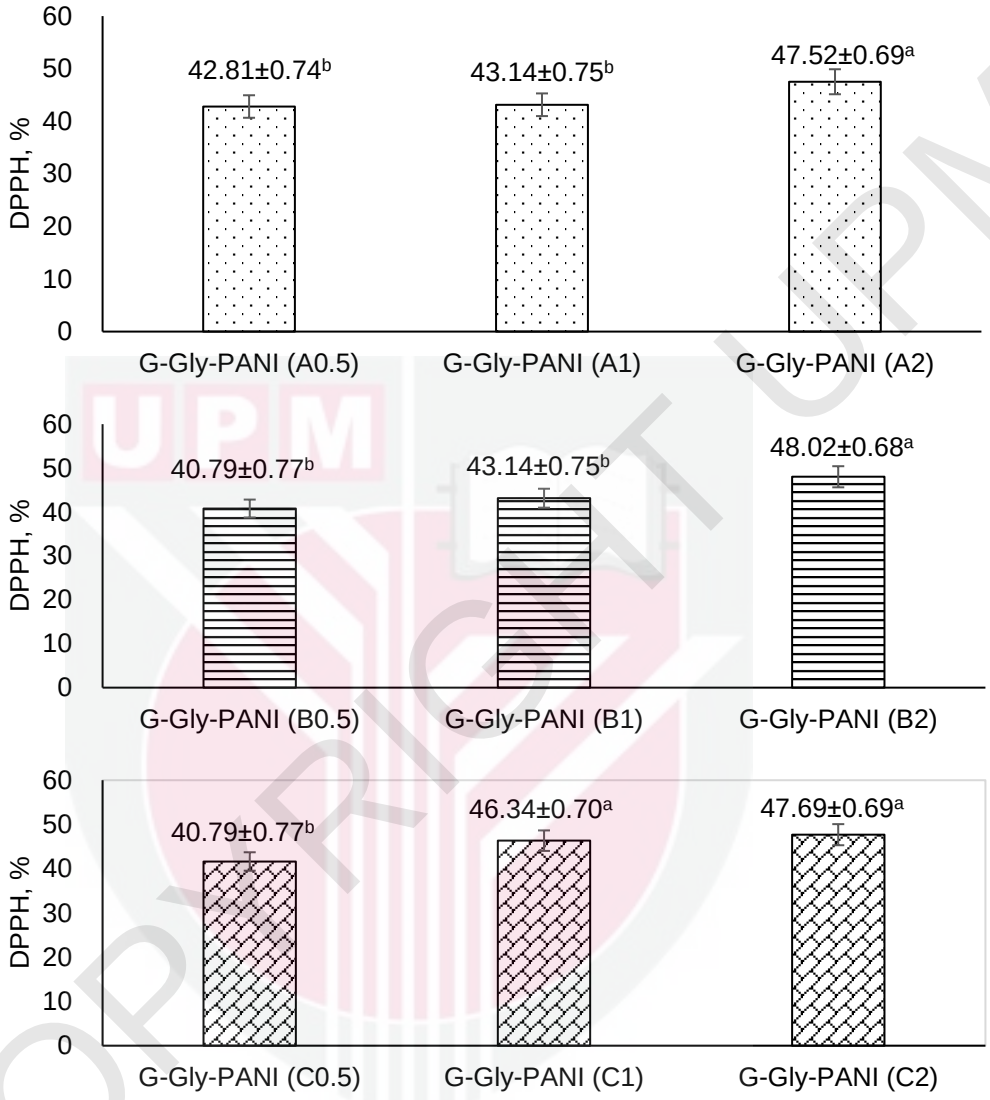

A=50μm≤x≤100μm; B=100μm≤x≤125μm;C=125μm≤x≤250μm (x: range size of PANI)

a,b, Different superscripts indicate a statistically difference ($p<0.05$) within the same column

Figure 4.17: Free radical scavenging activity of gelatin-based film

4.4 Efficiency and behavior of self-healing properties on PANI/gelatin-based film

4.4.1 Behavior of self-healing by water stimulation

Figures 4.18-4.21 illustrates the self-healing behavior of the gelatin-based film. The film was damaged by a razor blade, and the cracks between the edge were photographed by light microscope. Drops of water were added to the damaged zones of films to enable the occurrence of healing process. As shown in Figures 4.18-4.21, the fresh crack faded and could not be seen after five minutes of healing. The recovery or healing process of the sample was due to the self-complementary and mobile hydrogen bonding network sites (Luan et al., 2018). When the samples were incised, the weaker hydrogen bonds on the open cut sides were broken and linked with other non-associated groups. Once the open cut sections comes in contact with water, the broken hydrogen bonds are then associated once more – which drive the molecular chains to move, touch. and get tangled back, reverting to its original state.

Figure 4.18: Microscope images (x 10 magnification) of fresh-cut (left) and self-healed (right) film for gelatin-based film. Arrows indicate the incision line.

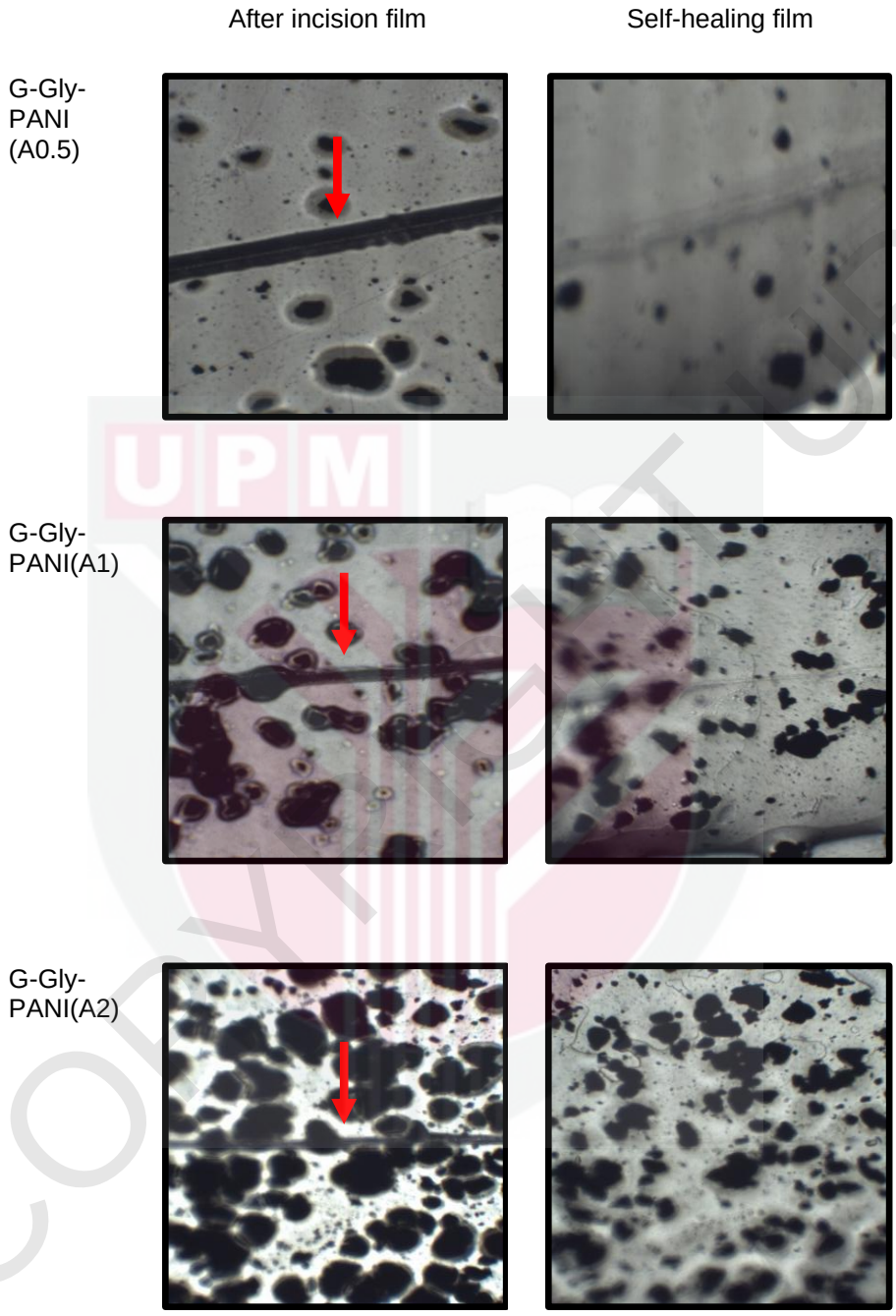

Figure 4.19: Light microscope images (x 10 magnification) of fresh-cut and self-healed film for PANI/gelatin-based film (A=50μm≤x≤100μm (x: range size of PANI))

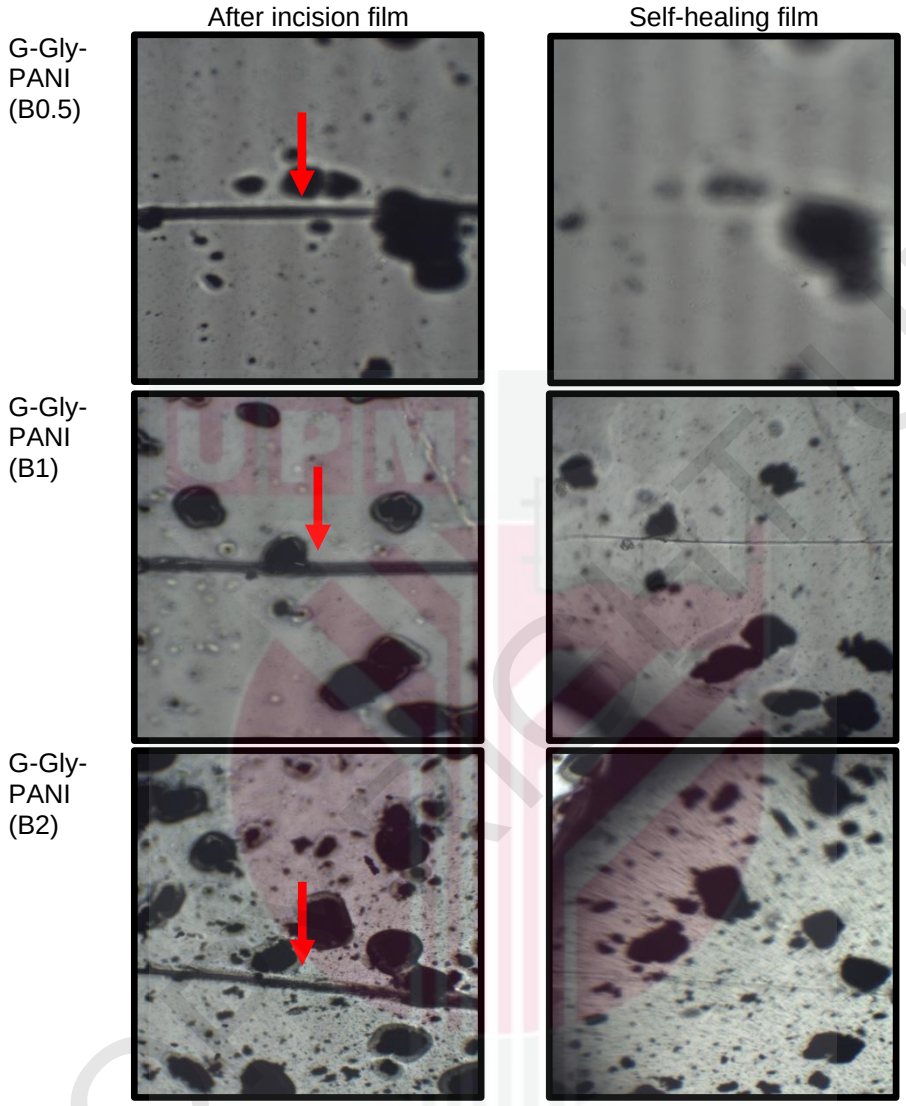

Figure 4.20: Light microscope images (x 10 magnification) of fresh-cut and self-healed film for PANI/gelatin-based film (B=100μm≤x≤125μm (x: range size of PANI))

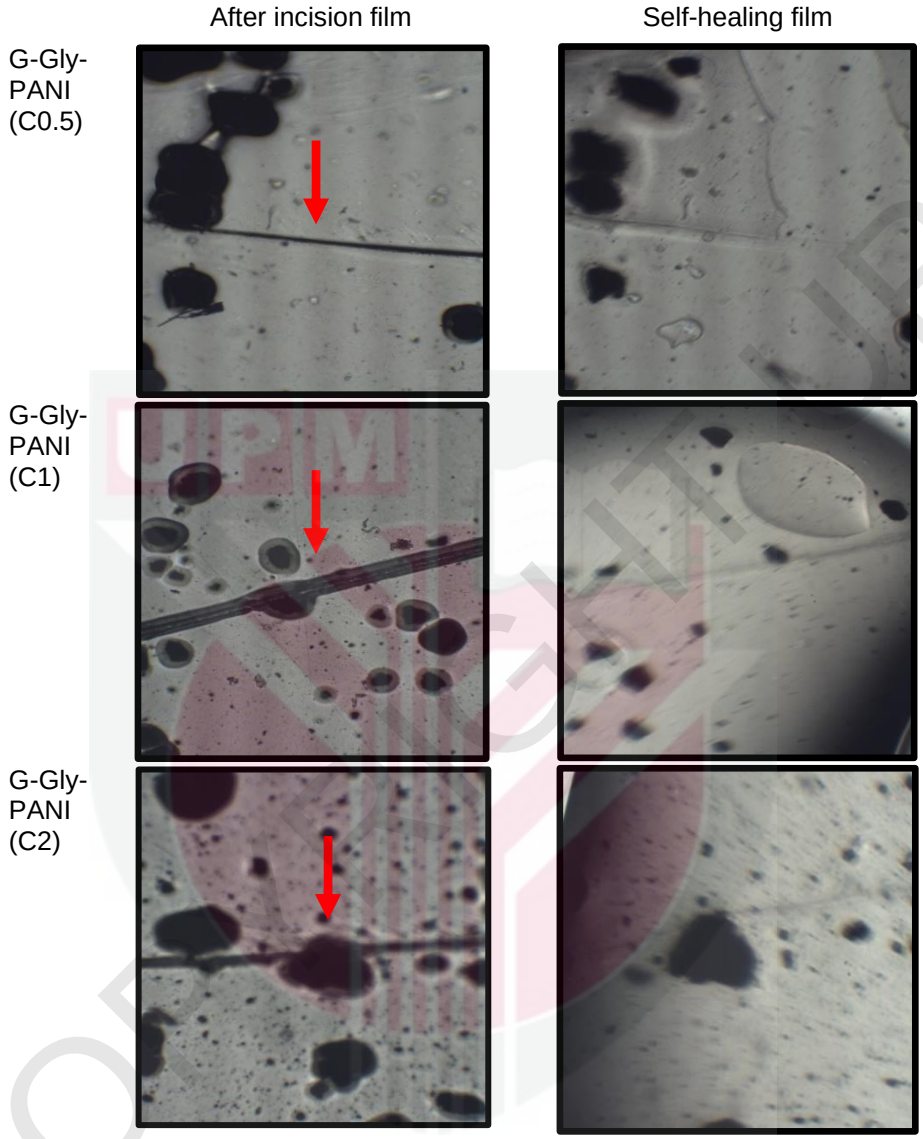

Figure 4.21:Light microscope images (x10 magnification) of fresh-cut and self-healed film for PANI/gelatin-based film (C=100μm≤x≤125μm (x: range size of PANI))

After healing for five minutes, new hydrogen bonding emerged in the gap due to the swelling of the damaged films and mobility of the polymer chains under the stimulus of the water (Song et al., 2017). The self-healing ability of the films could be ascribed to the water induced swelling and high mobility of the polymer network that facilitates the reconstruction of hydrogen bonding under the water assistance (Wittmer et al., 2018). Absorbed water interrupted the intermolecular

hydrogen bonds in the polymer and mobilized the polymer chains for the self-healing process. Originally, the stability of the secondary or triple helix structure was due to the formation of hydrogen bonds through glycine residues, which are present in α-chains (Ramachandran & Kartha, 1954). The hydrogen bonds were formed between hydrogen atoms of glycine and oxygen atom from -COOH groups (Figure 4.22 (a)) (Oakenfull & Scott, 2003). Thus, in the healing process with the existence of water, the hydrogen bonding at the cut interfaces can be developed in either way: (1) with -OH of two hydroproline or (2) with -C=O of gelatin network and -OH of hydroproline (Figure 4.20 (b)). The efficient intrinsic self-healing of the gelatin-based film is contributed to sufficient free hydroxyl groups at the open cut interfaces to reform hydrogen bond across the interfaces (Zhang and He 2015). Hence, the healing process of the gelatin-based films in this study was factorized by the hydrogen bonding that induced by the high amounts of glycine and hydroproline in the gelatin. During the healing process, the water in contact with the cutting part was also adsorbed into the films, with no other forces acting on it. The osmotic pressure of the water will cause the gelatin to swell and the network to mix and expand. Simultaneously, the elastic restoring force of the gelatin network will try to resist the expansion. When the opposing forces were balanced, at a given time, the gelatin network would stop absorbing water when the equilibrium was reached (Doi, 2013). Physical diffusion is one of the keys elements for the self-healing process. The additional water is referred as free water. Furthermore, glycerol in the film will also create the hydrophilic hydroxyl groups as active sites that gave attractions to the water molecules and facilitate the healing process (Nor et al., 2017; Sanyang et al., 2015). The swelling of the gelatin gave an impact on the tensile properties after self-healing and will be further discussed in the next section.

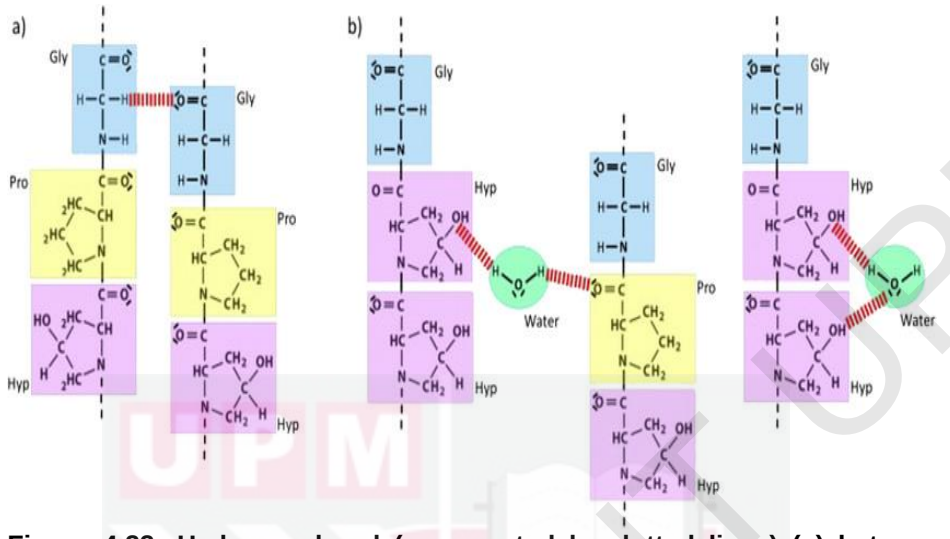

Figure 4.22: Hydrogen bond (represented by dotted lines) (a) between gelatin strands and (b) among gelatin strands and water molecules (Source: Duconseille et al. (2015)).

Figure 4.23 shows the graphical overview of the self-healing processed after incision by using stimuli of water for PANI/gelatin-based film. When the PANI/gelatin-based film was exposed to mechanical incision, the hydrophobic interlinked (bridges) between the gelatin chains ruptured in abundance, thereby exposing the hydrophobic PANI molecules to interstitial water contact and immediately formed an overlap junction to create water depletion region which facilitated the film healing. The adsorbed water molecules tend to form clusters rather than distribute homogoneusly into the polymer matrix (water-water interactions) (Canales et al., 2011). Thus, hydrophobic PANI aid in creating the water depletion on the cutting area and hydrogen bonding between the -NH group or -COOH group with water and later facilitated the healing process. This is manifested in the experimental observation (Figure 4.17-4.19). In the study by Sharma et al. (2017), the self-healing of the iongels was due to the hydrophobic interactions in the tail side of the 1-ethyl-3-methylimidazolim chloride ionic liquid in the gelatin that formed overlap junction and created water depletion and initiated the self-healing. Figure 4.24 shows the simplified illustration of film matrix interactions with glycerol and PANI.

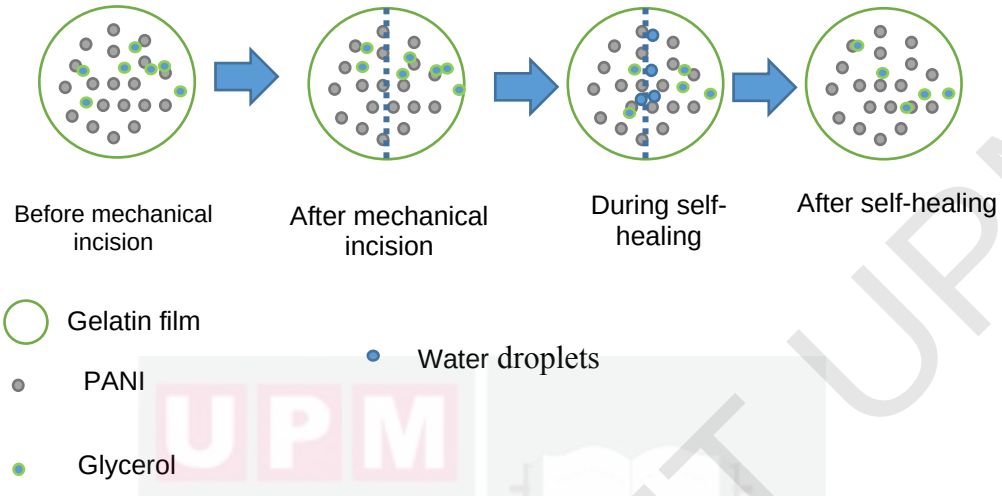

Figure 4.23: Graphical overview of the self-healing process

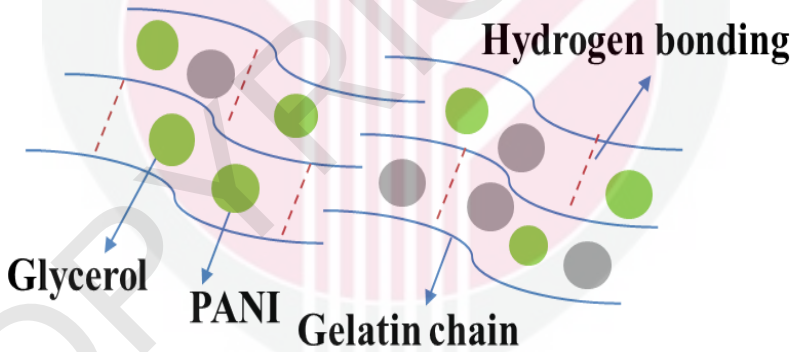

Figure 4.24: Scheme of gelatin matrix interactions with glycerol and PANI

4.4.2 Effect of mechanical strength of gelatin-based film after self-healing

Since the flexibility of molecular chains is also critical to the self-healing ability, the mechanical properties of the self-healed gelatin-based films were determined. It was found that the healed samples were stretched to different strains, depending on the samples as displayed in Table 4.16.

Based on the data tabulated in Table 4.16, TS and EAB of the self-healed films were reduced in compared to the before incision film. However, the strength of the films still can be considered to restore although the TS was not similar as before the incision. Previously, it has been explained that the intrinsic of the self-healing utilized the interactions between the chemical bonds, which include the reversibility of non-covalent bonds (hydrogen bond), to rearrange the polymer chains, and restore the destroyed interactions at damaged interfaces in the healing process. The tensile properties of the healed films still show decrement compared to the original film, which caused by the swelling effect during the healing process. When the water induced in between the cut open spaced, the water diffused into the network film due to the free volume for interdiffusion and formed hydrogen bonding with the free hyroxyl group in the protein network (hydrogen bonding). From the result obtained in Table 4.15, the TS values for high concentration of PANI incorporation in the gelatin-based film was increased after the healing process. This was due to the high concentration of hydrophobic PANI in the film that reduced the amount of water absorded by the film, resulting in less water being bound to act as other plasticizer on the film, reducing the weakening of the film structure and increased the TS (Suppakul et al., 2013). Moreover, after the healing process, the film absorb water using water stimuli and impact on the hardness of the film. Thus increasing the TS of the film after self-healed.

The swelling of the film also affected the EAB of the film. The EAB was significantly decreased for the self-healed film in comparison to the film before incision. The high reduction in EAB after self-healing processed was due to the numerous hydrogen bonding bonding between the gelatin that led to the reduction in the molecular mobility (Othman et al., 2019). In addition, the swelling process will undoubtedly impact the tensile properties of the films.

Table 4.16: The mechanical properties of the original and self-healing gelatin-based film.

*Sample	Before incision		After self-healed	
	TS(MPa)	EAB(%)	TS(MPa)	EAB(%)
G-Gly	14.83±1.11	96.44±5.32	14.15±0.50	19.5±2.12
G-Gly-PANI(A0.5)	9.41±3.04	52.35±15.35	13.35±3.74	12.00±0
G-Gly-PANI(A1)	19.48±2.67	46.75±0.35	16.50±2.12	8.5±3.54
G-Gly-PANI(A2)	19.59±1.54	31.62±6.27	15.50±2.12	4.00±0
G-Gly-PANI(B0.5)	14.97±0.13	70.21±2.48	14.30±8.06	24.50±24.5
G-Gly-PANI(B1)	21.92±0.75	50.84±4.31	8.46±0.63	12±2.83
G-Gly-PANI(B2)	19.89±2.54	31.41±0.94	14.99±0.16	10.6±1.10
G-Gly-PANI(C0.5)	10.02±0.40	95.88±1.71	16.35±0.10	11.27±1.26
G-Gly-PANI(C1)	8.51±1.86	105.52±8.51	13.34±0.68	8.33±0.79
G-Gly-PANI(C2)	4.62±0.49	93.23±1.59	13.56±0.79	14.05±0.76

4.4.3 Sorption isotherm and sorption model analysis of PANI/gelatin-based film

Moisture sorption isotherm for the film describes the relationship between the moisture content and water activity of the surrounding. Figures 4.25 shows the moisture content of the gelatin-based film, respectively, at different temperature (5, 30, and 40 °C) and RH (23,33,43,57,75%) for seven days. It can be seen that the moisture content of the films increased within 24 hours, which indicates the early stage of moisture sorption of the film. This phenomenon was due to the high partial pressure of saturated vapor at the initial stage (Chinma et al., 2015; Othman et al., 2019). After 24 hours, the moisture content of the film attained plateu, which indicates that the moisture content equilibrated with the RH (Mali et al., 2005). As apparent, the rate of water sorption declined with time as the moisture content inside the film was increased.

From the findings, moisture content of the films was seen to be influenced by the RH. Moisture content of the films stored at high RH conditioned contained a high amount of moisture content compared to film stored at low RH conditioned. For an example, the equilibrium moisture content (EMC) of G-Gly film at a temperature of 5 °C is 22.42% in 57% RH condition, while EMC of G-Gly film at the same temperature but different RH condition of 75% is 37.35%. In high RH condition, it contained a high amount of water molecules that can be adsorbed by the film. By increasing of moisture content at high RH, such a move caused the film to swell and open the new binding sites for water and increase the EMC (Chowdhury & Das, 2012). The addition of glycerol also contributes to the higher EMC. This can be related to the increased in the free volume in the films, which enhances the mobility of the polymeric chains that lead by the incorporation of glycerol between the protein chains, and also increased the active site to interact with the water (Hoque et al., 2011). Moreover, strong hygroscopic nature of gelatin and glycerol give impact on the G-Gly film to absorb moisture from the surrounding.

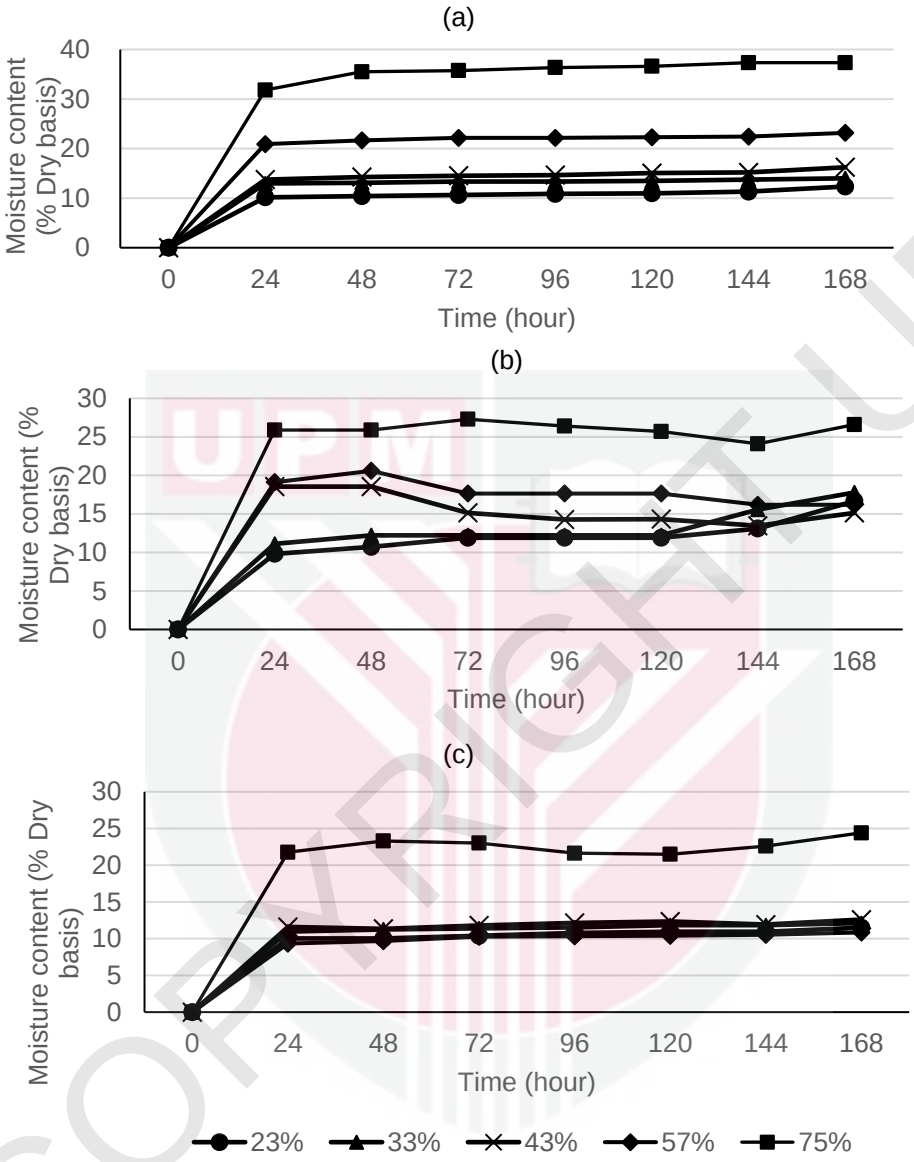

Figure 4.25: Water sorption data of G-Gly film at different RH (23,33,43, 57 and 75%) and temperature (a) 5 °C; (b) 30 °C and (c) 40 °C.

Moreover, more time was required for the moisture content of the films to achieve equilibrium at high RH. From the findings, for example, at 5 °C for 57% and 75% RH, the EMC was archived 96 and 144 hours, respectively. Previously, it was reported by Mostafa & Sourell, (2009) that the increase of equilibrium moisture content also features to a decrement in the vapor pressure insufficiency at high RH. This situation leads to the production of an atmosphere near the saturation that increasing the capability of the film will absorb extra moisture from the

atmosphere (Othman et al., 2019). The gap of water activity between the film and the surrounding also affected the time for the sorption activity to achieve equilibrium. Hence, the saturated water molecules in the surrounding also lead to spending extensive period than usual for the water sorption activity to reach equilibrium.

Besides, the effect of temperature on the water sorption of the films has also been studied and observed from the EMC of the film (Othman et al., 2017). Based on the Figure 4.23, the EMC of the films decreased as the temperature increased irrespective of the RH. This phenomenon occurred due to the binding characteristics of the water molecules in the film matrix. At high temperature, some of the water molecules are activated to the energy levels that allowed them to break away from the sorption sites in the film, thus decreased the amount of water absorded. This was related to the fact that, at high temperature, some water molecules are activated to energy levels that allowed them to break away from the sorption sites in the film (Bajpai et al., 2017). On the other hand, at low temperature, the intermolecular attractive forces between the active polar sites within the film matrix and the water vapor molecules are strong based on the less kinetic energy of vapor molecules.

Next, the water sorption data of the film analyzed at different temperature and RH was then fitted using rearranged Peleg's model. The data was plotted using $t/(M_t-M_i)$ versus time, t graph, to obtain the Peleg constants. Table A1-A3 listed out the k_1, water sorption rate and k_2, water sorption capacity, as well as R^2 values that were obtained from fitted curved. It can be observed that $k_1$and k_2 decreased with the increase of RH. The low k_1 value indicates that the film exhibits high initial water sorption rate (Peleg, 1988) and k_2 indicates the film exhibit high water adsorption capacity (Mali et al., 2005). This finding is consistent with the previous discussion, whereby the increase in RH resulted in an increased in EMC. Many polar groups like -COOH and-NH_2 along the gelatin molecules increase the EMC while increasing the RH. These groups act as strong binding sites for the water molecules to be adsorbed.

From another perspective, the k_2 values for PANI/gelatin-based film were higher than gelatin-based film. This indicates that the water sorption capacity of PANI/gelatin-based film was lower than gelatin-based film. This may be attributed to the fact that gelatin is a hydrophilic polymer with a number of polar groups along the macromolecular chains, which interact with the incoming vapor molecules that cause the water uptake (Bajpai et al., 2017). Meanwhile, the PANI/gelatin-based film has PANI as one of the constituents that does not interact with water due to the hydrophobicity properties of PANI. Hence, the water becomes less contact with the polar active sites of gelatin due the existence of PANI. In addition, the sorption rate for the PANI/gelatin-based film was faster compared to the gelatin-based film. Thus, PANI/gelatin-based film reached the equilibrium state early than gelatin-based film. This would mean there will be fewer chances for the film to hold more water and reduced the water

sorption capacity of the film. PANI is creating the water depletion in the near areas and thus increased the sorption rate.

Overall, based on the Peleg's model analysis, the findings are noteworthy to be determined since the sorption behavior of the film needs to be studied thoroughly before it can be used for the designated application, particularly in understanding the behavior of self-healing properties.

In line to investigate the water sorption isotherms of the film, the water sorption data of the films at different level of RH and temperature was then fitted using the GAB model (Equation 3.6, a_w/M_e versus a_w). The fitted curves resulted in a second order polynomial equation and the constant values calculated from the equation were used to determine the GAB constant parameter (k, W_m, and C) using equations 3.7-3.9. The GAB constant parameters as well as R^2 were tabulated in Table A4. The GAB constant parameters obtained were affiliated for factor correcting properties of a multilayer molecules (k), GAB monolayer moisture content (W_m), and Guggenheim constant (C). Among all the GAB constant parameters, W_m is the most crucial parameter to be studied (Akoy et al., 2013). The monolayer moisture content corresponds to the minimum moisture to avoid from auto-oxidation and improving the stability of the product throughout the storage period (Ogbonnaya Chukwu, 2010). W_m also indicates the number of water molecules that are strongly bound to the active sites grants on the surface of the substrate, considered as an optimum value in assuring stability of the substrate (Bajpai et al., 2017).

From the tabulated data in Table A4, W_m for all the sample films, decreased as the temperature increased from 5 °C to 30 °C but increased at 40 °C. At temperature of 30 °C, the total number of the active site for the water bindings was decreased owing to the physical and chemical changes in the film that were mainly caused by the temperature. In contrast, W_m was increased at 40 °C, which was caused by the ability to decrease the moisture content in the surrounding.

The values of W_m for gelatin-based film were higher in compared to the PANI/gelatin-based film, which was attributable to the presence of various polar groups along the gelatin chains, resulting in having more sites for attachments of water vapor molecules compared to the PANI/gelatin-basd film. Furthermore, the hydrophobic properties of the PANI block or disturbed the sorption of water molecules on the active site of gelatin. Moreover, the tortuous water pathway created by the PANI in the films lower the water permeability of the films, resulting in having lesser water adsorbtion to the sorption films (Othman et al., 2017).

As for the Guggenheim constant, C describes the adsorbent-adsorbate interactions. From the Table 4.19, the C values for all the films was less than 2. For the value of C, in that, between $0 < C < 2$, the isotherm adheres to type III

GAB isotherm (Bajpai et al., 2017). These findings were consistent with the studies by Al-Muhtaseb et al. (2002) and Saberi et al. (2015), which obtained sigmoidal shape curve data without a point of inflection (type III). Finally, for the value of K that provides a measure of interactions between the energy values of the molecules in the monolayer and that of water yield a value of less than 1 and more than 0. Additionally, the hydroxyl groups of glycerol on the sorption site of the matrix could increase the interactions energies between the water molecules on the second and higher water layers and polymer.

Among other models tested, only the GAB model can be used accurately to describe the gelatin-based film. Table A5-A7 show the isotherm models used in this study and the calculated constant values summarized in the table. The Smith constant, A (intercept) and B (slope) were computed from the linear regression of M versus -ln(1-a_w) line. The Halsey model constant were calculated from a linear plot of ln M vesus ln(-ln(a_w)) by taking the intercept (a) and slope (b). As for the Caurie model, the sorption data were fitted in a linear plot of ln (M) versus a_w. Smith Halsey and Caurie models, which show fewer acceptable performance in the experimental data fitting, where the R^2 for all temperatures were less than 0.95.

Further study on the effect of surrounding conditions (RH and temperature) on the self-healing behavior of PANI/gelatin-based film was investigated. For the range of RH, only 43%, 57%, and 75% were studied. These specific points were chosen based on the findings in the sorption analysis of the films, where the high RH has more significant effect in relation to EMC, sorption rate, sorption capacity, and W_m.

4.4.4 Effect of difference environmental conditions (temperature and RH) on the film self-healing ability

Previously, the self-healing behavior was observed by stimuli of water directly to the damaged part. In the following sub-section, the self-healing experiments were performed as a function time to evaluate the speed and progress of moisture-triggered process at different RH and temperature. The efficiency of the self-healing was different between the water-stimuli and moisture-stimuli. The self-healing was triggered by the moisture, depending on the relative humidity of the surrounding that provide the amount of water in the vapor state The self-healing processed of the gelatin-based films were stored at different RH (43%, 57% and 75%) and temperature (5 °C, 30 °C and 40 °C), and subsequently observed by image analysis.

The experiments revealed that the speed and degree of the self-healing process depends on the moisture content and temperature. Figure A1-A6 showed the self-healing processed at lower RH (43% and 57%) at different temperature. Under low RH conditions, the healing process tend to be slower and the

damaged does not fully heal. The film tend to resist the sorption due to the dense hydrogen-boding network, which resist the swelling at low RH (Lee & Lee, 2013). In fact, at low RH, the air surroundings contain less amount of water molecules compared to the high RH conditions, thus having less amount of moisture in contact with the films. Based on previously analyzed Peleg model, aspects of low sorption rate and capacity were observed at low RH, which attributed to the findings that the healing process was distorted and improperly heal.

Nevertheless, under high RH conditions (75%), the sample can be seen to self-heal almost to its full extent, irrespective of the different temperatures as illustrated in Figure 4.26-4.28. At high RH, the adsorbed moisture interrupts the intermolecular hydrogen bonds in the polymer mobilizing the former rigid fraction. Thus, the mobilized polymer has higher free of motion to trigger self-healing. In conjunction with the findings on the moisture sorption behavior at high RH, the film tends to swell and open up new bonding sites for the water to be adsorbed at the damage area. Hydrogen-boding of water to the accessible -COOH and $-NH_2$ in the active side of gelatin is responsible for gelatin sorption isotherm, which then supports the act of self-healing the damaged part. Figure 4.26 showed the healing process, in which the process is present as early in Day 4 at lower temperature compared to the high temperature 30 and 40 °C. In addition, the hygroscopic nature of gelatin and glycerol also affect the healing process through different temperature and RH. Based on the moisture sorption study in the previous section, the EMC of the plasticized film was higher compared to the unplasticized film, which helped heal the damaged film at low temperature and high RH condition.

As previously discussed in the GAB model sorption analysis, the W_m of the films indicates the maximum volume of water, which can be adsorbed by a single layer per gram of dry films (Strauss et al., 1991). The adsorption of water molecules must give changes corresponding to the mass change (water sorption analysis). Generally, all the films, including gelatin-based film and PANI/gelatin-based films, have W_m 0.1208-1.252 per gram of dry solids. According to the GAB model parameter, which is W_m, if assuming one hydrogen bonds with another water molecule, the maximum amount of hydrogen bonding in 1 g of composite film is at 0.1208 mol. However, if the amount exceeds that, the films will not adsorb any water as it has achieved the equilibrium state and maximum water adsorption capabilities. Thus, from the sorption model, the application of the water sorption analysis can be utilized in monitoring and characterizing the healing process.

*Sample	Day 0	Day 4	Day 7
G-Gly	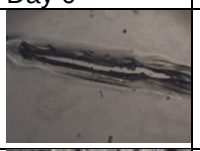		
G-Gly-PANI(A0.5)	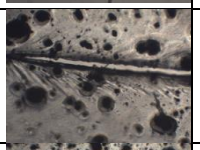	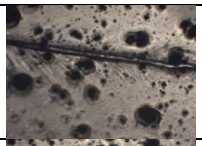	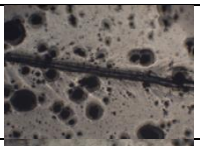
G-Gly-PANI(A1)	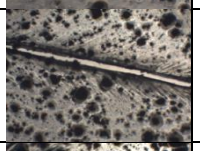	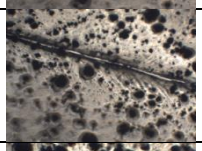	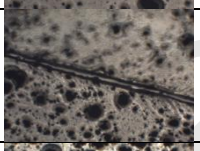
G-Gly-PANI(A2)	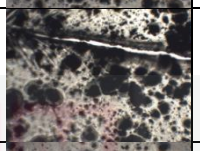	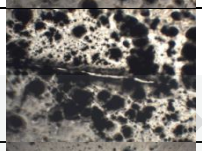	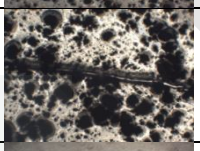
G-Gly-PANI(B0.5)	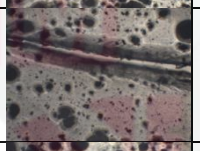	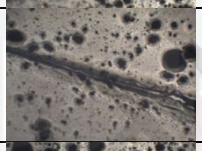	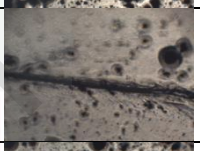
G-Gly-PANI(B1)	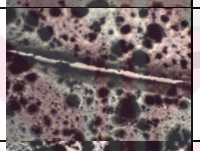	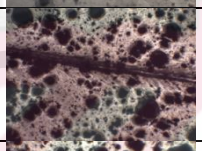	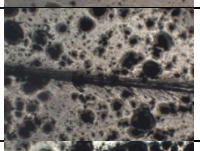
G-Gly-PANI(B2)	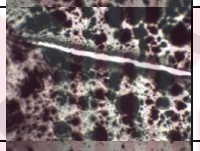	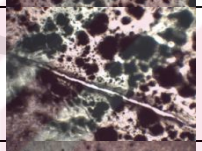	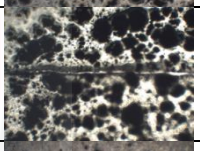
G-Gly-PANI(C0.5)	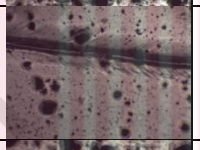	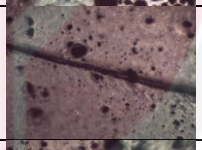	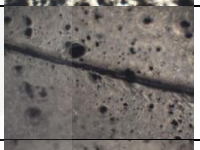
G-Gly-PANI(C1)	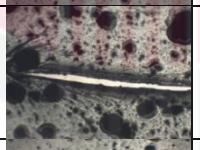	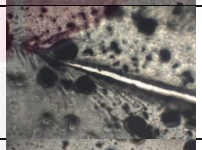	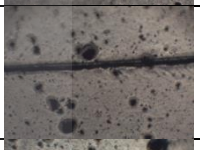
G-Gly-PANI(C2)	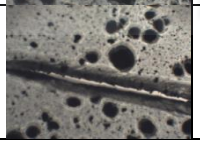	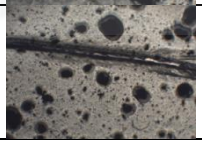	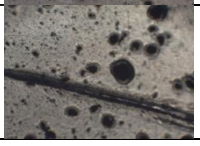

Figure 4.26: Light microscope (x10 magnification) image of self-healing progress at day 0, 4 and 7 at RH 75% and temperature 5 °C.

Sample	Day 0	Day 4	Day 7
G-Gly		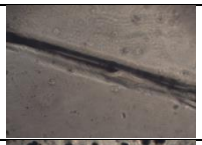	
G-Gly-PANI(A0.5)	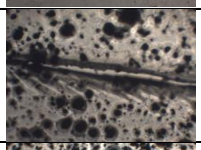	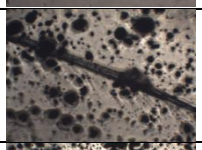	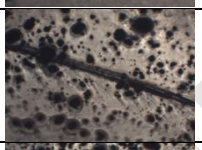
G-Gly-PANI(A1)	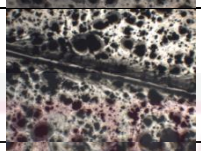	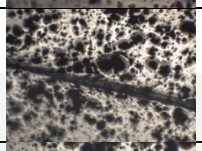	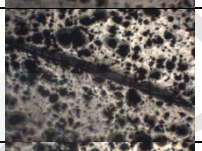
G-Gly-PANI(A2)	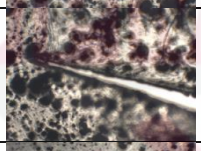	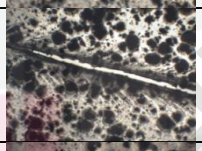	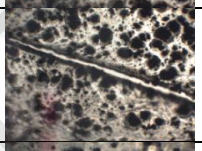
G-Gly-PANI(B0.5)	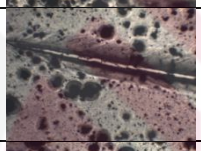	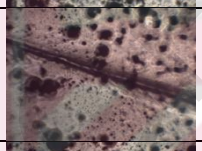	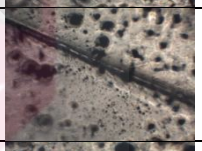
G-Gly-PANI(B1)	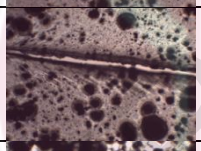	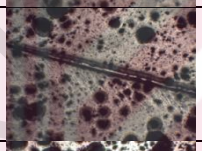	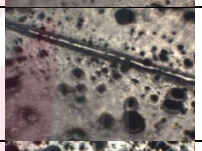
G-Gly-PANI(B2)	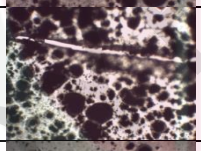	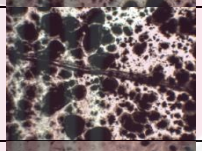	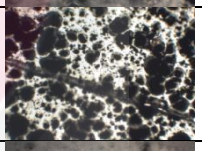
G-Gly-PANI(C0.5)	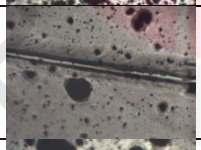	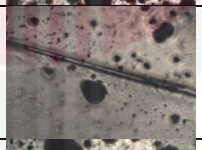	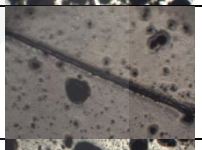
G-Gly-PANI(C1)	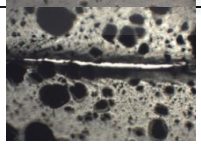	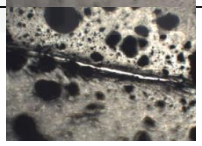	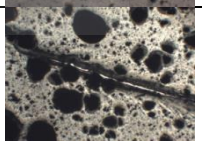
G-Gly-PANI(C2)	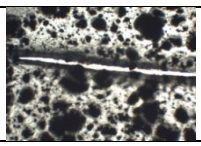	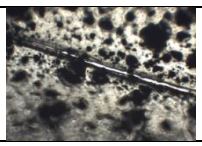	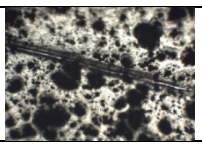

Figure 4.27: Light microscope image (x10 magnification) of self-healing progress at day 0, 4 and 7 at RH 75% and temperature 30 °C.

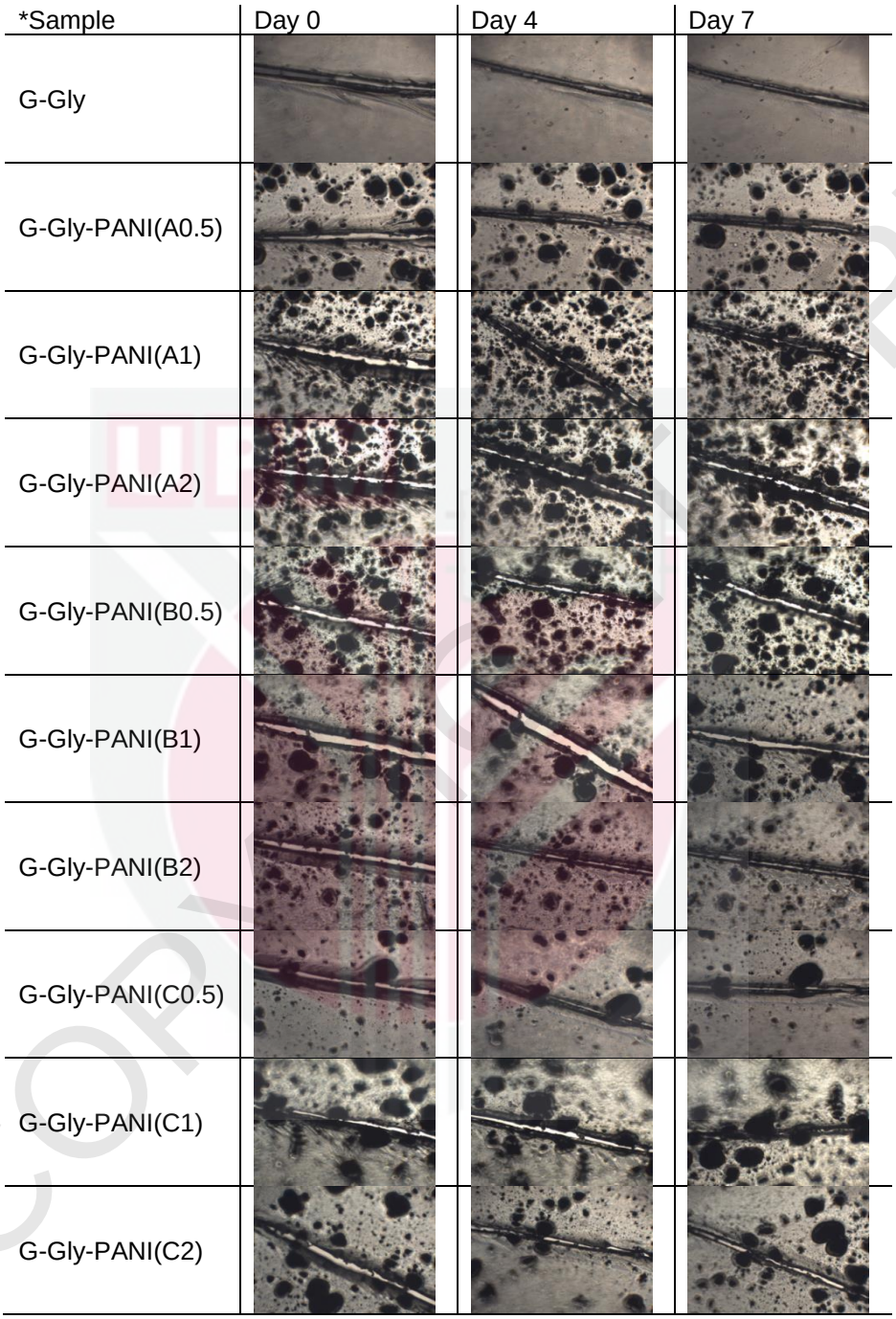

Figure 4.28: Light microscope (x10 magnification) image of self-healing progress at day 0, 4 and 7 at RH 75% and temperature 40 °C.

The experiments revealed that water is crucial for the self-healing process and certain water contents are needed to achieve complete self-healing. From the observations made, the self-healing process does not simply present itself at any given films that are in any temperature and RH except for the films stored at low temperature and high RH, which is inclusive of the nearly self-healing the incision part. Each of the films has its own equilibrium moisture content, as it has reached the maximum moisture to be adsorbed at a certain time.

In summary, this study has found that the damage PANI/gelatin-based film has the potential to be fully healed by physical interaction in the presence of moisture. Thus, the PANI/gelatin-based film can be categorized as a smart material with extended lifetimes with the capability to repair itself upon damage without the requirement for detection or repair by manual intervention. In addition, the self-healing of the film does affect the RH and temperature of the control surrounding. The healing process might not be fully healed if the film in question has reached saturated conditions at a certain time and is not able to adsorb more moisture to facilitate the healing process. Thus, as for the study for self-healing behavior, it is vital to consider the aspects of proper RH and temperature as it not only determined the stability and shelf life of the film but also the capabilities of the film's self-healing properties.

In application to be used for perishable fruit and vegetable packaging application such as strawberries, broccoli, asparagus or mushroom, the developed active gelatin-based film not only protect the products from deteriorate quickly by reducing the oxidation but can self-heal if the damaged occurs during handling and transportation. As explained before in the literature, perishable fruit and vegetables will continue respirates even after harvesting and give out gases and moisture. The moisture from the respiration process will help in the self-healing process when accidental damage occurred. Hence, the self-healable active gelatin-based film has advantage in keeping the longer shelf life of the product and the film itself.

CHAPTER 5

CONCLUSION AND RECOMMENDATION

This chapter reports the major conclusion derived from this study, summarizes the research problems and the objectives of the thesis, presents the key findings and contribution of the thesis, and proposes recommendations for future work.

5.1 Conclusions

In order to achieve the purpose of developing a novelty self-healing active film using gelatin extracted from red tilapia fish scale integrated with PANI as an active material for active film applications, four major sub-sections were reviewed and concluded. The fish scale of red tilapia is a good source of gelatin (4.34% dry weight basis), which contains 85.80% protein and abundance of glycine (20.79 g/100 g) and hydropoline (14.38 g/100 g). A high concentration of imino acids (glycine and hydroproline) contributes to superior filmogenic characteristics. Furthermore, the FTIR spectra revealed four distinct peaks: amide A, amide I, amide II, and amide III. Finally, the red tilapia gelatin extracted from the fish scales demonstrated strong film-forming characteristics for future development as a film. The gelatin film-forming solution was then modified by adding glycerol as a plasticizer to make gelatin-based films using the solution casting technique. The major variations in mechanical characteristics improved the film's flexibility by more than 90% while decreasing its tensile strength from 72.23 MPa to 14.83 MPa. The FTIR measurement revealed certain changes in the chemical structure of the plasticized gelatin-based film. In terms of WVP properties, the addition of glycerol as a plasticizer enhanced the WVP value owing to the plasticizer's hydrophilic capabilities. Based on the results, the feature properties of the films were investigated further as active films by incorporating PANI into the gelatin-based film using the solution blending process. PANI was created through oxidative polymerization of aniline. A digital shot showed a green dark patch, indicating that the PANI was spread throughout the gelatin matrix. According to the colour analysis, a* values rose as PANI sizes and concentrations increased, suggesting that the colour of PANI became dominant. There are no novel chemical interactions between PANI and gelatin, according to the FTIR chemical interaction study. Because of the different Tg values found, PANI and gelatin composites were termed heterogeneous and immiscible. Based on thermal analysis, due to the integration of PANI the low thermal stability and substantial weight loss compared to the G-Gly film was obtained. The mechanical characteristics of gelatin-based films were also changed owing to poor interfacial adhesion between PANI and gelatin at modest PANI loading sizes (A and B) into the film, regardless of PANI concentrations. As a result, the interaction mechanism was validated using morphological analysis and reinforcements in water resistance, mechanical characteristics, and thermal properties that were achievable between the matrix and filler. The

antioxidant activity of the PANI/gelatin-based film increased with increasing PANI loading, regardless of PANI size. Meanwhile, incorporation of the film with varied sizes of PANI had little influence on its antioxidant characteristics. As a result, the PANI/gelatin-based film may be employed for active film application. Next, for the development of damage repair, the design of active self-healing polymer materials requires tuning of the interactions between chemical processes, physical network remodelling, and interdiffusion of polymer chain segments. It is necessary to examine the roles of active compounds in the polymer. The reversible hydrogen bonding between the water molecules and the COOH of amino acids in the gelatin structure was responsible for the self-healing behaviour of the PANI/gelatin-based film. This research gave significant information on the healing process of self-healable active gelatin-based film. The influence of the surrounding environment, such as RH and temperature, was also regarded to initiate healing processes. According to the results, high RH and low temperature stimulate healing process, even when the film is not completely cured. Increasing the RH reduces the Peleg's constant values, which correspond to the sorption rate and capacity, based on the Peleg's constant k_1 and k_2 values. The GAB monolayer moisture content (Wm) gave important information on the maximum water absorbed by the film based on the GAB model isotherm, which may be related to the observation of the films healing process. Yet, the moisture adsorb was distribute on the whole film not only at the incision part until equilibrium was attained, rendering the healing process incomplete. Nonetheless, the procedure applied in this study was practical for the lab-scale purpose in developing these PANI/gelatin-based active self-healing films and show excellent benefits in scratch repair and have potential use in active film applications. The procedure applied was cheaper and ease to handle for the non-continuous process. The parameters and analysis studied can be used as reference to transfer to a continuous pilot-scale production. The most important aspects to be consider is especially the viscosity of the casting solution and the drying temperatures which cannot be simulated during a lab-scale production on a bench. These parameters have to be selected individually for each product when transferring the process to a pilot-scale or production-scale continuous process.

5.2 Recommendations and future works

The investigation presented in this thesis has improved our knowledge of the creation and performance of a self-healing red tilapia fish scale gelatin-based active film combined with PANI. Many concerns remain unresolved, and there are various areas where more study might be conducted-healable red tilapia's fish scale gelatin-based active film mixed with PANI. Many issues remain unsolved, and there are various areas where more study might be conducted. Further research in the following important areas will add functionality and improve the field of gelatin-based study:

- Modify the gelatin extraction method in a ‘greener’ ways without using chemical as pre-treatment - Chemical pre-treatment was used in this investigation since it is the most feasible and effective technique to

eliminate non-collegous proteins and diminerilization. This procedure may be substituted with a less harmful one, such as high-pressure processing.

- The practical application of gelatin-based film in extending food shelf-life should be studied further, particularly through the hurdle concept; previously, this study demonstrated the good antioxidant activity of the film with the incorporation of an active substance (PANI); thus, practical application should be used to validate the potential for extending food shelf-life. Furthermore, leaching investigations of the film with PANI inclusion in various media, as well as leachability tests, may be performed.
- Improved the interactions between the PANI and gelatin matrix by chemically graft PANI on the surface of the matrix. PANI available on the surface of the substrate is utilized in the first instance, for the free radical scaveging activity. This potentially will elevate their free radical scaveging capacity.
- The PANI/gelatin-based film may be used to pack chosen perishable vegetables under real-world storage settings to assess its effectiveness as active and self-healing packaging as well as its impact on the packed product

REFERENCES

Abdul Khalil, H. P. S., Banerjee, A., Saurabh, C. K., Tye, Y. Y., Suriani, A. B., Mohamed, A., Karim, A. A., Rizal, S., & Paridah, M. T. (2018). Biodegradable Films for Fruits and Vegetables Packaging Application: Preparation and Properties. In *Food Engineering Reviews* (Vol. 10, Issue 3, pp. 139–153). Springer New York LLC. https://doi.org/10.1007/s12393-018-9180-3

Abdullah, Cai, J., Hafeez, M. A., Wang, Q., Farooq, S., Huang, Q., Tian, W., & Xiao, J. (2022). Biopolymer-based functional films for packaging applications: A review. In *Frontiers in Nutrition* (Vol. 9). Frontiers Media S.A. https://doi.org/10.3389/fnut.2022.1000116

Abu-Thabit, N. Y. (2016). Chemical Oxidative Polymerization of Polyaniline: A Practical Approach for Preparation of Smart Conductive Textiles. *Journal of Chemical Education*, *93*(9), 1606–1611. https://doi.org/10.1021/acs.jchemed.6b00060

Acosta, S., Jiménez, A., Cháfer, M., González-Martínez, C., & Chiralt, A. (2015). Physical properties and stability of starch-gelatin based films as affected by the addition of esters of fatty acids. *Food Hydrocolloids*, *49*, 135–143. https://doi.org/10.1016/j.foodhyd.2015.03.015

Aguirre-Alvarez, G., Pimentel-González, D. J., Campos-Montiel, R. G., Foster, T., & Hill, S. E. (2011). The effect of drying temperature on mechanical properties of pig skin gelatin films. *CYTA - Journal of Food*, *9*(3), 243–249. https://doi.org/10.1080/19476337.2010.523902

Ahmad, M., & Benjakul, S. (2011). Food Hydrocolloids Characteristics of gelatin from the skin of unicorn leatherjacket (Aluterus monoceros) as influenced by acid pretreatment and extraction time. *Food Hydrocolloids*, *25*(3), 381–388. https://doi.org/10.1016/j.foodhyd.2010.07.004

Ahmad, T., Ismail, A., Ahmad, S. A., Khalil, K. A., Kee, L. T., Awad, E. A., & Sazili, A. Q. (2020). Extraction, characterization and molecular structure of bovine skin gelatin extracted with plant enzymes bromelain and zingibain. *Journal of Food Science and Technology*. https://doi.org/10.1007/s13197-020-04409-2

Ahmad, T., Ismail, A., Ahmad, S. A., Khalil, K. A., Teik Kee, L., Awad, E. A., & Sazili, A. Q. (2019). Physicochemical characteristics and molecular structures of gelatin extracted from bovine skin: effects of actinidin and papain enzymes pretreatment. *International Journal of Food Properties*, *22*(1), 138–153. https://doi.org/10.1080/10942912.2019.1576731

Aïssa, B., Therriault, D., Haddad, E., & Jamroz, W. (2012). Self-healing materials systems: Overview of major approaches and recent developed technologies. *Advances in Materials Science and Engineering*, *2012*. https://doi.org/10.1155/2012/854203

Akay, G., Hassan-Raeisi, A., Tuncaboylu, D. C., Orakdogen, N., Abdurrahmanoglu, S., Oppermann, W., & Okay, O. (2013). Self-healing hydrogels formed in catanionic surfactant solutions. *Soft Matter*, *9*(7), 2254–2261. https://doi.org/10.1039/c2sm27515e

Akoy, E., Von Hörsten, D., & Ismail, M. (2013). Moisture adsorption characteristics of solar-dried mango slices. *International Food Research Journal*, *20*(2), 883–890.

Alemán, A. ;, & Martínez-Alvarez, O. (2013). Marine collagen as a source of bioactive molecules: A review. *Journal of Natural Product*, *3*, 105–114.

Alfaro, A. da T., Balbinot, E., Weber, C. I., Tonial, I. B., & Alessandra, M.-L. (2014). Fish Gelatin: Characteristics, Functional Properties, Applications and Future Potentials. *Food Engineering Reviews*, *6*(4), 33–44.

Al-Muhtaseb, A. H., McMinn, W. A. M., & Magee, T. R. A. (2002). Moisture sorption isotherm characteristics of food products: A review. *Food and Bioproducts Processing: Transactions of the Institution of of Chemical Engineers, Part C*, *80*(2), 118–128. https://doi.org/10.1205/09603080252938753

Altamirano, M. M., Hernandez-Arana, A., Tello-Solis, S., & Calcagno, M. L. (1994). Spectrochemical evidence for the presence of a tyrosine residue in the allosteric site of glucosamine-6-phosphate deaminase from Escherichia coli. *European Journal of Biochemistry*, *220*(2), 409–413. https://doi.org/10.1111/j.1432-1033.1994.tb18638.x

Andersson, C., Järnström, L., Fogden, A., Mira, I., Voit, W., Zywicki, S., & Bartkowiak, A. (2009). Preparation and incorporation of microcapsules in functional coatings for self-healing of packaging board. *Packaging Technology and Science*, *22*(5), 275–291. https://doi.org/10.1002/pts.853

Andrade P, R. D., Lemus M, R., & Pérez C, C. E. (2011). Models of sorption isotherms for food: uses and limitations. *Vitae*, *18*, 325–334.

Annala, M., & Löfgren, B. (2006). Compatibilization of conductive polyethylene/ polyaniline blends. *Macromolecular Materials and Engineering*, *291*(7), 848–857. https://doi.org/10.1002/mame.200600071

AOAC International. (2016). Official methods of analysis of AOAC International. *Association of Official Analysis Chemists International*, 3172.

Arik Kibar, E. A., & Us, F. (2013). Thermal, mechanical and water adsorption properties of corn starch-carboxymethylcellulose/methylcellulose

biodegradable films. *Journal of Food Engineering*, *114*(1), 123–131. https://doi.org/10.1016/j.jfoodeng.2012.07.034

Aruoma, O. I. (2003). Methodological considerations for characterizing potential antioxidant actions of bioactive components in plant foods. *Mutation Research - Fundamental and Molecular Mechanisms of Mutagenesis*, *523–524*, 9–20. https://doi.org/10.1016/S0027-5107(02)00317-2

Asghar, A., & Henrickson, R. L. (1982). Chemical, biochemical, functional, and nutritional characteristics of collagen in food systems. In *Advances in Food Research* (Vol. 28, Issue C). https://doi.org/10.1016/S0065-2628(08)60113-5

ASTM. (2002). Standard test method for tensile properties of thin plastic sheeting: Method D882-02. In *Annual Book of ASTM standards*. American Society for Testing and Materials.

ASTM. (2005). *Standard test methods for water vapor transmission of materials-E96/E96-05. Philadelphia. i*, 1–14. https://doi.org/10.1520/E0096

Azmi, N. S., Basha, R. K., Tajul Arifin, N. N., Othman, S. H., & Mohammed, M. A. P. (2020). Functional properties of tilapia's fish scale gelatin film: Effects of different type of plasticizers. *Sains Malaysiana*, *49*(9), 2221–2229. https://doi.org/10.17576/jsm-2020-4909-19

Azmi, N. S., Kadir Basha, R., Othman, S. H., & Mohammed, M. A. P. (2019). Characterization of antioxidant tapioca starch/polyaniline composites film prepared using solution casting method. *Food Research*, *3*(4), 317–324. https://doi.org/10.26656/fr.2017.3(4).144

Backfolk, K., Holmes, R., Ihalainen, P., Sirviö, P., Triantafillopoulos, N., & Peltonen, J. (2007). Determination of the glass transition temperature of latex films: Comparison of various methods. *Polymer Testing*, *26*(8), 1031–1040. https://doi.org/10.1016/j.polymertesting.2007.07.007

Baghi, F., Gharsallaoui, A., & Dumas, E. (2022). *Advancements in Biodegradable Active Films for Food Packaging : Effects of Nano / Microcapsule Incorporation*. 1–44.

Bajpai, S., Awasthi, S., Singh Utiye, A., & Mishra, B. (2017). Investigation of Moisture Sorption Properties of Gelatin/Poly (Aniline)/Films. *SOJ Materials Science & Engineering*, *5*(2), 1–6. https://doi.org/10.15226/sojmse.2017.00147

Basha, R. K. (2011). *Development and Performance of Biomass Based Film Materials for Packaging of Fruits and Vegetables*. Hokkaido University.

Basha, R. K., Leong, K. Y., Othman, S. H., Talib, R. A., Naim, M. N., Hasnan, N. Z. N., & Azmi, N. S. (2021). Sorption characteristic of starch-based film. *Food Research*, *5*, 193–200. https://doi.org/10.26656/fr.2017.5(S1).056

Bergo, P., & Sobral, P. J. A. (2007). Effects of plasticizer on physical properties of pigskin gelatin films. *Food Hydrocolloids*, *21*(8), 1285–1289. https://doi.org/10.1016/j.foodhyd.2006.09.014

Bergo, P., Sobral, P. J. A., & Prison, J. M. (2010). Effect of glycerol on physical properties of cassava starch films. *Journal of Food Processing and Preservation*, *34*(SUPPL. 2), 401–410. https://doi.org/10.1111/j.1745-4549.2008.00282.x

Beygisangchin, M., Rashid, S. A., Shafie, S., Sadrolhosseini, A. R., & Lim, H. N. (2021). Preparations, properties, and applications of polyaniline and polyaniline thin films—a review. *Polymers*, *13*(12). https://doi.org/10.3390/polym13122003

Bhadra, J., Al-Thani, N. J., Madi, N. K., & Al-Maadeed, M. A. (2017). Effects of aniline concentrations on the electrical and mechanical properties of polyaniline polyvinyl alcohol blends. *Arabian Journal of Chemistry*, *10*(5), 664–672. https://doi.org/10.1016/j.arabjc.2015.04.017

Bhavaniramya, S., Vishnupriya, S., & Al-aboody, M. S. (2019). Grain & Oil Science and Technology Role of essential oils in food safety : Antimicrobial and antioxidant applications. *Grain & Oil Science and Technology*, *2*(2), 49–55. https://doi.org/10.1016/j.gaost.2019.03.001

Binder, W., Dohler, D., & Michael, P. (2013). Part One Design of Self-Healing Materials. *Self-Healing Polymers: From Principles to Applications*.

Boeva, Zh. A., & Sergeyev, V. G. (2014). Polyaniline: Synthesis, properties, and application. *Polymer Science Series C*, *56*(1), 144–153. https://doi.org/10.1134/S1811238214010032

Bourlieu, C., Guillard, V., Vallès-Pamiès, B., Guilbert, S., & Gontard, N. (2009). Edible moisture barriers: How to assess of their potential and limits in food products shelf-life extension? *Critical Reviews in Food Science and Nutrition*, *49*(5), 474–499. https://doi.org/10.1080/10408390802145724

Byjus. (2022, May 20). *Protein Structure and Levels of Protein*. https://byjus.com/chemistry/protein-structure-and-levels-of-protein/

Cadden, A. -M. (1988). Moisture Sorption Characteristics of Several Food Fibers. *Journal of Food Science*, *53*(4), 1150–1155. https://doi.org/10.1111/j.1365-2621.1988.tb13550.x

Cao, Y., Smith, P., & Heeger, A. J. (1992). Counter-ion processibility of conducting polyblends of polyaniline in bulk polymers. *Synthetic Metals*, *48*, 91–97.

Cao, Y., Treacy, G. M., Smith, P., & Heeger, A. J. (1993). Optical-quality transparent conductive polyaniline films. *Synthetic Metals*, *57*(1), 3526–3531. https://doi.org/10.1016/0379-6779(93)90470-H

Chang, P. R., Jian, R., Yu, J., & Ma, X. (2010). Fabrication and characterisation of chitosan nanoparticles/plasticised-starch composites. *Food Chemistry*, *120*(3), 736–740. https://doi.org/10.1016/j.foodchem.2009.11.002

Chen, J., Peng, Q., Thundat, T., & Zeng, H. (2019). Stretchable, Injectable, and Self-Healing Conductive Hydrogel Enabled by Multiple Hydrogen Bonding toward Wearable Electronics. *Chemistry of Materials*, *31*(12), 4553–4563. https://doi.org/10.1021/acs.chemmater.9b01239

Chia, M. R., Phang, S. W., & Ahmad, I. (2022). Emerging Applications of Versatile Polyaniline-Based Polymers in the Food Industry. In *Polymers* (Vol. 14, Issue 23). MDPI. https://doi.org/10.3390/polym14235168

Chinma, C. E., Ariahu, C. C., & Alakali, J. S. (2015). Effect of temperature and relative humidity on the water vapour permeability and mechanical properties of cassava starch and soy protein concentrate based edible films. *Journal of Food Science and Technology*, *52*(4), 2380–2386. https://doi.org/10.1007/s13197-013-1227-0

Cho, S. M., Gu, Y. S., & Kim, S. B. (2005). Extracting optimization and physical properties of yellowfin tuna (Thunnus albacares) skin gelatin compared to mammalian gelatins. *Food Hydrocolloids*, *19*(2), 221–229.

Cho, S. M., Kwak, K. S., Park, D. C., Gu, Y. S., Ji, C. I., & Jang, D. H. (2004). Processing optimization and functional properties of gelatin from shark (Isurus oxyrinchus) cartilage. *Food Hydrocolloids*, *18*(4), 573–579.

Chowdhury, T., & Das, M. (2012). Moisture sorption isotherm and isosteric heat of sorption of edible films made from blends of starch, amylose and methyl cellulose. *International Food Research Journal*, *19*(4), 1669–1678.

Chuaynukul, K., Nagarajan, M., Prodpran, T., Benjakul, S., & Prasarpran, S. (2017). Impacts of plasticizer and pre-heating conditions on properties of bovine and fish gelatin films fabricated by thermo-compression molding technique. *Italian Journal of Food Science*, *29*(3), 487–504.

Cordier, P., Tournilhac, F., Soulié-Ziakovic, C., & Leibler, L. (2008). Self-healing and thermoreversible rubber from supramolecular assembly. *Nature*, *451*(7181), 977–980. https://doi.org/10.1038/nature06669

Coupland, J. N., Shaw, N. B., Monahan, F. J., Dolores O'Riordan, E., & O'Sullivan, M. (2000). Modeling the effect of glycerol on the moisture sorption behavior of whey protein edible films. *Journal of Food Engineering*, *43*(1), 25–30. https://doi.org/10.1016/S0260-8774(99)00129-6

Cuq, B., Gontard, N., & Guilbert, S. (1997). Thermal properties of fish myofibrillar protein-based films as affected by moisture content. *Polymer*, *38*(10), 2399–2405. https://doi.org/10.1016/S0032-3861(96)00781-1

Das, M. P., R., S. P., Prasad, K., Jv, V., & M, R. (2017). Extraction and Characterization of Gelatin: a Functional Biopolymer. *International Journal of Pharmacy and Pharmaceutical Sciences*, *9*(9), 239. https://doi.org/10.22159/ijpps.2017v9i9.17618

Del Nobile, M. A., Conte, A., Cannarsi, M., & Sinigaglia, M. (2008). Use of biodegradable films for prolonging the shelf life of minimally processed lettuce. *Journal of Food Engineering*, *85*(3), 317–325. https://doi.org/10.1016/j.jfoodeng.2007.06.040

Ding, F., Wu, S., Wang, S., Xiong, Y., Li, Y., Li, B., Deng, H., Du, Y., Xiao, L., & Shi, X. (2015). Soft Matter hydrogel with autonomous self-healing ability †. *Soft Matter*. https://doi.org/10.1039/C5SM00587F

Dispenza, C., Leone, M., Presti, C. L., Librizzi, F., Spadaro, G., & Vetri, V. (2006). Optical properties of biocompatible polyaniline nano-composites. *Journal of Non-Crystalline Solid*, *352*, 3855–3580.

Dispenza, C., Sabatino, M.-A., Niconov, A., Chmielewska, D., & Spadaro, G. (2012). E-beam crosslinked, biocompatible functional hydrogels incorporating polyaniline nanoparticles. *Radition Physic and Chemistry*, *81*(1456–1459).

Doi, M. (2013). *Soft matter physics*. Oxford University Press.

Drago, E., Campardelli, R., Pettinato, M., & Perego, P. (2020). Innovations in Smart Packaging Concepts for Food : An Extensive Review. *Foods*, *9*(11), 1628. https://doi.org/https://doi.org/10.3390/foods9111628

Duconseille, A., Astruc, T., Quintana, N., Meersman, F., & Sante-Lhoutellier, V. (2015). Gelatin structure and composition linked to hard capsule dissolution: A review. *Food Hydrocolloids*, *43*, 360–376. https://doi.org/10.1016/j.foodhyd.2014.06.006

Etxabide, A., Uranga, J., Guerrero, P., & de la Caba, K. (2017). Development of active gelatin films by means of valorisation of food processing waste: A review. *Food Hydrocolloids*, *68*, 192–198. https://doi.org/10.1016/j.foodhyd.2016.08.021

Europe, P., & EPRO. (2022). *Plastics-the Facts 2022 OCTOBER 2022*.

Fainleib, A. M., & Purikova, O. H. (2019). Self-healing polymers: approaches of healing and their application. *Polymer Journal*, *41*(1), 4–18. https://doi.org/10.15407/polymerj.41.01.004

Federal, U., & Catarina, D. S. (2017). *Effect of drying method on mechanical , thermal and water absorption properties of enzymatically crosslinked gelatin hydrogels*. *89*, 745–755.

Flieger, J., Flieger, W., & Baj, J. (2021). Antioxidants : Classification , Natural Sources , Activity / Capacity Measurements, and Usefulness for the Synthesis of Nanoparticles. *Materials (Basel)*, *14*(15), 4135. https://doi.org/doi: 10.3390/ma14154135

Foggia, M. Di, Taddei, P., Torreggiani, A., Monica, D., & Tinti, A. (2012). Self-assembling peptides for biomedical applications: IR and Raman spectroscopies spectroscopies. *Proteomics Research Journal ·*, *2*(3), 231–272.

Foh, M. B. K., Kamara, M. T., Amadou, I., Foh, B. M., & Wenshui, X. (2011). Effect of enzymatic hydrolysis on the nutritional and functional properties of Nile tilapia (Oreochromis niloticus) proteins. *American Journal of Biochemistry and Mol Ecular Biology*, *1*(1), 54–67.

Francis, F. J. (1983). Colorimetry of food. In M. Peleg & E. B. Baley (Eds.), *Physical Properties of Food* (pp. 105–124).

Frankel, E. N., & Meyer, A. S. (2000). The problem of using one-dimensional method to evaluate multifunctional food and biological antioxidants. *Journal of the Science of Food and Agriculture*, *18*(13), 1925–1941. https://doi.org/https://doi.org/10.1002/1097-0010(200010)80:13%3C1925::AID-JSFA714%3E3.0.CO;2-4

Genies, E. M., & Lapkowski, M. (1987). Electrochemical in situ epr evidence of two polaron-bipolaron states in polyaniline. *Journal of Electroanalytical Chemistry*, *236*(1–2), 199–208. https://doi.org/10.1016/0022-0728(87)88027-0

Gennaddios, A., Weller, C. L., Hanna, M., & Froning, G. W. (1996). Mechanical and Barrier Properties of Egg Albumen Films. *Journal of Food Science*, *61*(3), 585–589. https://doi.org/10.1111/j.1365-2621.1996.tb13164.x

Ghadermazi, R., Hamdipour, S., Sadeghi, K., Ghadermazi, R., & Khosrowshahi Asl, A. (2019). Effect of various additives on the properties of the films and coatings derived from hydroxypropyl methylcellulose—A review. In *Food Science and Nutrition* (Vol. 7, Issue 11, pp. 3363–3377). Wiley-Blackwell. https://doi.org/10.1002/fsn3.1206

Ghasemlou, M., Khodaiyan, F., & Oromiehie, A. (2011). Physical , mechanical , barrier , and thermal properties of polyol-plasticized biodegradable edible film made from kefiran. *Carbohydrate Polymers*, *84*(1), 477–483. https://doi.org/10.1016/j.carbpol.2010.12.010

Giménez, B., Gómez-Estaca, J., Alemán, A., Gómez-Guillén, M. C., & Montero, M. P. (2009). Physico-chemical and film forming properties of giant squid (Dosidicus gigas) gelatin. *Food Hydrocolloids*, *23*(3), 585–592. https://doi.org/10.1016/j.foodhyd.2008.07.003

Girja, B. G., Sailaja, R. R. N., & Madras, G. (2005). Thermal degradation and mechanical properties of PET blends. *Polymer Degradation and Stability*, *90*, 147–153.

Gizdavic-Nikolaidis, M., Travas-Sejdic, J., Bowmaker, G. A., Cooney, R. P., Thompson, C., & Kilmartin, P. A. (2004). The antioxidant activity of conducting polymers in biomedical applications. *Current Applied Physics*, *4*(2–4), 347–350. https://doi.org/10.1016/j.cap.2003.11.045

Gizdavic-Nikolaidis, M., Travas-Sejdic, J., Kilmartin, P. A., Bowmaker, G. A., & Cooney, R. P. (2004). Evaluation of antioxidant activity of aniline and polyaniline. *Current Applied Physics*, *4*(2–4), 343–346. https://doi.org/10.1016/j.cap.2003.11.044

Gómez-Guillén, M. C., Pérez-Mateos, M., Gómez-Estaca, J., López-Caballero, E., Giménez, B., & Montero, P. (2009). Fish gelatin: a renewable material for developing active biodegradable films. *Trends in Food Science and Technology*, *20*(1), 3–16. https://doi.org/10.1016/j.tifs.2008.10.002

Gómez-Guillén, M. C., Turnay, J., Fernández-Diaz, M. D., Ulmo, N., Lizarbe, M. A., & Montero, P. (2002). *Structural and physical properties of gelatin extracted from different*. *16*, 25–34. https://doi.org/10.1016/S0268-005X(01)00035-2

González, P., Medina, C., Famá, L., & Goyanes, S. (2016). Biodegradable and non-retrogradable eco-films based on starch – glycerol with citric acid as crosslinking agent. *Carbohydrate Polymers*, *138*, 66–74. https://doi.org/10.1016/j.carbpol.2015.11.041

Gospodinova, N., & Terlemezyan, L. (1998). Conducting polymers prepared by oxidative polymerization: Polyaniline. *Progress in Polymer Science (Oxford)*, *23*(8), 1443–1484. https://doi.org/10.1016/S0079-6700(98)00008-2

Gueguen, J., Viroben, G., Noireaux, P., & Subirade, M. (1998). Influence of plasticizers and treatments on the properties of films from pea proteins. *Industrial Crops and Products*, *7*(2–3), 149–157. https://doi.org/10.1016/S0926-6690(97)00043-5

Guerrero, P., Nur Hanani, Z. A., Kerry, J. P., & De La Caba, K. (2011). Characterization of soy protein-based films prepared with acids and oils by compression. *Journal of Food Engineering*, *107*(1), 41–49. https://doi.org/10.1016/j.jfoodeng.2011.06.003

Gulyuz, U., & Okay, O. (2013). Self-healing polyacrylic acid hydrogels. *Soft Matter*, *9*(43), 10287–10293. https://doi.org/10.1039/c3sm52015c

Halliwell, B., & Gutteridge, J. M. (2015). *Free Radicals in Biology and Medicine* (5th ed.). Oxford University Press. https://doi.org/10.1093/acprof:oso/9780198717478.001.0001

Hao, S., Li, L., Yang, X., Cen, J., Shi, H, Boa, B., & He, J. (2009). The characteristics of gelatin extracted from sturgeon (Acipenser baeri) skin using various pretreatments. *Food Chemistry*, *115*, 124–128.

Haque, M. A., Kurokawa, T., Kamita, G., & Gong, J. P. (2011). Lamellar bilayers as reversible sacrificial bonds to toughen hydrogel: Hysteresis, self-recovery, fatigue resistance, and crack blunting. *Macromolecules*, *44*(22), 8916–8924. https://doi.org/10.1021/ma201653t

Haug, I. J., Draget, K. I., & Smidsrød, O. (2004). Physical behaviour of fish gelatin-κ-carrageenan mixtures. *Carbohydrate Polymers*, *56*(1), 11–19. https://doi.org/10.1016/j.carbpol.2003.10.014

Holze, R. (2011). Electrochimica Acta Copolymers — A refined way to tailor intrinsically conducting polymers &. *Electrochimica Acta*, *56*(28), 10479–10492. https://doi.org/10.1016/j.electacta.2011.04.013

Hoque, M. S., Benjakul, S., & Prodpran, T. (2011). Effects of partial hydrolysis and plasticizer content on the properties of film from cuttlefish (Sepia pharaonis) skin gelatin. *Food Hydrocolloids*, *25*(1), 82–90. https://doi.org/10.1016/j.foodhyd.2010.05.008

Hosseini, S. F., Rezaei, M., Zandi, M., & Farahmandghavi, F. (2016). Development of bioactive fish gelatin/chitosan nanoparticles composite films with antimicrobial properties. *Food Chemistry*, *194*, 1266–1274. https://doi.org/10.1016/j.foodchem.2015.09.004

Hosseinzadeh, H., & Ramin, S. (2018). *International Journal of Biological Macromolecules Fabrication of starch- graft -poly (acrylamide)/ graphene oxide / hydroxyapatite nanocomposite hydrogel adsorbent for removal of malachite green dye from aqueous solution*. *106*, 101–115.

Hsu, C. F., Peng, H., Basle, C., Travas-Sejdic, J., & Kilmartin, P. A. (2011). ABTS•+ scavenging activity of polypyrrole, polyaniline and poly(3,4-ethylenedioxythiophene). *Polymer International*, *60*(1), 69–77. https://doi.org/10.1002/pi.2912

Hsu, C. F., Peng, H., Zhang, L., Travas-Sejdic, J., & Kilmartin, P. A. (2009). Structural changes in polyaniline upon reaction with DPPH. *E-Journal of Surface Science and Nanotechnology*, *7*(April), 269–272. https://doi.org/10.1380/ejssnt.2009.269

Hsu, C. F., Zhang, L., Peng, H., Travas-Sejdic, J., & Kilmartin, P. A. (2008). Scavenging of DPPH free radicals by polypyrrole powders of varying levels of overoxidation and/or reduction. *Synthetic Metals*, *158*(21–24), 946–952. https://doi.org/10.1016/j.synthmet.2008.06.017

Hu, B., Chen, L., Lan, S., Ren, P., Wu, S., Liu, X., Shi, X., Li, H., Du, Y., & Ding, F. (2018). Layer-by-layer assembly of polysaccharide films with self-healing and antifogging properties for food packaging applications. *ACS*

Applied Nano Materials, *1*(7), 3733–3740. https://doi.org/10.1021/acsanm.8b01009

Hua, Y., Guo, X. F., Chen, Z. X., & Shu, Z. Bin. (2014). Preparation and characterization of collagen food packaging film. *Journal of Chemical and Pharmaceutical Research*, *6*(6), 740–745.

Humpolicek, P., Kasparkova, V., Saha, P., & Stejskal, J. (2012). Biocompatibility of polyaniline. *Synthetic Metals*, *162*, 722–727.

Irwandi, J., Faridayanti, S., Mohamed, E. S. M., Hamzah, M. S., Torla, H. H., & Che Man, Y. B. (2009). Extraction and characterization of gelatin from different marine fish species in Malaysia. *International Food Research Journal*, *16*(3), 381–389.

Ismail, M. N., Ibrahim, M. S., & Abd El-Ghaffar, M. A. (1998). Polyaniline as an antioxidant and antirad in SBR vulcanizates. *Polymer Degardation and Stability*, *62*, 337–347.

Jafari, H., Lista, A., Siekapen, M. M., Ghaffari-Bohlouli, P., Nie, L., Alimoradi, H., & Shavandi, A. (2020). Fish collagen: Extraction, characterization, and applications for biomaterials engineering. *Polymers*, *12*(10), 1–37. https://doi.org/10.3390/polym12102230

Jahit, I. S., Nazmi, N. N. M., Isa, M. I. N., & Sarbon, N. M. (2016). *Preparation and physical properties of gelatin/CMC/chitosan composite films as affected by drying temperature*. *23*(3), 1068–1074.

Jomlapeeratikul, P., Poomsa-Ad, N., & Wiset, L. (2017). Effect of Drying Temperatures and Plasticizers on the Properies of Konjac Flour Film. *Journal of Food Process Engineering*, *40*(3). https://doi.org/10.1111/jfpe.12443

Jongjareonrak, A., Benjakul, S., Visessanguan, W., Prodpran, T., & Tanaka, M. (2006). Characterization of edible films from skin gelatin of brownstripe red snapper and bigeye snapper. *Food Hydrocolloids*, *20*(4), 492–501. https://doi.org/10.1016/j.foodhyd.2005.04.007

Kamal-Eldin, A., & Pokorn, J. (2005). *Analysis of lipid oxidation*.

Kamalesh, S., Tan, P., Wang, J., Lee, T., Kang, E.-T., & Wang, C.-H. (2000). Biocompatibility of electroactive polymers in tissues. *Journal of Biomedical Research*, *52*, 467–478.

Kanatt, S. R., Rao, M. S., Chawla, S. P., & Sharma, A. (2012). Active chitosan-polyvinyl alcohol films with natural extracts. *Food Hydrocolloids*, *29*(2), 290–297. https://doi.org/10.1016/j.foodhyd.2012.03.005

Kang, H., Tabata, Y., & Ikada, Y. (1999). *Fabrication of porous gelatin sca ! olds for tissue engineering*. *20*(February), 2–7.

Karim, A. A., & Bhat, R. (2009). Fish gelatin: properties, challenges, and prospects as an alternative to mammalian gelatins. *Food Hydrocolloids*, *23*(3), 563–576. https://doi.org/10.1016/j.foodhyd.2008.07.002

Kausch, H., & Jud, K. (1982). Molecular aspects of crack formation and healing in glassy polymers . *Plastics and Rubber Processing and Applications*, *2*(3), 265–268.

Kavoosi, G., Dadfar, S. M. M., Mohammadi Purfard, A., & Mehrabi, R. (2013). Antioxidant and antibacterial properties of gelatin films incorporated with carvacrol. *Journal of Food Safety*, *33*(4), 423–432. https://doi.org/10.1111/jfs.12071

Kerry, J. P., Grady, M. N. O., & Hogan, S. A. (2006). Past , current and potential utilisation of active and intelligent packaging systems for meat and muscle-based products : A review. *Meat Science*, *74*, 113–130. https://doi.org/10.1016/j.meatsci.2006.04.024

Kim, H.-S., Hobbs, H. I., Wang, I., Rutten, M. J., & Wanser, C. C. (2009). Biocompatible composites of polyanilne nanofibers and collagen. *Synthetic Metals*, *159*, 1313–1318.

Korossis, S. (2018). Structure-Function Relationship of Heart Valves in Health and Disease. *Structural Insufficiency Anomalies in Cardiac Valves*, 1–38. https://doi.org/10.5772/intechopen.78280

Kumar, A. B., Saikia, J. P., & Konwar, B. K. (2010). Swift heavy ion irradiation induced enhancement in the antioxidant activity and biocompatibility of polyaniline nanofiber. *Nanotechnology*, *21*, 1–8.

Lai, H. M., & Padua, G. W. (1998). Water vapor barrier properties of zein films plasticized with oleic acid. *Cereal Chemistry*, *75*(2), 194–199. https://doi.org/10.1094/CCHEM.1998.75.2.194

Lee, D. S., Kit L., Y., & Poergiovanni, L. (2008). Active and intelligent packaging. In *Food packaging science and technology* (pp. 445–473). CRC Press.

Lee, S. W., & Lee, D. (2013). Integrated study of water sorption/desorption behavior of weak polyelectrolyte layer-by-layer films. *Macromolecules*, *46*(7), 2793–2799. https://doi.org/10.1021/ma400076d

Lewandowska, K. (2009). Miscibility and thermal stability of poly(vinyl alcohol)/chitosan mixtures. *Thermochimica Acta*, *493*(1–2), 42–48. https://doi.org/10.1016/j.tca.2009.04.003

Li, J. H., Miao, J., Wu, J. L., Chen, S. F., & Zhang, Q. Q. (2014). Preparation and characterization of active gelatin-based films incorporated with natural antioxidants. *Food Hydrocolloids*, *37*, 166–173. https://doi.org/10.1016/j.foodhyd.2013.10.015

Li, W., Jiang, Z., Yang, Z., Zhao, N., & Yuan, W. (2013). Self-healing efficiency of cementitious materials containing microcapsules filled with healing adhesive: Mechanical restoration and healing process monitored by water absorption. *PLoS ONE*, *8*(11), 1–18. https://doi.org/10.1371/journal.pone.0081616

Liau, W. Bin, Sun, Y. T., Yang, L. Y., Wang, L. Y., Chiu, W. Y., Hsieh, K. H., & Tseng, S. M. (2006). Morphology and characterization of conductive films based on polyaniline-coated polystyrene latexes. *Journal of Applied Polymer Science*, *102*(6), 5406–5413. https://doi.org/10.1002/app.24995

Limpan, N., Prodpran, T., Benjakul, S., & Prasarpran, S. (2010). Properties of biodegradable blend films based on fish myofibrillar protein and polyvinyl alcohol as influenced by blend composition and pH level. *Journal of Food Engineering*, *100*(1), 85–92. https://doi.org/10.1016/j.jfoodeng.2010.03.031

Limpisophon, K., Tanaka, M., Weng, W. Y., Abe, S., & Osako, K. (2009). Characterization of gelatin films prepared from under-utilized blue shark (Prionace glauca) skin. *Food Hydrocolloids*, *23*(7), 1993–2000. https://doi.org/10.1016/j.foodhyd.2009.03.014

Liu, J., Yong, H., Liu, Y., Qin, Y., Kan, J., & Liu, J. (2019). Preparation and characterization of active and intelligent films based on fish gelatin and haskap berries (Lonicera caerulea L.) extract. *Food Packaging and Shelf Life*, *22*. https://doi.org/10.1016/j.fpsl.2019.100417

Luan, Y. G., Zhang, X. A., Jiang, S. L., Chen, J. H., & Lyu, Y. F. (2018). Self-healing Supramolecular Polymer Composites by Hydrogen Bonding Interactions between Hyperbranched Polymer and Graphene Oxide. *Chinese Journal of Polymer Science (English Edition)*, *36*(5), 584–591. https://doi.org/10.1007/s10118-018-2025-y

Lukasiewicz, M., Ptaszek, P., Ptaszek, A., & Bednarz, S. (2014). Polyaniline-starch blends: Synthesis, rheological, and electrical properties. *Starch/Staerke*, *66*(7–8), 583–594. https://doi.org/10.1002/star.201300147

Lv, I.-C., Huang, Q.-Y., Ding, W., Xiao, X.-H., Zhang, H.-Y., & Xiong, L.-X. (2019). Fish gelatin: The novel potential applications. *Journal of Functional Foods*, *63*, 103581.

Mahmoodani, F., & See, S. F. (2013). *Optimization of gelatin extraction and physico-chemical properties of catfish (Clarias gariepinus) bone gelatin Optimization of gelatin extraction and physico-chemical properties of catfish (Clarias gariepinus) bone gelatin*. *January*.

Mali, S., Sakanaka, L. S., Yamashita, F., & Grossmann, M. V. E. (2005). Water sorption and mechanical properties of cassava starch films and their relation to plasticizing effect. *Carbohydrate Polymers*, *60*(3), 283–289. https://doi.org/10.1016/j.carbpol.2005.01.003

Marana, J. P., Sivakumara, V., Sridharb, R., & Immanuel, V. P. (2013). Development of model for mechanical properties of tapioca starch based edible films. *Industrial Crops and Products*, *42*, 159–168.

Mariod, A. A., & Adam, H. F. (2013). Review: Gelatin, Source, Extraction and Industrial Applications. *Acta Sci. Pol., Technol. Aliment.*, *12*(2), 135–147. https://doi.org/10.1002/eji.200939488

Marsh, K., & Bugusu, B. (2007). Food Packaging—Roles, Materials, and Environmental Issues. *Journal of Food Science*, *72*(3), 39–55. https://doi.org/10.1111/j.1750-3841.2007.00301.x

Mauldin, T. C., & Kessler, M. R. (2010). Self-healing polymers and composites. *International Materials Reviews*, *55*(6), 317–346. https://doi.org/10.1179/095066010X12646898728408

Mchught, T. H., & Krochta, J. M. (1994). *Iournal o f Agricultural andFd Chemistrv*. *42*(4), 0–4.

Min, G. (1999). Conducting polymers and their application in the film industry - polyaniline/polyimide blended films. *Syn1*, *102*, 1163–1166.

Mohamad, S. N., Ismail, N. F., & Hamzah, A. (2021). *Red Hybrid Tilapia (Oreochromis spp .) Broodstock Development Programme in Malaysia : Status , Challenges and Prospects for Future Development*. *1*, 73–81.

Mohammad, A. W., Kumar, A. G., & Basha, R. K. (2014a). Optimization of enzymatic hydrolysis of tilapia (Oreochromis Spp.) scale gelatine. *International Aquatic Research*, *7*(1), 27–39. https://doi.org/10.1007/s40071-014-0090-6

Mohammad, A. W., Kumar, A. G., & Basha, R. K. (2014b). Optimization of enzymatic hydrolysis of tilapia (Oreochromis Spp.) scale gelatine. *International Aquatic Research*, *7*(1), 27–39. https://doi.org/10.1007/s40071-014-0090-6

Mohammadi, B., Pirsa, S., & Alizadeh, M. (2019). Preparing chitosan–polyaniline nanocomposite film and examining its mechanical, electrical, and antimicrobial properties. *Polymers and Polymer Composites*, *27*(8), 507–517. https://doi.org/10.1177/0967391119851439

Mohilner, D. M., Adams, R. N., & Argersinger, W. J. (1962). Investigation of the Kinetics and Mechanism of the Anodic Oxidation of Aniline in Aqueous Sulfuric Acid Solution at a Platinum Electrode. *Journal of the American Chemical Society*, *84*(19), 3618–3622. https://doi.org/10.1021/ja00878a003

Montero, P., & Gómez-Guillén, M. C. (2000). Extracting conditions for megrim (Lepidorhombus boscii) skin collagen affect functional properties of the

resulting gelatin. *Journal of Food Science*, *65*(3), 434–438. https://doi.org/10.1111/j.1365-2621.2000.tb16022.x

Mostafa, H. M., & Sourell, H. (2009). Equilibrium Moisture Content of Some Bioplastic Materials for Agricultural Use. *Agricultural Engineering International: CIGR Journal*, *0*(0), 1–10.

Muyonga, J. H., Cole, C. G. B., & Duodu, K. G. (2004). Characterisation of acid soluble collagen from skins of young and adult Nile perch (Lates niloticus). *Food Chemistry*, *85*(1), 81–89. https://doi.org/10.1016/j.foodchem.2003.06.006

Nagai, T., Izumi, M., & Ishii, M. (2004). *Fish scale collagen . Preparation and partial characterization*. 239–244. https://doi.org/10.1111/j.1365-2621.2004.00777.x

Nalinanon, S., Benjakul, S., Visessanguan, W., & Kishimura, H. (2008). Improvement of gelatin extraction from bigeye snapper skin using pepsin-aided process in combination with protease inhibitor. *Food Hydrocolloids*, *22*(4), 615–622. https://doi.org/10.1016/j.foodhyd.2007.01.012

Nand, A. V., Ray, S., Easteal, A. J., Waterhouse, G. I. N., Gizdavic-Nikolaidis, M., Cooney, R. P., Travas-Sejdic, J., & Kilmartin, P. A. (2011). Factors affecting the radical scavenging activity of polyaniline. *Synthetic Metals*, *161*(13–14), 1232–1237. https://doi.org/10.1016/j.synthmet.2011.04.010

Nand, A. V., Ray, S., Travas-Sejdic, J., & Kilmartin, P. A. (2012). Characterization of polyethylene terephthalate/polyaniline blends as potential antioxidant materials. *Materials Chemistry and Physics*, *134*(1), 443–450. https://doi.org/10.1016/j.matchemphys.2012.03.015

Narkar, A. R., Barker, B., Clisch, M., Jiang, J., & Lee, B. P. (2016). PH Responsive and Oxidation Resistant Wet Adhesive based on Reversible Catechol-Boronate Complexation. *Chemistry of Materials*, *28*(15), 5432–5439. https://doi.org/10.1021/acs.chemmater.6b01851

Nascimento, S., Surita, F., & Cecatti, J. (2012). Physical exercise during pregnancy: a systematic review. *Curr Opin Obstet Gynecol*, *24*(6), 387–394. https://doi.org/10.1097/GCO.0b013e328359f131.

Nataraj, D., Sakkara, S., HN, M., & Reddy, N. (2018). Properties and applications of citric acid crosslinked banana fibre-wheat gluten films. *Industrial Crops and Products*, *124*(July), 265–272. https://doi.org/10.1016/j.indcrop.2018.07.076

Nikoo, M., Xu, X., Development, A. C., & Ehsani, A. (2011). *International Aquatic Research Characterization of gelatin from the skin of farmed Amur sturgeon Acipenser schrenckii*. *January*.

Ninan, G., Joseph, J., & Aliyamveettil, Z. A. (2014). A comparative study on the physical, chemical and functional properties of carp skin and mammalian gelatins. *Journal of Food Science and Technology*, *51*(9), 2085–2091.

Nor, M. H. M., Nazmi, N. N. M., & Sarbon, N. M. (2017a). Effects of plasticizer concentrations on functional properties of chicken skin gelatin films. *International Food Research Journal*, *24*(5), 1910–1918.

Nor, M. H. M., Nazmi, N. N. M., & Sarbon, N. M. (2017b). Effects of plasticizer concentrations on functional properties of chicken skin gelatin films Effects of plasticizer concentrations on functional properties of chicken skin gelatin films. *International Food Reserach Journal*, *24*(5), 1910–1918.

Nordin, N., Othman, S. H., Rashid, S. A., & Basha, R. K. (2020). Effects of glycerol and thymol on physical, mechanical, and thermal properties of corn starch films. *Food Hydrocolloids*, *106*(March), 105884. https://doi.org/10.1016/j.foodhyd.2020.105884

Nur Hanani, Z. A., Roos, Y. H., & Kerry, J. P. (2014). Use and application of gelatin as potential biodegradable packaging materials for food products. *International Journal of Biological Macromolecules*, *71*, 94–102. https://doi.org/10.1016/j.ijbiomac.2014.04.027

Nurilmala, M., Suryamarevita, H., Hizbullah, H. H., Jacoeb, Agoes, M., & Ochiai, Y. (2022). Fish skin as a biomaterial for halal collagen and gelatin. *Saudi Journal of Biological Sciences*, *29*(2).

Oakenfull, D., & Scott, A. (2003). Gelatin gels in deuterium oxide. *Food Hydrocolloids*, *17*(2), 207–210.

Ogbonnaya Chukwu. (2010). Moisture-Sorption Study of Dried Date Fruits. *AU Journal of Technology*, *13*(3), 175–180.

Othman, S. H., Amirah, S., Edwal, M., Risyon, N. P., Basha, R. K., & Talib, R. A. (2017). Water Sorption and water permeability properties of edible film made from potato peel waste. *Food Science and Technology (Campinas)*, *37*, 63–70.

Othman, S. H., Kechik, N. R. A., Shapi'i, R. A., Talib, R. A., & Tawakkal, I. S. M. A. (2019). Water sorption and mechanical properties of starch/chitosan nanoparticle films. *Journal of Nanomaterials*, *2019*. https://doi.org/10.1155/2019/3843949

Palaniappan, S., & John, A. (2008). Polyaniline materials by emulsion polymerization pathway. *Progress in Polymer Science (Oxford)*, *33*(7), 732–758. https://doi.org/10.1016/j.progpolymsci.2008.02.002

Park, S. K., Rhee, C. O., Bae, D. H., & Hettiarachchy, N. S. (2001). Mechanical Properties and Water-Vapor Permeability of Soy-Protein Films Affected by

Calcium Salts and Glucono- δ -lactone. *Journal of Agriculture Food Chemical*, *15 mL*, 2308–2312.

Parsa, A., & Ghani, S. A. (2009). The improvement of free-radical scavenging capacity of the phosphate medium electrosynthesized polyaniline. *Electrochimica Acta*, *54*(10), 2856–2860. https://doi.org/10.1016/j.electacta.2008.11.022

Paschoalick, T. M., Garcia, F. T., Sobral, P. J. A., & Habitante, A. M. Q. B. (2003). Characterization of some functional properties of edible films based on muscle proteins of Nile Tilapia. *Food Hydrocolloids*, *17*(4), 419–427. https://doi.org/10.1016/S0268-005X(03)00031-6

Peleg, M. (1988). An Empirical Model for the Prediction. *Journal of Food Science*, *53*(4), 1216–1217.

Perazzo, K. K. N. C. L., Carlos De Vasconcelos Conceição, A., Pires Dos Santos, J. C., De Jesus Assis, D., Souza, C. O., & Druzian, J. I. (2014). Properties and antioxidant action of actives cassava starch films incorporated with green tea and palm oil extracts. *PLoS ONE*, *9*(9), 1–13. https://doi.org/10.1371/journal.pone.0105199

Phadke, A., Zhang, C., Arman, B., Hsu, cheng-C., Mashelkar, R. A., Kele, A. K., Tauber, M. J., Arya, G., & Verghese, S. (2012). *Rapid self-healing hydrogels*. *109*(12), 4383–4388. https://doi.org/10.1073/pnas.1201122109/-/DCSupplemental

Pirsa, S., & Mohammadi, B. (2021). Conducting/biodegradable chitosan-polyaniline film; Antioxidant, color, solubility and water vapor permeability properties. *Main Group Chemistry*, *20*(2), 133–147. https://doi.org/10.3233/MGC-210007

Pomeranz, Y., & Meloan, C. E. (2000). *Food Analysis: Theory and Practice* (3rd Editio). Aspen Publication.

Prabhakar, P. K., Raj, S., Anuradha, P. R., Sawant, S. N., & Doble, M. (2011). Biocampatibility studies on polyaniline and polyaniline-silver nanoparticle coated polyurethane composite. *Colloids and Surfaces B: Biointerfaces*, *86*, 146–153.

Pud, A. A. (1994). Stability and degradation of conducting polymers in electrochemical systems. *Synthetic Metals*, *66*, 91–97.

Pushpadass, H. A., Marx, D. B., & Hanna, M. A. (2008). Effects of extrusion temperature and plasticizers on the physical and functional properties of starch films. *Starch/Staerke*, *60*(10), 527–538. https://doi.org/10.1002/star.200800713

Quirós-Sauceda, A. E., Palafox-Carlos, H., Sáyago-Ayerdi, S. G., Ayala-Zavala, J. F., Bello-Perez, L. A., Álvarez-Parrilla, E., De La Rosa, L. A., González-

Córdova, A. F., & González-Aguilar, G. A. (2014). Dietary fiber and phenolic compounds as functional ingredients: Interaction and possible effect after ingestion. *Food and Function*, *5*(6), 1063–1072. https://doi.org/10.1039/c4fo00073k

Ramachandran, G. N., & Kartha, G. (1954). Structure of Collagen. *Nature*, *174*, 269–270.

Ramos, M., Valdés, A., Beltrán, A., & Garrigós, M. (2016). Gelatin-Based Films and Coatings for Food Packaging Applications. *Coatings*, *6*(4), 41. https://doi.org/10.3390/coatings6040041

Reátegui-Pinedo, N., Salirrosas, D., Sánchez-Tuesta, L., Quiñones, C., Jáuregui-Rosas, S. R., Barraza, G., Cabrera, A., Ayala-Jara, C., Martinez, R. M., Baby, A. R., & Prieto, Z. A. (2022). Characterization of Collagen from Three Genetic Lines (Gray, Red and F1) of Oreochromis niloticus (Tilapia) Skin in Young and Old Adults. *Molecules*, *27*(3). https://doi.org/10.3390/molecules27031123

Robertson, G. L. (2008). *Food packaging Principles and Practice* (Issue May 2007).

Roff, C. F., & Allen Foegeding, E. (1996). Dicationic-induced gelation of pre-denatured whey protein isolate. *Food Hydrocolloids*, *10*(2), 193–198. https://doi.org/10.1016/S0268-005X(96)80034-8

Ross-Murphy, S. B. (1997). Structure and Rheology of Gelatin Gels. *The Imaging Science Journal*, *45*(3–4), 205–209.

Saberi, B., Vuong, Q., Chockchaisawasdee, S., Golding, J., Scarlett, C., & Stathopoulos, C. (2015). Water Sorption Isotherm of Pea Starch Edible Films and Prediction Models. *Foods*, *5*(4), 1. https://doi.org/10.3390/foods5010001

Said, N. S., Howell, N. K., & Sarbon, N. M. (2021). A Review on Potential Use of Gelatin-based Film as Active and Smart Biodegradable Films for Food Packaging Application. In *Food Reviews International*. Bellwether Publishing, Ltd. https://doi.org/10.1080/87559129.2021.1929298

Said, N. S., & Sarbon, N. M. (2022a). Physical and Mechanical Characteristics of Gelatin-Based Films as a Potential Food Packaging Material: A Review. In *Membranes* (Vol. 12, Issue 5). MDPI. https://doi.org/10.3390/membranes12050442

Said, N. S., & Sarbon, N. M. (2022b). *Physical and Mechanical Characteristics of Gelatin-Based Films as a Potential Food Packaging Material : A Review*.

Said, N. S., & Sarbon, N. M. (2022c). Physical and Mechanical Characteristics of Gelatin-Based Films as a Potential Food Packaging Material: A Review.

In *Membranes* (Vol. 12, Issue 5). MDPI. https://doi.org/10.3390/membranes12050442

Saikia, J. P., Banerjee, S., Konwar, B. K., & Kumar, A. (2010). Biocompatible novel starch/polyaniline composites: Characterization, anti-cytotoxicity and antioxidant activity. *Colloids and Surfaces B: Biointerfaces*, *81*(1), 158–164. https://doi.org/10.1016/j.colsurfb.2010.07.005

Sánchez-Moreno, C. (2002). Methods Used to Evaluate the Free Radical Scavenging Activity in Foods and Biological Systems. *Food Science and Technology International*, *8*(3), 121–137. https://doi.org/10.1106/108201302026770

Sanyang, M. L., Sapuan, S. M., Jawaid, M., Ishak, M. R., & Sahari, J. (2015a). Effect of glycerol and sorbitol plasticizers on physical and thermal properties of sugar palm starch based films. *Recent Advances in Environment, Ecosystems and Development Effect*, *April*, 157–162.

Sanyang, M. L., Sapuan, S. M., Jawaid, M., Ishak, M. R., & Sahari, J. (2015b). Effect of plasticizer type and concentration on tensile, thermal and barrier properties of biodegradable films based on sugar palm (Arenga pinnata) starch. *Polymers*, *7*(6), 1106–1124. https://doi.org/10.3390/polym7061106

Sanyang, M. L., Sapuan, S. M., Jawaid, M., Ishak, M. R., & Sahari, J. (2016). Effect of plasticizer type and concentration on physical properties of biodegradable films based on sugar palm (arenga pinnata) starch for food packaging. *Journal of Food Science and Technology*, *53*(1), 326–336. https://doi.org/10.1007/s13197-015-2009-7

Sarabia, A. I., Gómez-Guillén, M. C., & Montero, P. (2000). The effect of added salts on the viscoelastic properties of fish skin gelatin. *Food Chemistry*, *70*(1), 71–76. https://doi.org/10.1016/S0308-8146(00)00073-X

Scherr, E. M., MacDiarmid, A. G., Manohar, S. K., Masters, J. G., Sun, Y., Tang, X., Druy, M. A., Glatkowski, P. J., Cajipe, V. B., Fischer, J. E., Cromack, K. R., Jozefowicz, M. E., Ginder, J. M., McCall, R. P., & Epstein, A. J. (1991). Polyaniline: Oriented films and fibers. *Synthetic Metals*, *41*(1–2), 735–738. https://doi.org/10.1016/0379-6779(91)91173-8

Shafiur Rahman, M. (2007). *Handbook of Food Preservation, Second Edition - Google Books* (pp. 587–608).

Shaikh, S., Yaqoob, M., & Aggarwal, P. (2021). An overview of biodegradable packaging in food industry. In *Current Research in Food Science* (Vol. 4, pp. 503–520). Elsevier B.V. https://doi.org/10.1016/j.crfs.2021.07.005

Shalini, R., & Singh, A. (2009). *Biobased Packaging Materials for the Food Industry*. *5*, 16–20.

Sharma, A., Rawat, K., Solanki, P. R., & Bohidar, H. B. (2017). Self-healing gelatin ionogels. *International Journal of Biological Macromolecules*, *95*, 603–607. https://doi.org/10.1016/j.ijbiomac.2016.11.103

Siparsky, G. L., Voorhees, K. J., Dorgan, J. R., & Schilling, K. (1997). Water transport in polylactic acid (PLA), PLA/polycaprolactone copolymers, and PLA/polyethylene glycol blends. *Journal of Environmental Polymer Degradation*, *5*(3), 125–136.

Siracusa, V. (2012). Food packaging permeability behaviour: A report. *International Journal of Polymer Science*, *2012*(i). https://doi.org/10.1155/2012/302029

Siriwardhana, C., Ali, S. S., Roberts, B., & Stewart, R. (2014). A systematic review of resilience and mental health outcomes of conflict-driven adult forced migrants. *Conflict and Health*, *8*(1). https://doi.org/10.1186/1752-1505-8-13

Skorb, E. V, & Andreeva, D. V. (2015). *Self-healing properties of layer-by-layer assembled multilayers*. *November 2014*. https://doi.org/10.1002/pi.4899

Sockalingam, K., & Abdullah, H. Z. (2015). *Extraction and Characterization of Gelatin Biopolymer from Black Tilapia (Oreochromis mossambicus) Scales*. *020053*. https://doi.org/10.1063/1.4919191

Song, G., Zhang, L., He, C., Fang, D. C., Whitten, P. G., & Wang, H. (2013). Facile fabrication of tough hydrogels physically cross-linked by strong cooperative hydrogen bonding. *Macromolecules*, *46*(18), 7423–7435. https://doi.org/10.1021/ma401053c

Song, Y., Meyers, K. P., Gerringer, J., Ramakrishnan, R. K., Humood, M., Qin, S., Polycarpou, A. A., Nazarenko, S., & Grunlan, J. C. (2017). Fast Self-Healing of Polyelectrolyte Multilayer Nanocoating and Restoration of Super Oxygen Barrier. *Macromolecular Rapid Communications*, *38*(10), 1–7. https://doi.org/10.1002/marc.201700064

Songchotikunpan, P., Tattiyakul, J., & Supaphol, P. (2008). *Extraction and electrospinning of gelatin from fish skin*. *42*, 247–255. https://doi.org/10.1016/j.ijbiomac.2007.11.005

Soo, P. Y., & Sarbon, N. M. (2018). Preparation and characterization of edible chicken skin gelatin fi lm incorporated with rice fl our. *Food Packaging and Shelf Life*, *15*(August 2017), 1–8. https://doi.org/10.1016/j.fpsl.2017.12.009

Srinivasa, P. C., Ramesh, M. N., Kumar, K. R., & Tharanathan, R. N. (2003). Properties and sorption studies of chitosan-polyvinyl alcohol blend films. *Carbohydrate Polymers*, *53*(4), 431–438. https://doi.org/10.1016/S0144-8617(03)00105-X

Stejskal, J., & Gilbert, R. G. (2002). POLYANILINE. PREPARATION OF A CONDUCTING POLYMER (IUPAC Technical Report). *Pure Appl. Chem.Russia J. Janca (France); N. Gospodinova (France); M. Helmstedt (Germany); I. Krivka (Czech Republic); P. Mokreva (Bulgaria J. Prokes (Czech Republic); A. Riede (Germany); E. Rozova (Russia); I. Sapurina (Russia); T. Shishkanova (France);*, *74*(5), 857867. https://doi.org/10.1351/pac200274050857

Strauss, U. P., Porcja, R. J., & Chen, S. Y. (1991). Volume Effects of Starch-Water Interactions. In H. Levine & L. Slade (Eds.), *Advances in Experimental Medicine and Biology* (pp. 351–363). Plenum Press.

Sudár, A., Móczó, J., Vörös, G., & Pukánszky, B. (2007). The mechanism and kinetics of void formation and growth in particulate filled PE composites. *Express Polymer Letters*, *1*(11), 763–772. https://doi.org/10.3144/expresspolymlett.2007.105

Suderman, N., Isa, M. I. N., & Sarbon, N. M. (2018). The effect of plasticizers on the functional properties of biodegradable gelatin-based film: A review. *Food Bioscience*, *24*(111–149).

Suhag, R., Kumar, N., Petkoska, A. T., & Upadhyay, A. (2020). Film formation and deposition methods of edible coating on food products: A review. *Food Research International*, *136*(March), 109582. https://doi.org/10.1016/j.foodres.2020.109582

Sun, P. D., Foster, C. E., & Boyington, J. C. (2004). Overview of protein structural and functional folds. *Current Protocols in Protein Science / Editorial Board, John E. Coligan ... [et Al.]*, *Chapter 17*, 1–189. https://doi.org/10.1002/0471140864.ps1701s35

Suppakul, P., Chalernsook, B., Ratisuthawat, B., Prapasitthi, S., & Munchukangwan, N. (2013). Empirical modeling of moisture sorption characteristics and mechanical and barrier properties of cassava flour film and their relation to plasticizing-antiplasticizing effects. *LWT - Food Science and Technology*, *50*(1), 290–297. https://doi.org/10.1016/j.lwt.2012.05.013

Tang, J., Jing, X., Wang, B., & Wang, F. (1988). Infrared spectra of soluble polyaniline. *Synthetic Metals*, *24*(3), 231–238. https://doi.org/10.1016/0379-6779(88)90261-5

Tarique, J., Sapuan, S. M., & Khalina, A. (2021). Effect of glycerol plasticizer loading on the physical , mechanical , thermal , and barrier properties of arrowroot (Maranta arundinacea) starch biopolymers. *Scientific Reports*, 1–17. https://doi.org/10.1038/s41598-021-93094-y

Thakur, V. K., & Kessler, M. R. (2015). Self-healing polymer nanocomposite materials: A review. *Polymer*. https://doi.org/10.1016/j.polymer.2015.04.086

Tian, Z., Yu, H., Wang, L., Saleem, M., Ren, F., Ren, P., Chen, Y., Sun, R., Sun, Y., & Huang, L. (2014a). Recent progress in the preparation of polyaniline nanostructures and their applications in anticorrosive coatings. *RSC Advances*, *4*(54), 28195–28208. https://doi.org/10.1039/c4ra03146f

Tian, Z., Yu, H., Wang, L., Saleem, M., Ren, F., Ren, P., Chen, Y., Sun, R., Sun, Y., & Huang, L. (2014b). Recent progress in the preparation of polyaniline nanostructures and their applications in anticorrosive coatings. *RSC Advances*, *4*(54), 28195–28208. https://doi.org/10.1039/c4ra03146f

Tong, Y., & Ying, T. (2013). Gelling strength improvement and characterization of a gelatin from scales of bighead carp (Aristichthys nobilis). *Journal of Food, Agriculture and Environment*, *11*(1), 146–150.

Tongnuanchan, P., Benjakul, S., & Prodpran, T. (2012). Properties and antioxidant activity of fish skin gelatin film incorporated with citrus essential oils. *Food Chemistry*, *134*(3), 1571–1579. https://doi.org/10.1016/j.foodchem.2012.03.094

Tongnuanchan, P., Benjakul, S., & Prodpran, T. (2013). Physico-chemical properties, morphology and antioxidant activity of film from fish skin gelatin incorporated with root essential oils. *Journal of Food Engineering*, *117*(3), 350–360. https://doi.org/10.1016/j.jfoodeng.2013.03.005

Tongnuanchan, P., Benjakul, S., & Prodpran, T. (2014). Structural, morphological and thermal behaviour characterisations of fish gelatin film incorporated with basil and citronella essential oils as affected by surfactants. *Food Hydrocolloids*, *41*, 33–43. https://doi.org/10.1016/j.foodhyd.2014.03.015

Tongnuanchan, P., Benjakul, S., Prodpran, T., & Nilsuwan, K. (2015). Emulsion film based on fish skin gelatin and palm oil: Physical, structural and thermal properties. *Food Hydrocolloids*, *48*, 248–259. https://doi.org/10.1016/j.foodhyd.2015.02.025

Tongnuanchan, P., Benjakul, S., Prodpran, T., Pisuchpen, S., & Osako, K. (2016). Mechanical, thermal and heat sealing properties of fish skin gelatin film containing palm oil and basil essential oil with different surfactants. *Food Hydrocolloids*, *56*, 93–107. https://doi.org/10.1016/j.foodhyd.2015.12.005

Tongnuanchan, P., Benjakul, S., Prodpran, T., & Songtipya, P. (2011). Characteristics of film based on protein isolate from red tilapia muscle with negligible yellow discoloration. *International Journal of Biological Macromolecules*, *48*, 758–767.

Tu, Q., Zhang, Q., Wang, Y., Jiao, Y., Xiao, J., Peng, T., & Wang, J. (2019). Antibacterial properties of poly(dimethylsiloxane) surfaces modified with graphene oxide-catechol composite. *Progress in Organic Coatings*, *129*, 247–253. https://doi.org/10.1016/j.porgcoat.2019.01.011

Tuncaboylu, D. C., Argun, A., Sahin, M., Sari, M., & Okay, O. (2012). Structure optimization of self-healing hydrogels formed via hydrophobic interactions. *Polymer*, *53*(24), 5513–5522. https://doi.org/10.1016/j.polymer.2012.10.015

Tyuftin, A. A., & Kerry, J. P. (2021). Gelatin films : Study review of barrier properties and implications for future studies employing biopolymer films. *Food Packaging and Shelf Life*, *29*(May), 100688. https://doi.org/10.1016/j.fpsl.2021.100688

Vanin, F. M., Sobral, P. J. A., Menegalli, F. C., Carvalho, R. A., & Habitante, A. M. Q. B. (2005). Effects of plasticizers and their concentrations on thermal and functional properties of gelatin-based films. *Food Hydrocolloids*, *19*(5), 899–907. https://doi.org/10.1016/j.foodhyd.2004.12.003

Vermeiren, L., Devlieghere, F., van Beest, M., de Kruijf, N., & Debevere, J. (2000). Developement in the Active Packaging of Foods. *The Journal of Food Technology in Africa*, *5*(1), 6–13.

Villasante, J., Martin-Lujano, A., & Almajano, M. P. (2020). Characterization and Application of Gelatin Films with Pecan Walnut and Shell Extract (Carya illinoiensis). *Polymers*, *12*(6), 1424–1446.

Wang, J., Zhu, L. H., Li, J., & Tang, H. Q. (2007). Antioxidant activity of polyaniline nanofibers. *Chinese Chemical Letters*, *18*(8), 1005–1008. https://doi.org/10.1016/j.cclet.2007.05.056

Wei, Y., Tang, X., Sun, Y., & Focke, W. W. (1989). A study of the mechanism of aniline polymerization. *Journal of Polymer Science Part A: Polymer Chemistry*, *27*(7), 2385–2396. https://doi.org/10.1002/pola.1989.080270720

Weng, W., & Wu, F. (2015). Water resistance and mechanical property improvement of tilapia (Tilapia zillii) scale gelatin films by dehydrated thermal treatment. *Journal of Food Science and Technology*, *52*(6), 3358–3366. https://doi.org/10.1007/s13197-014-1401-z

Weng, W., Zheng, H., & Su, W. (2014). Characterization of edible films based on tilapia (Tilapia zillii) scale gelatin with different extraction pH. *Food Hydrocolloids*. https://doi.org/10.1016/j.foodhyd.2014.03.026

Wilson, C. T., Harte, J., & Almenar, E. (2018). Effects of sachet presence on consumer product perception and active packaging acceptability - A study of fresh-cut cantaloupe. *Lwt*, *92*(February), 531–539. https://doi.org/10.1016/j.lwt.2018.02.060

Wittmer, A., Wellen, R., Saalwächter, K., & Koschek, K. (2018). Moisture-meidated self-healing kinetics and molecular dynamics in modified polyurethane urea polymers. *Polymer*. https://doi.org/10.1016/j.polymer.2018.07.059

Woo, E. M., & Jang, F. H. (1999). Phase structure and miscibility in blend of poly(4-methyl styrene) with poly(cyclohexyl methacrylate). *Polymer*, *40*(13), 3803–3808. https://doi.org/10.1016/S0032-3861(98)00581-3

Wool, R. P., & O'Connor, K. M. (1981). A theory of crack healing in polymers. *Journal of Applied Physics*, *52*(10), 5953–5963. https://doi.org/10.1063/1.328526

Xu, Y., Wu, Q., Sun, Y., Bai, H., & Shi, G. (2010). Three-dimensional self-assembly of graphene oxide and DNA into multifunctional hydrogels. *ACS Nano*, *4*(12), 7358–7362. https://doi.org/10.1021/nn1027104

Xu, Y. X., Kim, K. M., Hanna, M. A., & Nag, D. (2005). Chitosan-starch composite film: Preparation and characterization. *Industrial Crops and Products*, *21*(2), 185–192. https://doi.org/10.1016/j.indcrop.2004.03.002

Yadav, A. S., & Bhatnagar, D. (2007). Free radical scavenging activity, metal chelation and antioxidant power of some of the Indian spices. *BioFactors*, *31*(3–4), 219–227. https://doi.org/10.1002/biof.5520310309

Yang, H., Wang, Y., Zhou, P., & Regenstein, J. M. (2008). Effects of alkaline and acid pretreatment on the physical properties and nanostructures of the gelatin from channel catfish skins. *Food Hydrocolloids*, *22*(1541–1550).

Yang, L., & Paulson, A. T. (2000). Mechanical and water vapour barrier properties of edible gellan films. *Food Research International*, *33*(7), 563–570. https://doi.org/10.1016/S0963-9969(00)00092-2

Yavuz, A. G., Uygun, A., & Bhethanabotla, V. R. (2009). Substituted polyaniline/chitosan composites: Synthesis and characterization. *Carbohydrate Polymers*, *75*(3), 448–453. https://doi.org/10.1016/j.carbpol.2008.08.005

Yoon, J. S., Jung, H. W., Kim, M. N., & Park, E. S. (2000). Diffusion coefficient and equilibrium solubility of water molecules in biodegradable polymers. *Journal of Applied Polymer Science*, *77*(8), 1716–1722. https://doi.org/10.1002/1097-4628(20000822)77:8<1716::AID-APP8>3.0.CO;2-F

Yulistiani, F., Khairunisa, N., & Fitiana, R. (2020). The effect of glycerol concentration and breadfruit flour mass on edible film characteristics. *Journal of Physics: Conference Series*, *1450*(1). https://doi.org/10.1088/1742-6596/1450/1/012001

Zaiter, A., Becker, L., Karam, M. C., & Dicko, A. (2016). Effect of particle size on antioxidant activity and catechin content of green tea powders. *Journal of Food Science and Technology*, *53*(4), 2025–2032. https://doi.org/10.1007/s13197-016-2201-4

Zareh, E. N., Moghadam, P. N., Azariyan, E., & Sharifian, I. (2011). Conductive and Biodegradable polyaniline/starch Blends and Their Composites with Polystrene polyaniline/starch Blends and Their Composites with Polystrene. *Iranian Polymer Journal*, *20*(4), 319–328.

Zemskov, S. V., Jonkers, H. M., & Vermolen, F. J. (2014). A mathematical model for bacterial self-healing of cracks in concrete. *Journal of Intelligent Material Systems and Structures*, *25*(1), 4–12. https://doi.org/10.1177/1045389X12437887

Zhang, F., Xu, S., & Wang, Z. (2010). Pre-treatment optimization and properties of gelatin from freshwater fish scales. *Food and Bioproducts Processing*, *9*(May), 185–193. https://doi.org/10.1016/j.fbp.2010.05.003

Zhang, X., & He, J. (2015). Hydrogen-Bonding-Supported Self-Healing Antifogging Thin Films. *Scientific Reports*, *5*, 1–4. https://doi.org/10.1038/srep09227

Zhang, Z., Qian, S., & Ma, H. (2014). Investigating mechanical properties and self-healing behavior of micro-cracked ECC with different volume of fly ash. *Construction and Building Materials*, *52*, 17–23. https://doi.org/10.1016/j.conbuildmat.2013.11.001

Zhou, P., & Regenstein, J. M. (2005). Effects of alkaline and acid pretreatments on Alaska pollock skin gelatin extraction. *Journal of Food Science*, *70*(6), c392–c396. https://doi.org/10.1111/j.1365-2621.2005.tb11435.x

Zin, N. H. M., Wahab, W. A., & Ariffin, N. N. (2019). Extraction of collagen and gelatin from the scales of different freshwater fish. *International Journal of Allied Health Sciences*, *3*(2), 894–903.

*Sample	Day 0	Day 4	Day 7
G-Gly			
G-Gly-PANI(A0.5)	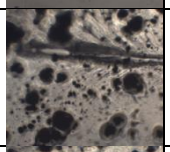	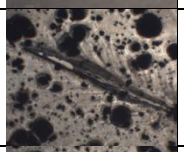	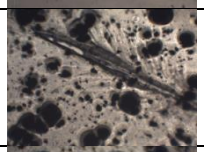
G-Gly-PANI(A1)	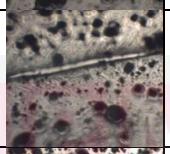	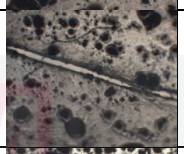	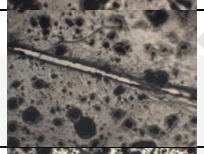
G-Gly-PANI(A2)	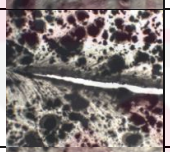	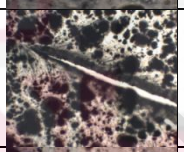	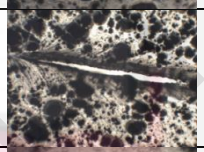
G-Gly-PANI(B0.5)	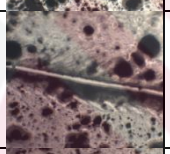	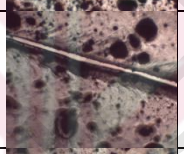	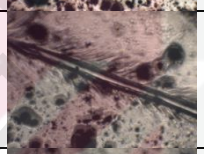
G-Gly-PANI(B1)	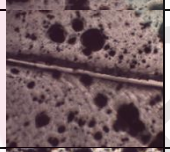	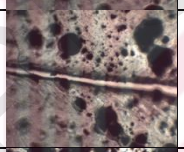	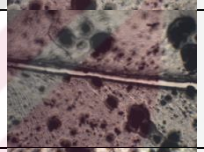
G-Gly-PANI(B2)	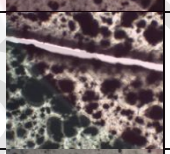	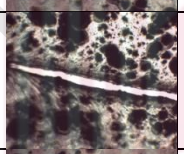	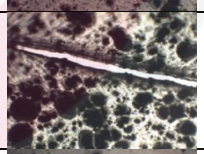
G-Gly-PANI(C0.5)	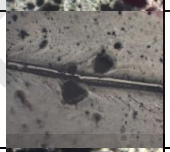	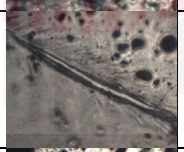	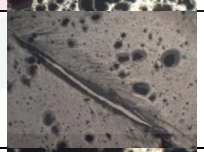
G-Gly-PANI(C1)	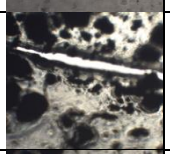	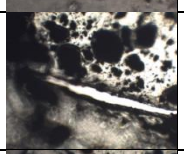	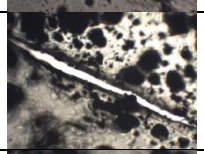
G-Gly-PANI(C2)	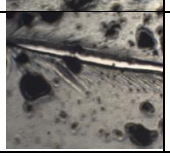	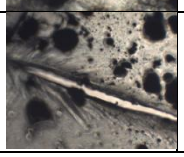	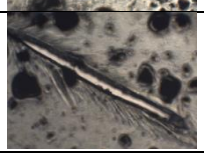

Figure A1: Light microscope image (10x magnification) of self-healing progress at day 0, 4 and 7 at RH 43% and temperature 5 °C

*Sample	Day 0	Day 4	Day 7
G-Gly			
G-Gly-PANI(A0.5)	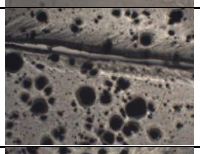	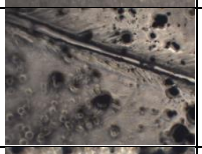	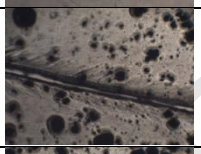
G-Gly-PANI(A1)	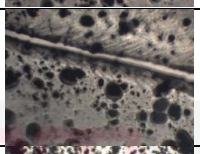	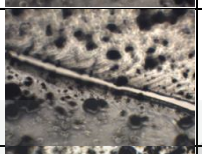	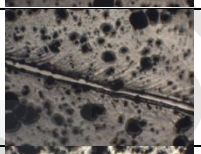
G-Gly-PANI(A2)	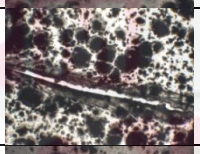	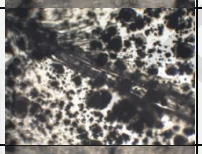	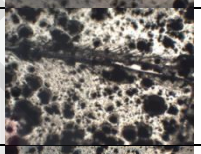
G-Gly-PANI(B0.5)	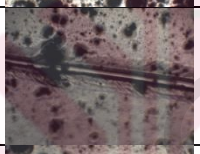	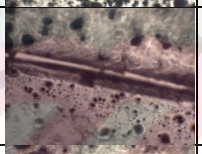	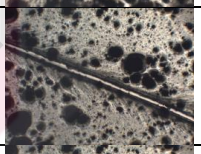
G-Gly-PANI(B1)	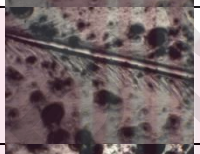	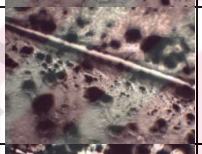	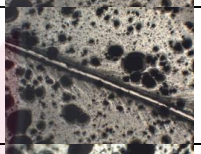
G-Gly-PANI(B2)	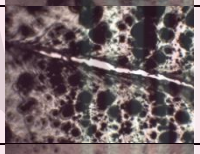	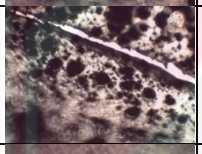	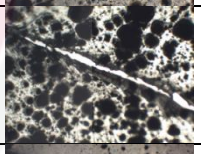
G-Gly-PANI(C0.5)	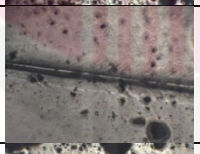	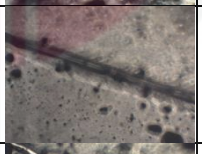	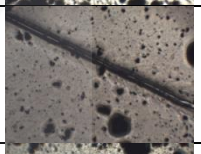
G-Gly-PANI(C1)	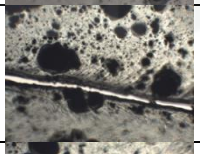	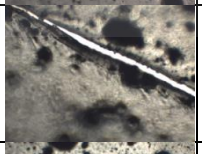	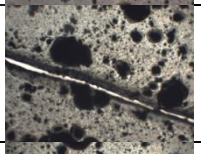
G-Gly-PANI(C2)	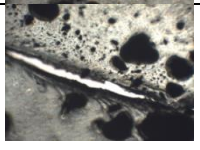	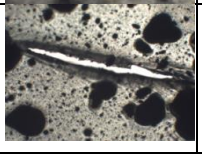	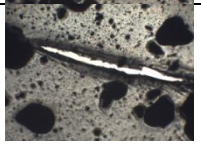

Figure A2: Light microscope image (x10 magnification) of self-healing progress at day 0, 4 and 7 at RH 43% and temperature 30 °C

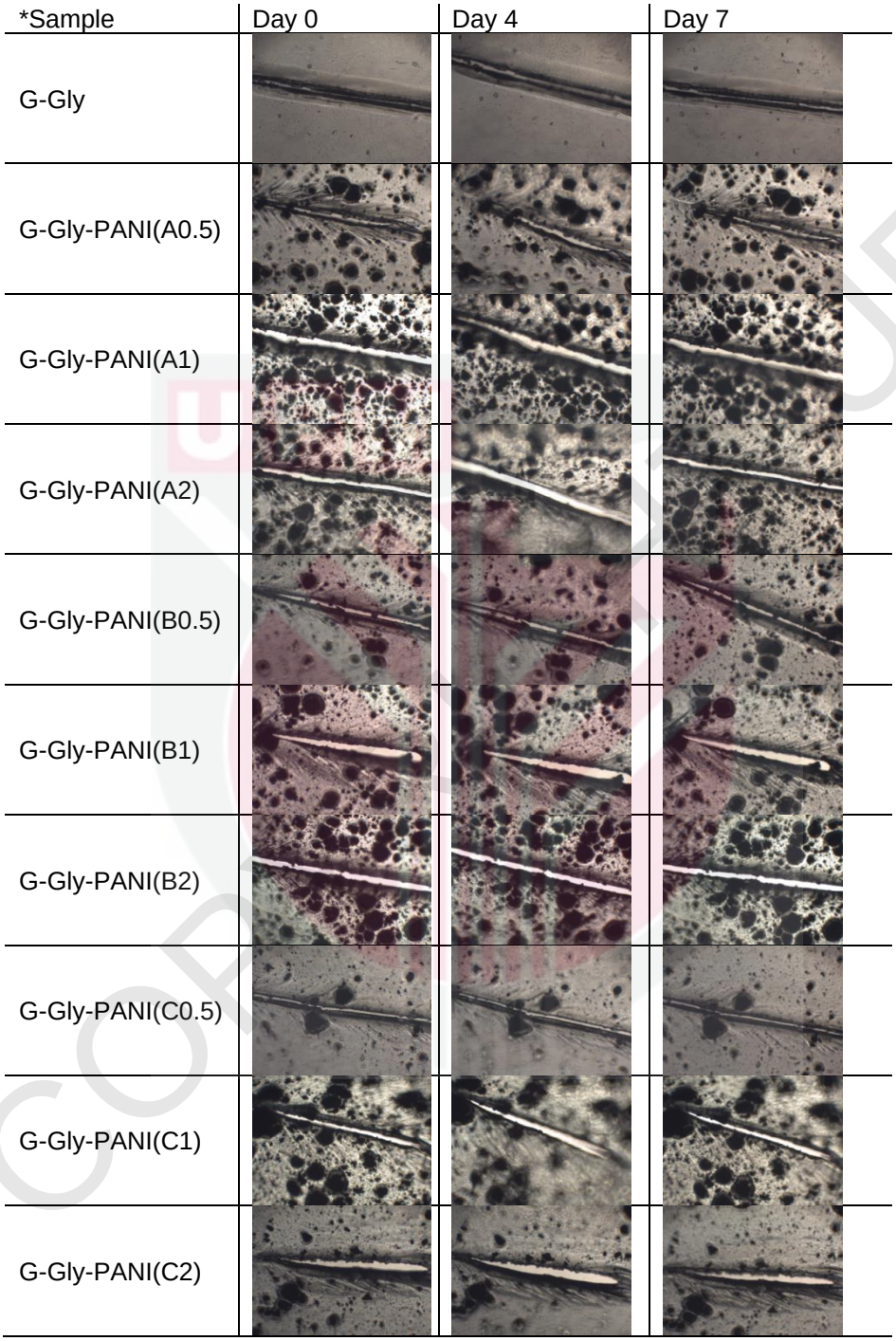

Figure A3: Light microscope (x10 magnification) image of self-healing progress at day 0, 4 and 7 at RH 43% and temperature 40 °C

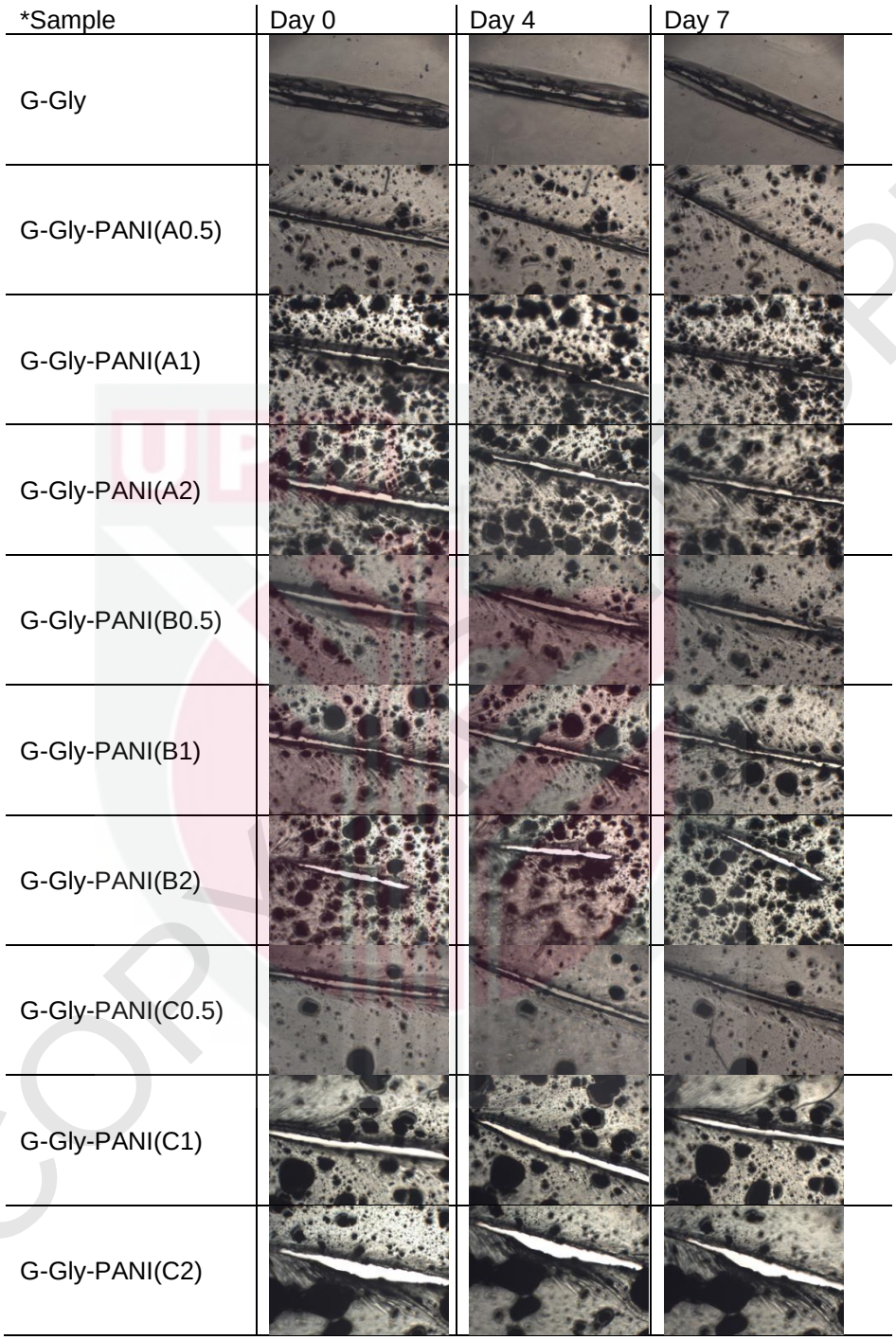

Figure A4: Light microscope (x10 magnification) image of self-healing progress at day 0, 4 and 7 at RH 57% and temperature 5 °C

*Sample	Day 0	Day 4	Day 7
G-Gly			
G-Gly-PANI(A0.5)	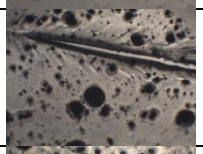	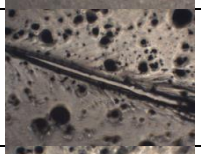	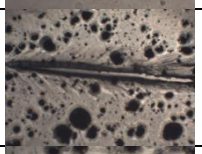
G-Gly-PANI(A1)	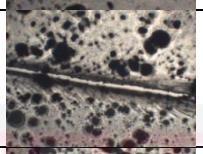	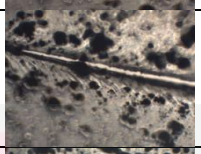	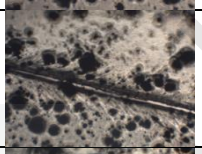
G-Gly-PANI(A2)	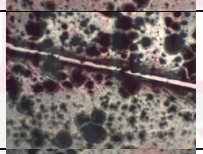	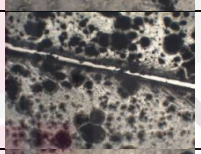	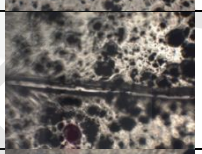
G-Gly-PANI(B0.5)	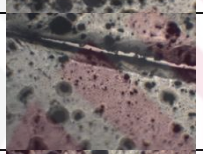	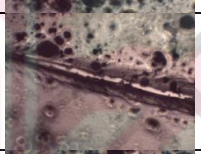	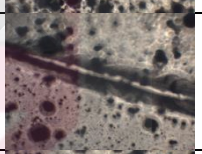
G-Gly-PANI(B1)	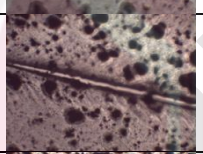	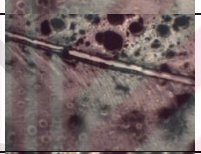	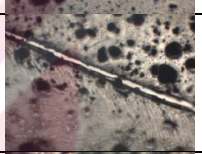
G-Gly-PANI(B2)	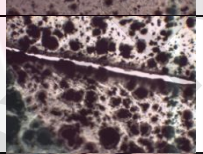	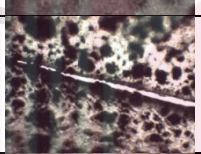	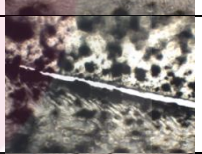
G-Gly-PANI(C0.5)	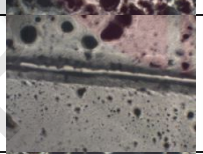	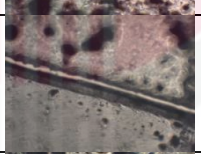	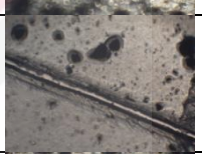
G-Gly-PANI(C1)	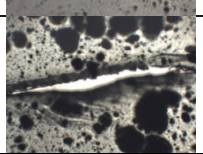	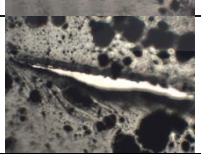	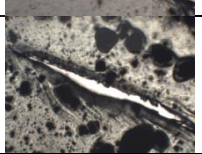
G-Gly-PANI(C2)	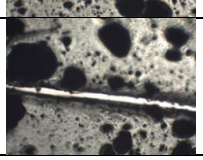	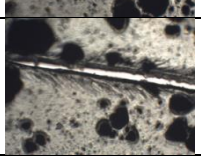	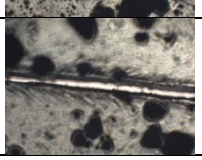

Figure A5: Light microscope image (x10 magnification) of self-healing progress at day 0, 4 and 7 at RH 57% and temperature 30 °C

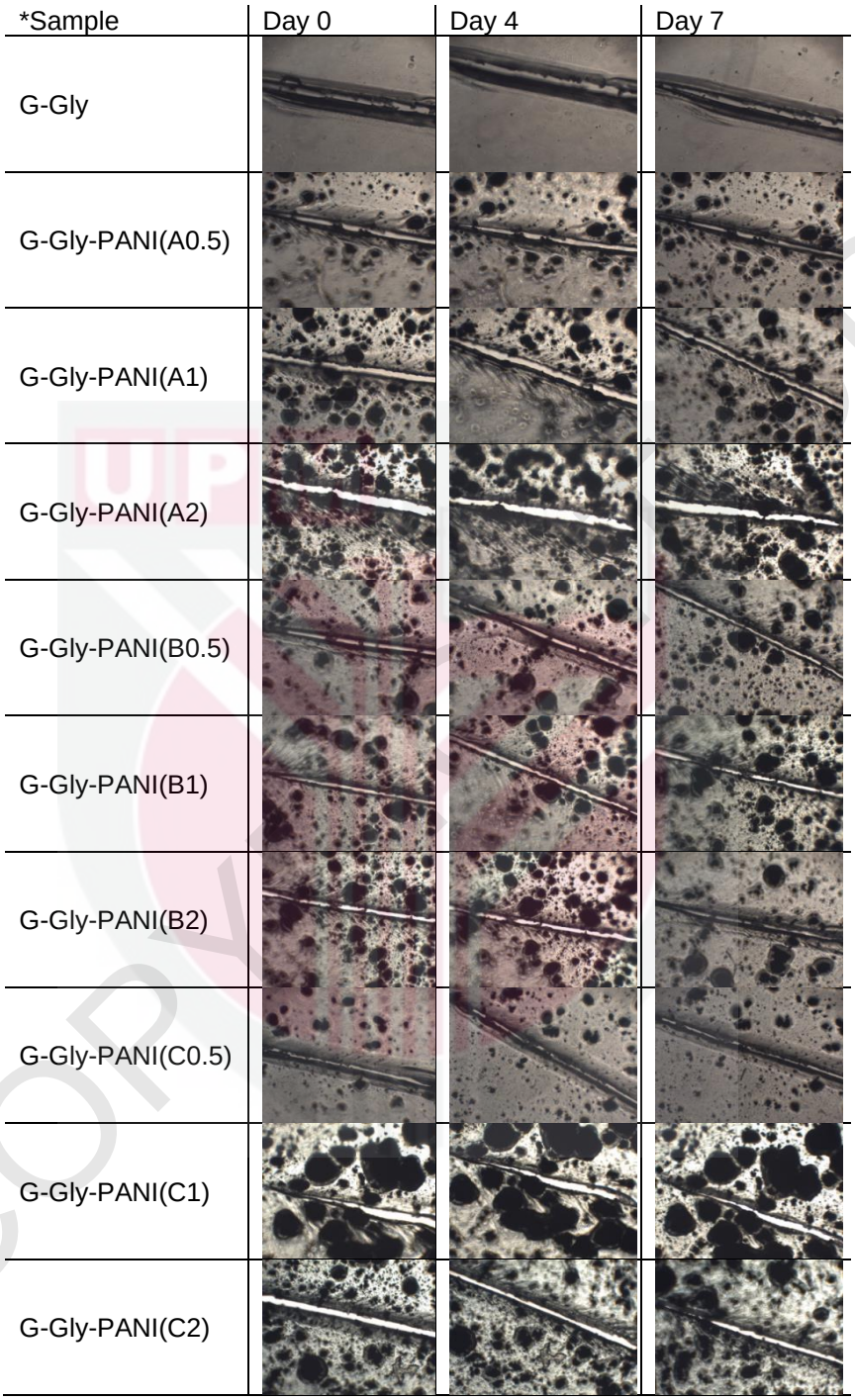

Figure A6: Light microscope (x10 magnification) image of self-healing progress at day 0, 4 and 7 at RH 57% and temperature 40 °C

Table A1: Water Sorption rate (k_1), water sorption capacity (k_2) and regression square (R^2) obtained from water sorption data fitted to Peleg model for the films at temperature 5 °C

RH (%)	Constant	Sample films									
		G-Gly	G-Gly-PANI (A0.5)	G-Gly-PANI (A1)	G-Gly-PANI (A2)	G-Gly-PANI (B0.5)	G-Gly-PANI (B1)	G-Gly-PANI (B2)	G-Gly-PANI (C0.5)	G-Gly-PANI (C1)	G-Gly-PANI (C2)
23	k_1	1.1141	1.3417	0.1966	0.1616	1.099	0.7091	0.0365	0.5599	0.3482	0.166
	k_2	0.1233	0.2200	0.2019	0.2704	0.1819	0.1003	0.0645	0.1303	0.137	0.1045
	R^2	0.9795	0.9859	0.9980	0.9993	0.9952	0.992	0.996	0.9965	0.9959	0.9639
33	k_1	0.3141	0.5744	0.1307	0.2554	0.1347	0.1553	0.0568	0.0452	0.0385	0.1158
	k_2	0.0994	0.1780	0.1098	0.1408	0.1302	0.0795	0.0578	0.0939	0.1032	0.0946
	R^2	0.9981	0.9987	0.9973	0.9996	0.9991	0.9992	0.9990	0.9998	0.9993	0.9988
43	k_1	0.5066	0.1285	1.3148	1.7359	0.1371	0.3836	0.2929	0.1950	0.1117	0.1434
	k_2	0.083	0.1483	0.0983	0.0537	0.0961	0.0853	0.0555	0.0837	0.0806	0.1005
	R^2	0.09916	0.9991	0.9795	0.8798	0.9994	0.9917	0.9927	0.09968	0.9958	0.9972
57	k_1	0.1398	0.4382	0.6609	0.6311	0.1377	0.1697	0.1446	0.0409	0.366	0.3167
	k_2	0.0523	0.0389	0.0504	0.1313	0.029	0.0387	0.0319	0.028	0.0725	0.0591
	R^2	0.9985	0.9595	0.9617	0.9952	0.09949	0.9902	0.9902	0.9919	0.9805	0.9868
75	k_1	0.0934	0.0416	0.1941	0.0005	0.0608	0.0836	0.0461	0.0658	0.0954	0.0379
	k_2	0.0298	0.0398	0.0253	0.0412	0.032	0.0291	0.0248	0.0205	0.0401	0.0336
	R^2	0.0991	0.9937	0.9697	0.9999	0.9971	0.9936	0.994	0.9979	0.9949	0.9966

Table A2: Water Sorption rate (k_1), water sorption capacity (k_2) and regression square (R^2) obtained from water sorption data fitted to Peleg model for at temperature 30 °C

RH (%)	Constant	Sample films									
		G-Gly	G-Gly-PANI (A0.5)	G-Gly-PANI (A1)	G-Gly-PANI (A2)	G-Gly-PANI (B0.5)	G-Gly-PANI (B1)	G-Gly-PANI (B2)	G-Gly-PANI (C0.5)	G-Gly-PANI (C1)	G-Gly-PANI (C2)
23	k_1	2.1034	1.8259	3.9932	1.4234	0.0535	1.0379	0.4016	2.8518	9.7792	1.6476
	k_2	0.0876	0.5398	0.5979	0.2095	0.1286	0.2019	0.1194	0.1964	0.2742	0.1014
	R^2	0.8772	0.8995	0.8967	0.9746	0.9916	0.9863	0.9966	0.9581	0.9037	0.9623
33	k_1	1.8997	0.6446	6.6211	2.0994	0.1026	0.3813	0.2777	0.0415	1.8217	0.3117
	k_2	0.0786	0.2017	0.3316	0.1536	0.1176	0.1366	0.1215	0.1362	0.142	0.1219
	R^2	0.8401	0.9542	0.9483	0.9487	0.9947	0.9952	0.9966	0.9896	0.9796	0.9822
43	k_1	0.5081	0.2407	0.309	0.007	0.1102	0.4467	0.0406	0.1362	0.0014	0.3408
	k_2	0.0645	0.1342	0.1433	0.1005	0.0717	0.01134	0.08888	0.0415	0.1188	0.0771
	R^2	0.9262	0.9955	0.9839	0.9958	0.9967	0.985	0.9986	0.9896	0.9967	0.9767
57	k_1	0.4528	0.0175	0.392	0.3726	0.0551	0.2524	0.1808	0.6583	0.2633	0.1409
	k_2	0.0537	0.0523	0.0861	0.1403	0.0611	0.0766	0.0643	0.1138	0.0822	0.0758
	R^2	0.8989	0.9998	0.9834	0.9969	0.9984	0.992	0.9965	0.9911	0.9961	0.9973
75	k_1	0.019	0.0252	0.0608	0.0729	0.0637	0.0517	0.2498	0.0894	0.1935	0.1136
	k_2	0.0296	0.0394	0.0422	0.0371	0.0364	0.0433	0.0332	0.0516	0.048	0.0365
	R^2	0.8819	0.9997	0.0999	0.9914	0.9979	0.9972	0.9819	0.9955	0.9797	0.9826

Table A3: Water Sorption rate (k_1), water sorption capacity (k_2) and regression square (R^2) obtained from water sorption data fitted to Peleg model at temperature 40 °C

RH (%)	Constant	Sample films									
		G-Gly	G-Gly-PANI (A0.5)	G-Gly-PANI (A1)	G-Gly-PANI (A2)	G-Gly-PANI (B0.5)	G-Gly-PANI (B1)	G-Gly-PANI (B2)	G-Gly-PANI (C0.5)	G-Gly-PANI (C1)	G-Gly-PANI (C2)
23	k_1	0.4496	0.3746	0.345	0.5791	0.7189	1.5145	1.0326	4.4278	4.7904	0.3767
	k_2	0.0975	0.2387	0.2067	0.1126	0.2157	0.183	0.1424	0.3121	0.1909	0.2587
	R^2	0.9965	0.9986	0.9968	0.9953	0.9939	0.9788	0.975	0.8634	0.9221	0.9797
33	k_1	0.2679	0.3814	0.4224	0.1726	0.684	0.7251	0.0779	1.3445	0.396	1.8799
	k_2	0.0914	0.121	0.1274	0.1017	0.1902	0.1081	0.128	0.2181	0.348	0.14
	R^2	0.9988	0.9985	0.9988	0.9954	0.9837	0.9931	0.9957	0.9315	0.9833	0.9719
43	k_1	0.2377	0.2663	0.1917	0.3941	0.6748	0.7995	1.2721	1.2221	1.5068	0.1037
	k_2	0.0844	0.0896	0.0953	0.088	0.0841	0.0977	0.167	0.1198	0.0732	0.1315
	R^2	0.9981	0.9991	0.9993	0.0997	0.09909	0.9906	0.9714	0.9779	0.8837	0.9932
57	k_1	0.4081	0.1235	0.1555	0.441	0.01162	0.4178	0.3594	2.4505	2.2086	1.3266
	k_2	0.1033	0.0823	0.1298	0.0802	0.0939	0.1124	0.1166	0.1251	0.0862	0.1007
	R^2	0.9981	0.9994	0.9958	0.9941	0.9956	0.9914	0.9942	0.9549	0.8607	0.9749
75	k_1	0.1058	0.0316	0.0535	0.103	0.4013	0.0392	0.6154	1.1168	0.0977	1.0782
	k_2	0.0451	0.0366	0.0193	0.0357	0.0666	0.0502	0.077	0.0386	0.0641	0.0429
	R^2	0.9908	0.9969	0.9988	0.0992	0.9002	0.9767	0.9175	0.9097	0.9288	0.9306

Table A4: GAB constant parameters for the films at different temperatures

Temperature (°C)	Constant	Sample films									
		G-Gly	G-Gly-PANI (A0.5)	G-Gly-PANI (A1)	G-Gly-PANI (A2)	G-Gly-PANI (B0.5)	G-Gly-PANI (B1)	G-Gly-PANI (B2)	G-Gly-PANI (C0.5)	G-Gly-PANI (C1)	G-Gly-PANI (C2)
5	k	0.3007	0.3230	0.1113	0.3313	0.1567	-0.0404	0.2860	0.2511	0.2864	0.3327
	W_m	0.3556	0.2620	0.0736	0.1497	0.1622	0.1208	0.4272	0.1591	0.2208	0.3165
	C	-0.3080	-0.1696	-0.0100	-0.0500	-0.0532	-0.0308	-0.4425	-0.0492	-0.1039	-0.2397
	R^2	0.9990	0.9694	0.9928	0.9423	0.9733	0.8188	0.9990	0.9701	0.9938	0.9899
30	k	0.2123	0.2428	-0.0342	-0.2492	0.2091	0.2224	0.2632	0.1735	0.1758	0.2297
	W_m	0.3604	0.2157	0.1598	0.2022	0.2119	0.3076	0.4723	0.1830	0.2040	0.2844
	C	-0.3176	-0.1018	-0.0515	-0.0822	-0.0969	-0.2153	-0.6215	-0.0708	-0.0884	-0.1831
	R^2	0.9961	0.9900	0.9300	0.9974	0.9986	0.9900	0.9187	0.9900	0.9900	0.9900
40	k	0.6273	0.3241	0.1742	0.3115	0.0970	0.2960	0.2455	0.3022	0.2438	0.2975
	W_m	1.2512	0.2670	0.2049	0.2992	0.1319	0.3027	0.3945	0.2428	0.2535	0.2584
	C	4.9871	-0.1707	-0.0904	-0.2174	-0.0358	-0.2218	-0.3931	-0.1374	-0.1470	-0.1574
	R^2	0.9900	0.9900	0.9900	0.9900	0.9900	0.9900	0.9900	0.9900	0.9900	0.9900

Table A5: Smith constant parameters for the films at different temperatures

Temperature (°C)	Constant	Sample films									
		G-Gly	G-Gly-PANI (A0.5)	G-Gly-PANI (A1)	G-Gly-PANI (A2)	G-Gly-PANI (B0.5)	G-Gly-PANI (B1)	G-Gly-PANI (B2)	G-Gly-PANI (C0.5)	G-Gly-PANI (C1)	G-Gly-PANI (C2)
5	A	3.6125	6.7396	2.9763	8.8906	5.8376	3.3216	2.3527	5.3583	4.9021	4.1301
	B	0.9239	0.5847	8.8270	3.6465	1.4556	1.8145	0.9518	2.9885	2.0725	1.3445
	R^2	0.9230	0.0683	0.5542	0.7736	0.7097	0.9507	0.9883	0.9163	0.9631	0.8978
30	A	3.9666	5.7625	10.421	7.1933	5.7058	3.8682	2.5116	6.4454	5.6399	4.3754
	B	0.1736	1.1847	1.1285	0.0716	0.9245	0.6937	0.6337	0.7857	0.7924	0.7209
	R^2	0.8998	0.9708	0.8970	0.0091	0.9623	0.9699	0.9490	0.9462	0.9852	0.9471
40	A	1.1156	5.4667	5.8455	5.2241	8.6926	4.8368	3.4809	5.9133	5.5471	5.6670
	B	0.1424	1.3739	1.0999	0.9477	0.2382	0.7971	0.3147	1.2734	0.5860	1.0541
	R^2	0.6855	0.8347	0.7726	0.5749	0.5273	0.7366	0.6325	0.8268	0.6486	0.7613

Table A6: Halsey constant parameters for the films at different temperatures

Temperature (°C)	Constant	Sample films									
		G-Gly	G-Gly-PANI (A0.5)	G-Gly-PANI (A1)	G-Gly-PANI (A2)	G-Gly-PANI (B0.5)	G-Gly-PANI (B1)	G-Gly-PANI (B2)	G-Gly-PANI (C0.5)	G-Gly-PANI (C1)	G-Gly-PANI (C2)
5	a	1.4003	1.9421	2.3317	2.3806	1.8799	1.4299	0.2860	1.9072	1.7711	1.5627
	b	0.1429	0.0449	0.2113	0.2282	0.1475	0.2605	0.4272	0.2783	0.2206	0.1746
	R^2	0.8754	0.0456	0.8695	0.8540	0.7137	0.9151	0.9990	0.9250	0.9447	0.8446
30	a	1.3989	1.8457	2.3950	1.9810	1.8165	1.0355	1.8165	1.9250	1.7950	1.5524
	b	0.0289	0.1198	0.0668	0.1335	0.0977	0.1414	0.0977	0.0605	0.0871	0.0986
	R^2	0.8607	0.9455	0.8412	0.8809	0.9384	0.9235	0.9384	0.5859	0.9725	0.9191
40	a	0.1699	1.8138	1.8511	1.7067	2.1802	1.6538	0.2455	1.8768	1.7639	1.8215
	b	0.0750	0.1361	0.0469	0.1182	0.0305	0.0934	0.3945	0.1194	0.0620	0.1045
	R^2	0.6156	0.7732	0.6694	0.7312	0.4427	0.6549	0.9900	0.7508	0.5548	0.6862

Table A7: Caurie constant parameters for the films at different temperatures

Temperature (°C)	Constant	Sample films									
		G-Gly	G-Gly-PANI (A0.5)	G-Gly-PANI (A1)	G-Gly-PANI (A2)	G-Gly-PANI (B0.5)	G-Gly-PANI (B1)	G-Gly-PANI (B2)	G-Gly-PANI (C0.5)	G-Gly-PANI (C1)	G-Gly-PANI (C2)
5	A	1.2415	1.9008	2.0902	2.1331	1.7030	1.1368	0.7825	1.5863	1.5207	1.3680
	r	-0.4366	-0.1187	-0.6602	-0.6309	-0.4659	-0.8014	-0.6748	-0.8756	-0.6855	0.5350
	R^2	0.8424	0.0328	0.8748	0.6922	0.7333	0.8984	0.9940	0.9435	0.9397	0.8167
30	A	1.3666	1.7127	2.3216	1.8320	1.7080	1.3152	0.8792	1.8360	1.6976	1.4435
	r	-0.8860	-0.3658	-0.2024	-0.4095	-0.2986	-0.3297	-0.4302	-0.2312	-0.2675	-0.2998
	R^2	0.8349	0.9086	0.7960	0.8538	0.9027	0.9245	0.8810	0.8830	0.9458	0.8762
40	A	0.0905	1.6668	1.8009	1.5799	2.1579	1.5547	1.2347	1.7477	1.6990	1.7100
	r	-0.2207	-0.4067	-0.1393	-0.3514	-0.0503	-0.2753	-0.1564	-0.3527	-0.1808	-0.3094
	R^2	0.5493	0.7119	0.6071	0.6653	0.3917	0.5863	0.4735	0.6927	0.4863	0.6202

LIST OF PUBLICATIONS

Azmi, N. S., Kadir Basha, R., Othman, S. H., and Mohammed, M. A. P. (2019). Characterization of antioxidant tapioca/starch/polyaniline composites film prepared using solution casting method. *Food Research,* 3(4), 317-324.

Azmi, N. S., Kadir Basha, R., Arifin, N. N. T, Othman, S. H., and Mohammed, M. A. P. (2020). Functional properties of tilapia's fish scale gelatin film: effects of different type of plasticizers. *Sains Malaysiana,* 49 (9): 221-2229.

Basha, R.K., Leong, K.Y., Othman, S.H., Talib, R.A., Naim, M.N., Hasnan, N.Z.N. and Azmi, N.S. (2021). Sorption characteristic of starch-based film. *Food Research,* 5(Suppl. 1): 193-200.

Azmi, N. S., Kadir Basha, R., Othman, S. H., and Mohammed, M. A. P., Wakisaka, M. and Ariffin, S. H. Development of fish scale gelatin-based film and its effect on anti-fogging properties for packaging of mushrooms (Submitted to Journal of Food Science and Technology)